THURSTON AIRCRAFT CORPORATION
AIRCRAFT & MARINE ENGINEERING - AIRFRAME MANUFACTURING
BOX 450 SANFORD AIRPORT, SANFORD, MAINE 04073 • 207/324-3313

Final Report

HYDROFOIL SEAPLANE DESIGN

Contract N00019-69-C-0475

Report No. 6912

May 1970

Prepared by: Nicholas J. Vagianos
Vice President Engineering

David B. Thurston
President

Thurston Aircraft Corporation

UNCLASSIFIED

DISCLAIMER NOTICE

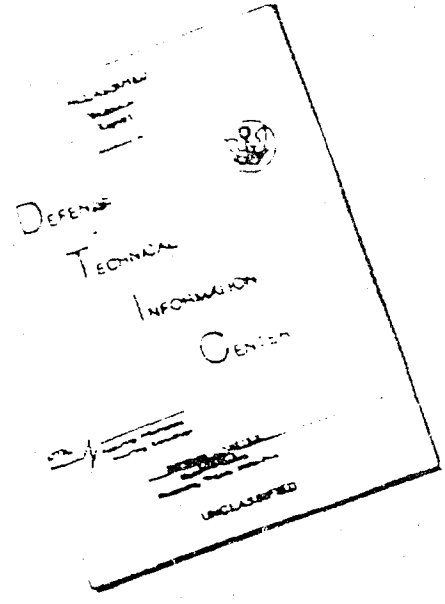

THIS DOCUMENT IS BEST QUALITY AVAILABLE. THE COPY FURNISHED TO DTIC CONTAINED A SIGNIFICANT NUMBER OF PAGES WHICH DO NOT REPRODUCE LEGIBLY.

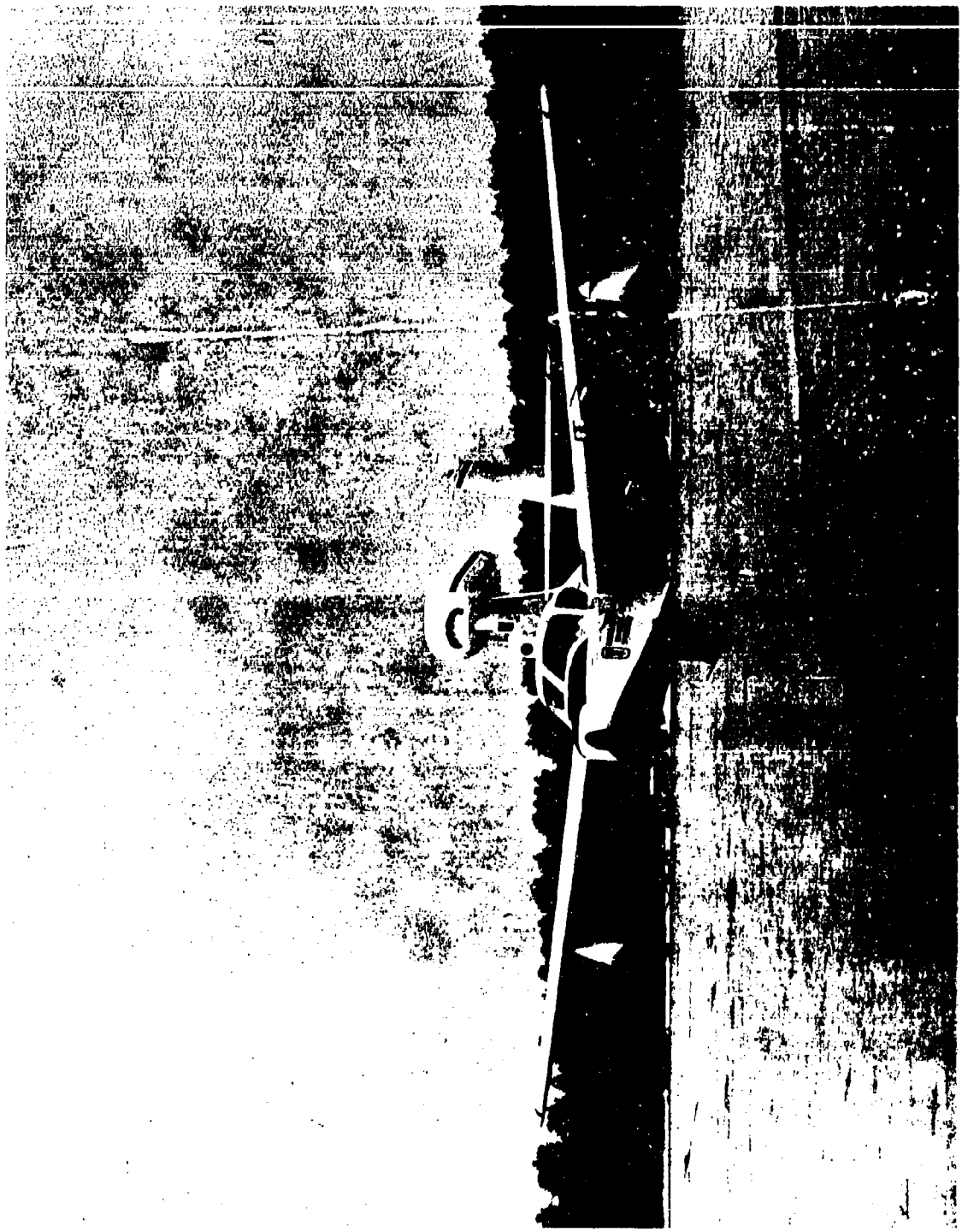

Thurston Aircraft Corporation HRV-1 Equipped with Supercavitating Hydrofoil

TABLE OF CONTENTS

NOMENCLATURE

a	Lift curve slope
A	Aspect ratio b^2/S; and for foils with dihedral $2(d/c)\cot\Gamma$
b	Span, feet
c	Chord, feet
cg	Center of Gravity
C_D	Drag coefficient, $D/\frac{1}{2}\rho V^2 S$
C_{D_p}	Profile drag coefficient
C_L	Lift coefficient, $L/\frac{1}{2}\rho V^2 S$
C_L'	Section lift coefficient, $L/\frac{1}{2}\rho V^2 c$
$C_{L,d}$	Design lift coefficient of hydrofoil (lift due to bottom shape)
C_M	Moment coefficient, $M/\frac{1}{2}\rho V^2 Sc$
C_p	Pressure coefficient $(p - p_\infty)/q_\infty$
d	Depth, feet
D	Drag, pounds
f	Trailing edge flap
F	Froude number, $V/\sqrt{gc}$
g	Gravitational acceleration, ft/sec^2
L	Lift, pounds
p	Static pressure
q	Dynamic pressure, $\frac{1}{2}\rho V^2$
R_e	Reynold's Number, $\rho cV/\mu$
S	Projected area, $feet^2$ (S_w for wings; S_H for hydrofoil)
V	Velocity, feet/second
x	Distance from hydrofoil leading edge, measured aft along chord, feet
y	Distance from hydrofoil chord line, measured upward, feet

α Angle of attack; angle between hydrofoil chord and free steam velocity vector, measured in plane perpendicular to hydrofoil transverse axis, degrees

γ Central angle of circular arc hydrofoil, radians

Γ Dihedral angle, degrees

δ Flap deflection, degrees

Λ Sweep angle, degrees

μ Viscosity, $lb\text{-}sec/ft^2$

ρ Density, slugs per cubic foot, $lb\text{-}sec^2/ft^4$

σ Cavitation number, $(p_\infty - p)/q_\infty$

Subscripts:

c cavity

v vapor

τ Trim angle; angle between hydrofoil chord and airplane reference line (equivalent of aerodynamic incidence), degrees

BLANK PAGE

1. Hydrofoil Seaplane History

While this brief history of hydrofoil seaplane design and development is not intended to be comprehensive, an effort has been made to illustrate the lineage of hydrofoil research dating back over one hundred years to the original experiments of Thomas Moy.

Using water as a test medium, Moy towed a lightweight boat on England's Surrey Canal during 1861. This test vehicle was fitted with three cambered planes of subsonic airfoil profile pinned along the spanwise axis and mounted below the keel. The boat rose above the water surface as speed was increased, while the inventor noted the planes developed increased lift and trimmed to reduce drag as speed was increased (Ref. 1).

Foretelling the configuration of the Piaggio P.C.7 built in 1929, the Frenchmen Emmanuel Farcot in 1869 and Tissandier in 1893 both developed craft fitted with underwater propellers and submerged inclined planes. Tissandier's "glider boat" was also equipped with wings, as was a model craft built by Clement Ader in 1895. Ader's design incorporated two adjustable underwater bow foils and a planing horizontal tail. Ader further developed this configuration through 1904 into a variable sweep wing air cushion vehicle having a concave lower wing surface to entrap the air cushion, certainly a remarkable development half a century ahead of its time.

During 1897 a catamaran boat equipped with a series of four high aspect ratio hydrofoils and an underwater propeller driven by a steam engine was successfully "flown" over the Seine carrying one man at 20 miles per hour. Developed by H. F. Phillips and Comte de Lambert, this design was improved through 1907 at which time it was powered by an Antionette internal combustion engine and was capable of carrying two men over the water at a speed of thirty four miles per hour.

Professor Enrico Forlanini of Milan applied for a ladder foil patent in 1905 "to permit boats and flying machines to lift out of contact with the water surface when propelled, thereby offering much less resistance and as a consequence be capable of attaining much higher speeds." While suitable engines prevented Forlanini from attaining flight, he continued his experiments through the development of an air propelled vehicle employing the original ladder hydrofoil system. Built in 1906, this craft lifted clear of the water and reached a speed of 38 knots (43mph).

1907 appears to have been the first acceleration point for hydrofoil development. In that year: Orville and Wilbur Wright, familiar with the work of Phillips and Comte de Lambert, experimented with copper sheet hydrofoils mounted on a test bed operated in the Miami River at Dayton, Ohio; G. R. Napier announced his concept for spring loaded variable incidence hydrofoils that would vary lift with heave to maintain stable flight - granted a

British patent in 1911, there is no record that Napier ever built a working model of this system which is similar to the principle behind variable angle trailing edge (flapped) hydrofoils; the American L. E. Simpson developed the design for a variable incidence submerged foil craft; the Italians Crocco and Ricaldoni built and tested a boat equipped with tandem (bow and stern) surface piercing hydrofoils. Driven by cambered variable pitch reversing propellers of dural sheet and a 100 h.p. engine, this vehicle exceeded a foil borne speed of 50 mph while carrying two men.

Also during 1907, the American Peter Cooper Hewitt developed a tandem ladder foil test vehicle which weighed 2500 pounds and reached 30 mph; at this speed, only the lowest foils remained submerged.

While most of the preceding development programs employed boats or boat-type test beds, much of this experimentation was directed toward flight from water as well as the determination of section lift and drag characteristics using water as the fluid medium. Early aircraft experimenters realized the advantages of a large, smooth, and relatively obstruction free launching and landing area offered by a calm water surface - provided they could overcome the dual problems of hydrodynamic suction and drag present during water take off.

Finally, the first powered airplane to take off from water was demonstrated at Marseilles, France by Henri Fabre on March 28, 1910. Employing a canard arrangement of three low aspect ratio 15% thick cambered float/foils and powered by a Gnome engine, Fabre's design carried him a distance of approximately 500 yards at a height of six feet above the water surface. The Fabre floats were designed to provide lift whether running submerged, upon the water surface, or in flight - and probably contributed the additional lift necessary for a successful water take off with minimum thrust.

It is interesting to note that on page 146 of his 1918 Edition of "Military Airplanes", Grover C. Loening shows the Fabre float to have considerably less drag than other known floats of the period and an L/D value of 6- over twice that of any other float tested.

Impressed with Forlanini's work, the Italian General A. Guidoni determined during 1910 to achieve flight with a hydrofoil seaplane. Starting with Forlanini's ladder foil system, which he soon discarded because of the heaving and pitching associated with differential and rapid unporting of the foils, Guidoni equipped each float of his twin float Farman F.1 biplane with a tandem cascade system of three positive d edral hydrofoils per strut. Variations of this system were successfully flown by Guidoni on three Farman aircraft, the F.1, F.2, and F.3; although experimentation probably continued through 1913, there is little documentation

concerning the detail design and test results of Guidoni's useful work.

A second period of accelerated hydrofoil aircraft development began in 1911. In fact, with the exception of supersonic flight, there is little in the aircraft field to date that was not tried in some form by or during 1911. This includes Voisin's amphibian (using Fabre floats), Curtiss' retractable landing gear, and Avro's ventilated step floats. By 1911, engines and the state of the art of aircraft design had reached a level such that: Glen Curtiss made his first flight from water using a pusher biplane equipped with tandem floats and a forward mounted six foot span hydrofoil; the first British water take off was accomplished by Cdr. Schwann in a tractor Avro biplane having ventilated step twin floats each mounting two struts fitted with two cascade aluminum alloy hydrofoils of 40 inch span and 4 inch chord (a tandem cascade system similar to Guidoni's). The foils were positioned 4 inches apart, set at 3° incidence, had a camber depth of 8% chord, and the upper foil was located 20 inches below the water surface. So by 1911, aircraft developed in France, Italy, Great Britain, and the United States had succeeded in conducting sustained flight off water.

Another 1911 American seaplane, The Michigan Steel Boat Company's "Flying Fish," was equipped with a single, beam width, narrow chord hydrofoil mounted below the aluminum hull. A single seat tractor flying boat of short wingspan, the "Flying Fish" skimmed along the water surface supported by the flat hydrofoil and a planing section of the hull afterbody - possibly the first planing tail hull. During 1911, this design traveled from Detroit to Cleveland at an average speed of 50 mph, although maximum speeds of 70 mph were recorded when the "Flying Fish" lifted clear of the water except for the planing tail.

The first significant attempt to develop an airplane capable of rough water or open-sea operation was supported by the British Admiralty during 1911. Lt. Charles Burney, R.N. conducted towing experiments that year leading to the design and development of the Burney X.2 during 1912, and the final X.3 configuration of 1913 intended for shipboard stowage. (Fig. 1.) Influenced by the work of Forlanini and Guidoni, the Burney designs employed a split Tietjens cascade hydrofoil system with two struts forward and one aft. Water taxiing power was supplied by small counterrotating propellers tandem mounted between the forward foils and driven from the engine through a clutch system. In theory, the water propellers would get the X.3 foilborne, the flight propeller would be clutched in, and take off through rough seas completed in airplane fashion. In practice, various stability problems resulted from both water and air torque reactions when the respective propellers were engaged, compounded no doubt by inadequate aerodynamic control during unporting. Wrecked during a towing encounter with a hidden sandbar, this interesting project was terminated during late 1913. The various torque problems bounding

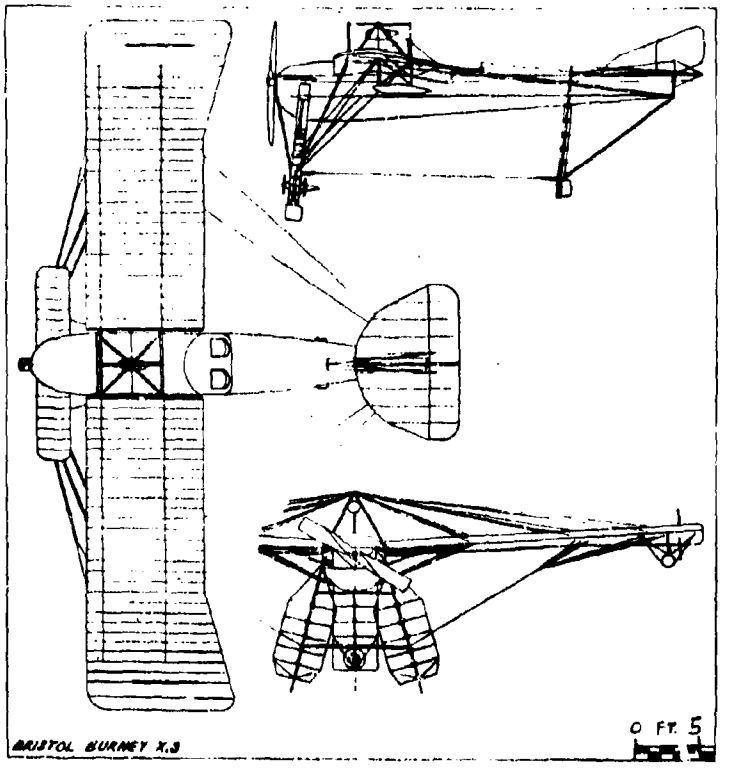

Fig. 1

Burney X. 3 Hydrofoil Seaplane

Tietjens Split Cascade System

Power Plant: 200 hp Canton-Unne
Span: 57'-10"
Length: 36'-8"
Wing Area: 500 sq.ft.

the X-3 were similar to those experienced by the Piaggio P.C.7 in 1929.

During 1914 the Wright brothers were again testing hydrofoils in the Miami River. Their main interest lay in stopping water from breaking away from the upper surface of cambered foils too soon (speedwise) and thus preventing the subsequent loss of lift. Tests were conducted with cambered sheet steel "hydrovanes" having an auxiliary narrow cambered strip of steel placed just above the leading edge. While this slotted hydrofoil was apparently successful in delaying breakaway beyond the speed possible with a plain (subcavitating) hydrofoil, it was only applied by the Wrights to one seaplane design built in 1915. Possibly they were really seeking a means for obtaining an improved C_L for their aircraft, but if so, such a design was never flown by them. At this same time, Handley-Page in England was wind tunnel testing and developing his slotted wing to a new level of lift and stall attitude capability; apparently neither group being aware of the others efforts in the same field.

World War I terminated hydrofoil seaplane research for many years, until the series of Schneider Trophy Contest races revived determined interest in the development of high performance water based aircraft. Although the only seaplane attempting water take off from hydrofoils never made the starting line, the configuration and design data for the Italian Piaggio P.C. 7 represent a bold design attempt to achieve seaplane performance comparable with landplanes by minimizing frontal area (Fig. 2).

Designed by Piaggio's Chief Engineer, Giovanni Pegna for the 1929 Schneider Trophy Contest and financed by both Piaggio and the Italian government, the P.C. 7 was a relatively small airplane of 3709 pounds gross weight. Described in Jane's All The World's Aircraft of 1932, page 232c, and more fully by Benjamin Posniak (now a Senior Project Manager at N S R D C) in an article for the Italian press published in 1934, the P.C. 7 used a split Tietjens hydrofoil system having two foils forward instead of floats and two small foils superimposed aft below the tail surfaces. Initial tests revealed difficulties with the water screw due to torque as well as clutch slip caused by oil and water seepage; when attempts to correct these problems proved unsuccessful, further development of this interesting design was abandoned. However, since this configuration was so far ahead of its time, and could serve as a stepping stone for future high performance seaplane development (with jet engines precluding propeller problems), a few of the P.C. 7 design details are presented for reference purposes:

Type: Experimental single seat cantilever monoplane racing seaplane.
Power Plant: 850 hp Isotta-Fraschini engine of 12 cylinders
Wing: Cantilever; 3 spars; plywood covered and watertight; wing surface water cooling radiators.
Fuselage: Built-up watertight plywood structure; fuel in fuselage.

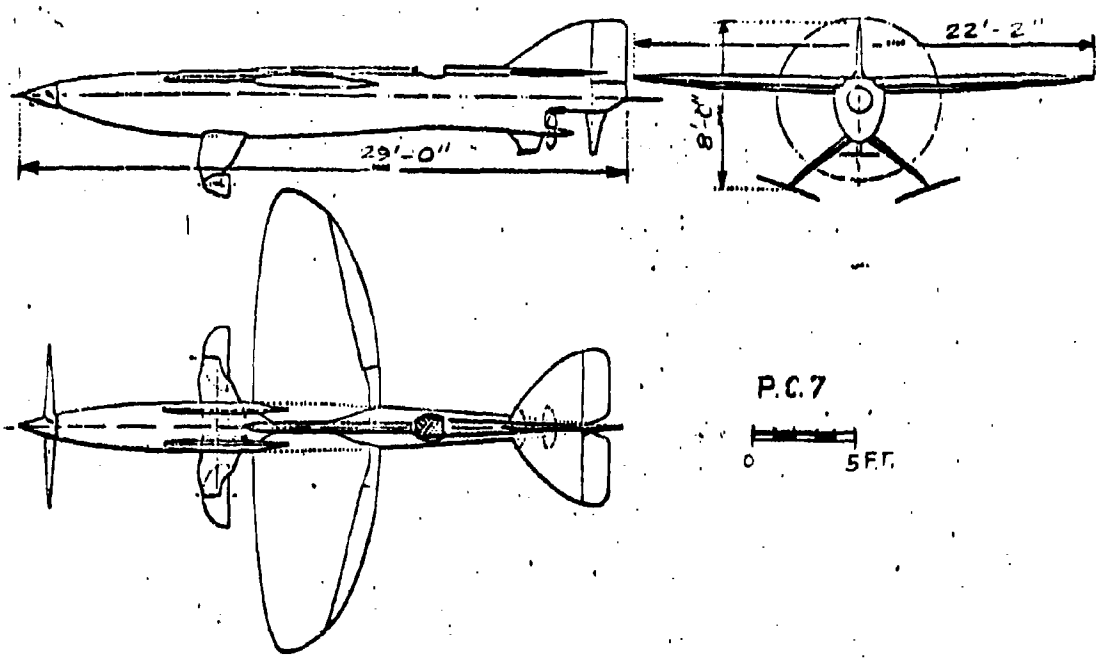

Fig. 2

Piaggio P.C. 7
Schneider Trophy Racer

Tietjens Split Flat Monofoil System

Power Plant: 850 hp Isotta-Fraschini
Length: 29'-0"
Wing Area: 106.3 sq. ft.

Tail Surfaces: Same as wing; watertight
Flotation: Watertight structure having two watertight compartments in fuselage plus welded aluminum alloy tanks; rests on water by floating on the wing, fuselage, and tail

Operation: The 850 hp IF engine drives the water screw until the P.C. 7 is foilborne, at which point the propeller is clear of the water and engaged for flight.

Span: 22'-2" Height: 8'
Length: 29' Wing Area: 106.3 sq. ft. total including fuselage area - 90.9 sq. ft. net

Weight Empty: 3093 lb.
Useful Load: 616 lb.
Gross Weight 3709 lb.

Estimated maximum speed: 373 mph.

Following the failure of the P.C. 7 to achieve water borne flight, primarily due to mechanical causes rather than basic configuration, hydrofoil seaplane design received virtually no emphasis until Edo Aircraft studies begun in 1957 developed the JRF-5G amphibian equipped with a Grunberg supercavitating hydrofoil system (Fig. 3). This configuration was extensively evaluated by Edo and at the U. S. Naval Air Test Center, Patuxent River, Maryland through 1964.

The Grunberg foil system as adapted to the JRF-5G consisted of a supercavitating hydrofoil near the airplane center of gravity and two planing bow skids; this arrangement was used to permit evaluation of the hydrofoil while providing safety in the event of foil failure. This system used the largest supercavitating hydrofoil built up to that time and the first supercavitating foil mounted on a seaplane. The bow skids served the dual purpose of (1) properly trimming the airplane during transition through the hump speed regime and (2) preventing the airplane from diving if the submerged foil failed. Both the large hydrofoil and the bow skids were retracted hydraulically to permit ramp approaches and land operations, and were locked in the up and down positions.

The water performance and test results obtained with the JRF-5G are discussed under Section VI of this study.

Subsequent to the JRF-5G program, Edo initiated design and tank studies during 1964 to develop a single, surface-piercing, supercavitating hydrofoil for application to the Grumman HU-16 Albatross Amphibian. To flight test this concept in scale form,

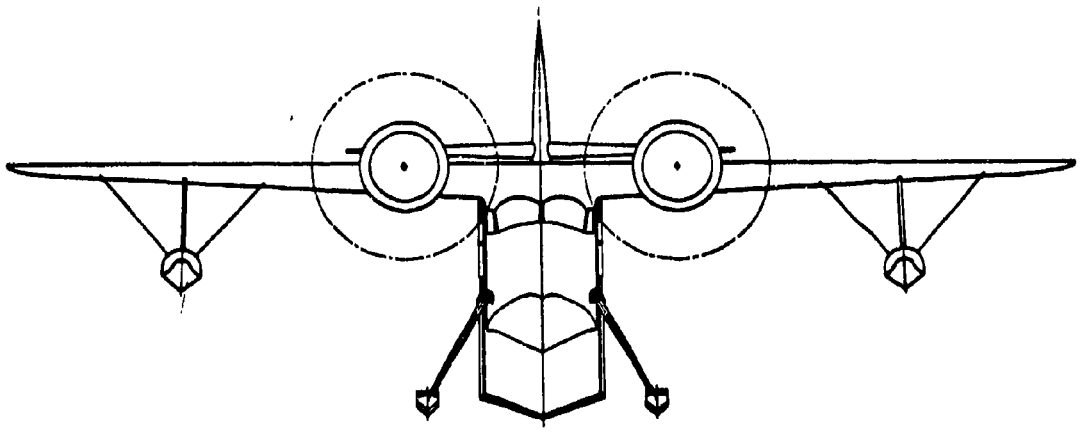

FRONT VIEW

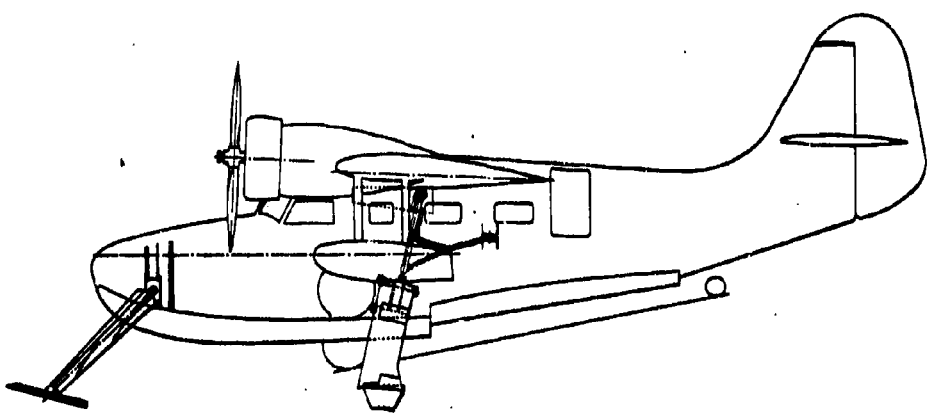

SIDE VIEW

Fig. 3 JRF-5G Airplane
BuNo 37782

TEST AIRPLANE WITH GRUNBERG HYDROFOIL SYSTEM

Span: 49'-0"
Length: 38'-4"
Wing Area: 375 sq. ft.
Gross Weight - 9570 pounds

the Thurston HRV-1 (Skimmer LA-4A) Amphibian was equipped in 1966 with a single foil similar to the Edo design but 1/2.47 scale size of that necessary for HU-16 evaluation (Fig. 4). This supercavitating foil was flown on the HRV-1 during 14 November 1966, representing the first known flight of an airplane equipped with a single surface-piercing hydrofoil. The detail flight test program was successfully completed with 41 data runs recorded; operational results are presented in Section V.

SPAN	38'-0"
AREA	170 SQ FT
LENGTH	23'-6"
TEST WT.	2300 LBS.
ENGINE	180 HP

FIG. 4

HRV-1 ARRANGEMENT AND SPRAY PATTERNS WITH HYDROFOIL NO. 1

SCALE : 1/64

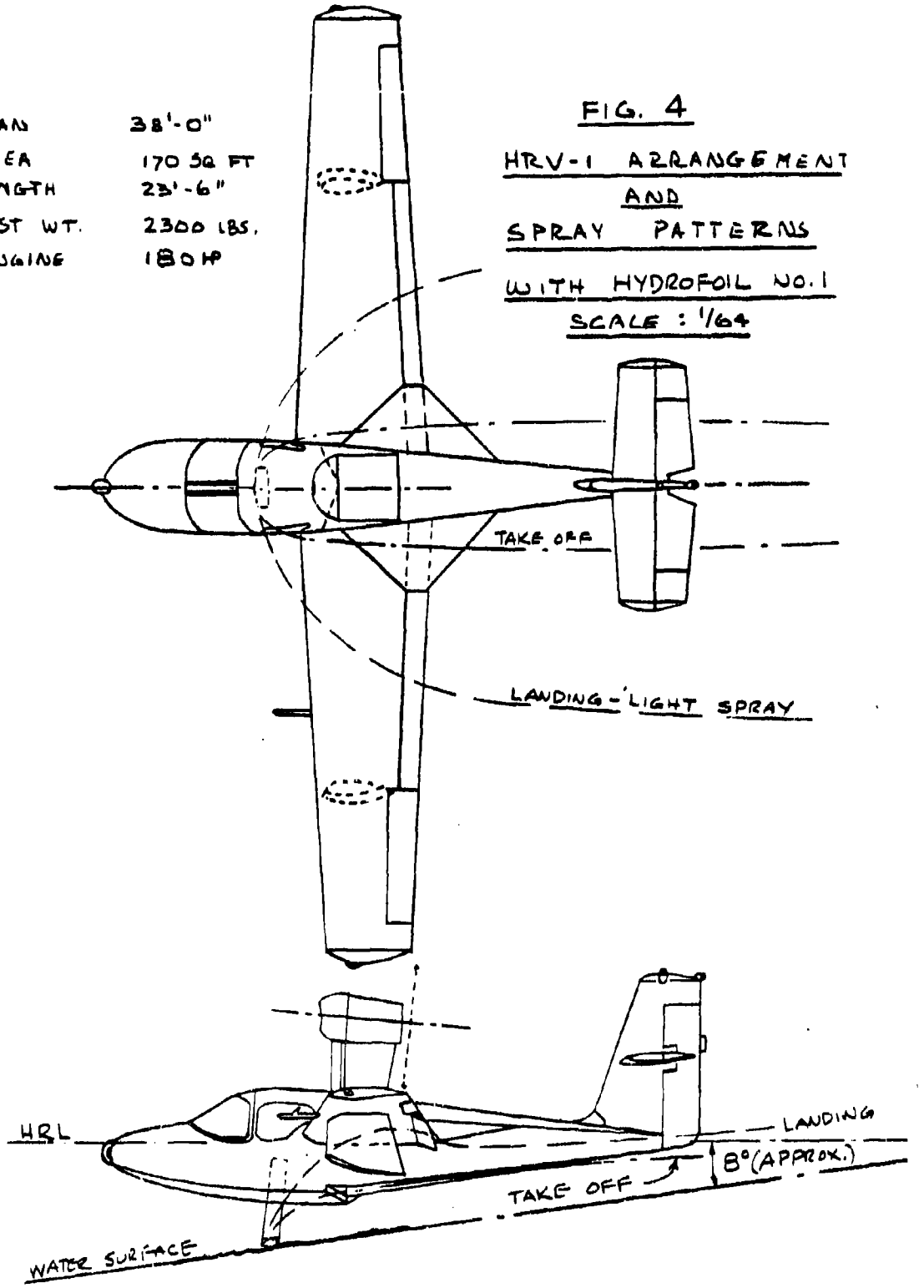

II. Description and Classification of Hydrofoil Systems

Since no comprehensive description of the various hydrofoil systems is available, an effort has been made to classify tested as well as possible arrangements. Refer to Figures 5 through 21.

Fig. 5. The Single Hydrofoil system consists of one hydrofoil placed slightly ahead of the cg, with some type of vehicle stabilization provided in addition to the foil; such as the wing, tail, and control surfaces of a seaplane. The single hydrofoil supports a predetermined percentage of the gross weight at unporting. Conceivably the single hydrofoil arrangement could be either a monofoil, a hoop foil, or a ladder foil; the Thurston HRV-1, the only seaplane flown with this type of arrangement, employs a single, positive dihedral, super-cavitating monofoil.

Fig. 6. The Grunberg system employs a main foil (continuous, split, or monofoil) positioned behind the cg, with two hydro-skis or floats forward skimming the water surface and stabilizing the vehicle. With this design, the main foil arrangement carries most of the unporting design load, while stabilizing members provide a small percentage of the design lift (with respect to load distribution, the Grunberg System is similar to the Canard System). This foil arrangement has been used on the JRF-5G seaplane (see Fig. 3).

Figs. 7-10. The Tandem Hydrofoil systems consist of foil arrangements at the bow and stern with each foil array carrying about 50% of the unporting design load. The foils could be monofoils, split, or continuous hoop or ladder foils, or a combination of any of these; however, most of such arrangements are not practical, considering the associated drag, weight, and cost. As a result, this system is unsuitable for seaplane application compared to the single hydrofoil system. Further, undesirable lateral and longitudinal trim problems could develop during unporting in heavy seas.

Figs. 11-14. The Tietjens Hydrofoil system has a forward main hydrofoil that carries most (60% - 90%) of the unporting design load, with a smaller hydrofoil arrangement in the stern carrying the remainder. The lifting surfaces at the bow and stern could consist of monofoils, or split or continuous hoop or ladder hydrofoils; again these arrangements are not practical for aircraft application. One split Tietjens arrangement that was tested for seaplane operation, the Burney X.2 and X.3 of 1912 and 1913 had two cascaded foil struts at the bow and a similar cascaded set of foils at the stern (see Fig. 1).

Description and Classification of Hydrofoil Systems (Con't)

Figs. 15 and 16. The A. G. Bell Hydrofoil system, named after the inventor who employed hydrofoils on his HD-4 boat of 1919, is one of a number of more complex hydrofoil systems. The arrangement consisted of a main foil at the cg supporting over half of the load, with smaller stabilizing foil arrangements at the bow and stern. Bell's original split system had two ladder arrangements amidships, with smaller single ladder arrays at the bow and stern. Due to drag, weight, and cost, this and similar complex systems are considered impractical for aircraft use.

Figs. 17-20. The Canard Hydrofoil system positions a main hydrofoil arrangement located behind the cg carrying 60%-90% of the unporting design load, with a smaller hydrofoil located at the bow. The array at the bow and amidships could consist of monofoils, split or continuous hoop or ladder foils, or a combination of these. Again, this system results in too much drag, weight, and cost to be practical for modern aircraft application. However, one split Canard system, the Fabre, using cambered hydrofoil floats, achieved the first powered flight from water in 1910 (See Pg. 2). Using another design approach, Guidoni flew a twin-float mounted tandem split Canard system successfully in Italy during 1910 and for several years thereafter (See Pg. 2).

It is evident that many of these foil systems overlap. Since foil arrangements are frequently mentioned by the designer's name as well as by planform arrangement, it was considered advisable to present configurations under both classifications.

A comprehensive illustration of possible hydrofoil arrangements is presented in Figure 21, together with conventional nomenclature for each configuration.

5. SINGLE HYDROFOIL SYSTEM

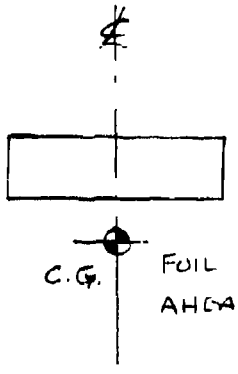

6. GRUNBERG SYSTEM

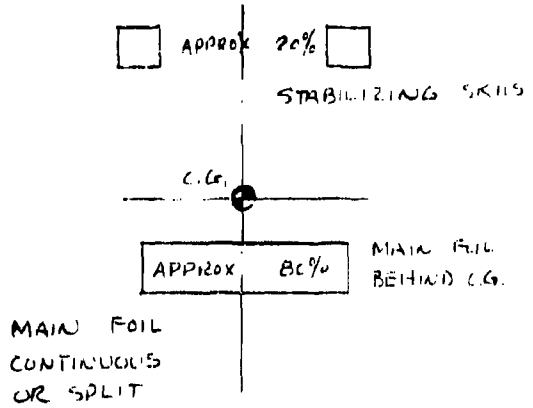

TANDEM HYDROFOIL SYSTEMS

7. CONVENTIONAL

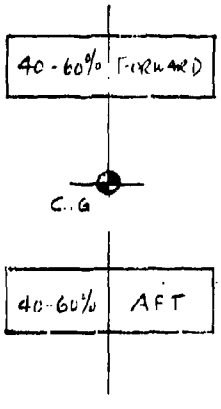

8. SPLIT

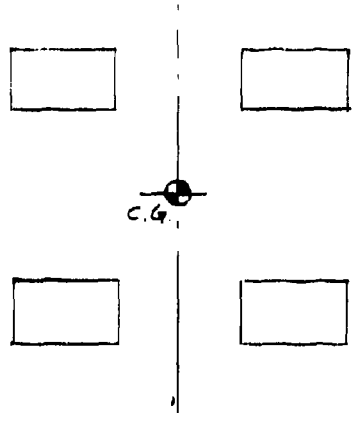

9. SPLIT

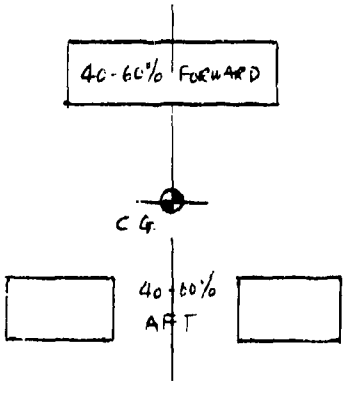

10. SPLIT

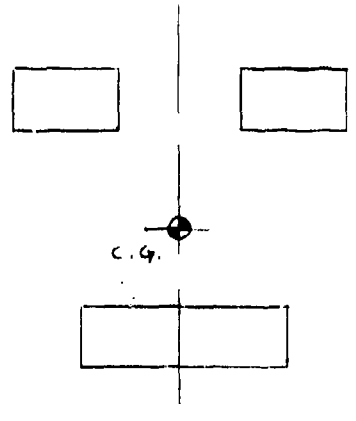

TIETJENS HYDROFOIL SYSTEMS

11. CONVENTIONAL

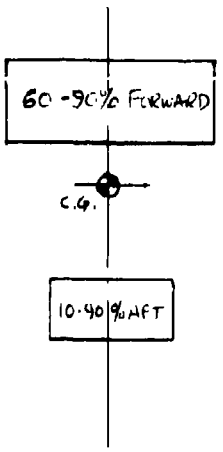

12. SPLIT (BURNEY)

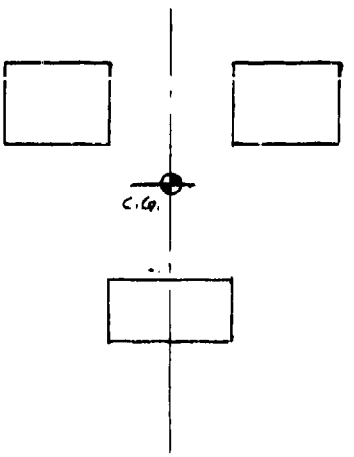

13. SPLIT

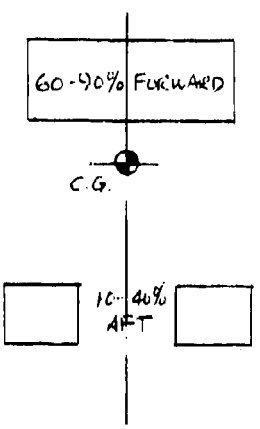

14. SPLIT

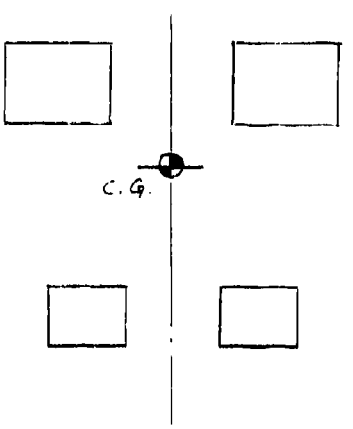

A.G. BELL HYDROFOIL SYSTEMS

15. CONTINUOUS MAIN FOIL

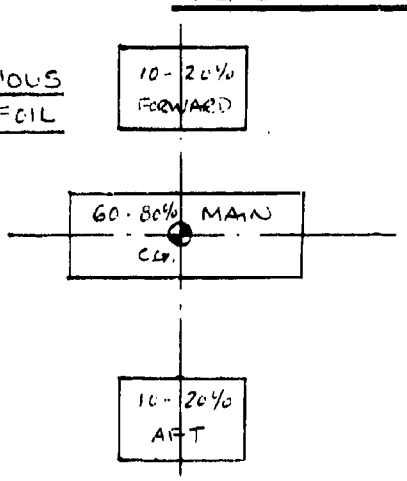

16. SPLIT (A.G. BELL)

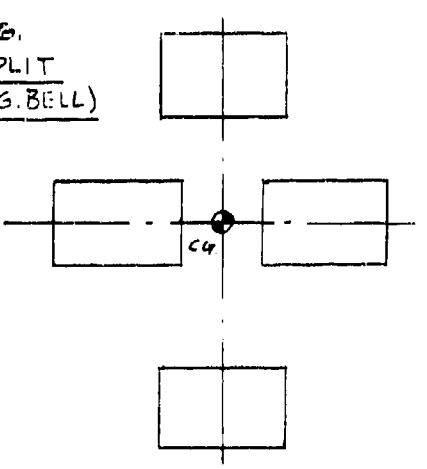

CANARD HYDROFOIL SYSTEMS

17. CONVENTIONAL

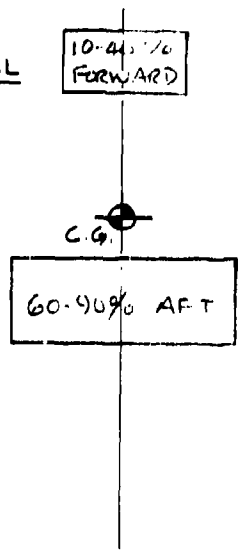

18. SPLIT

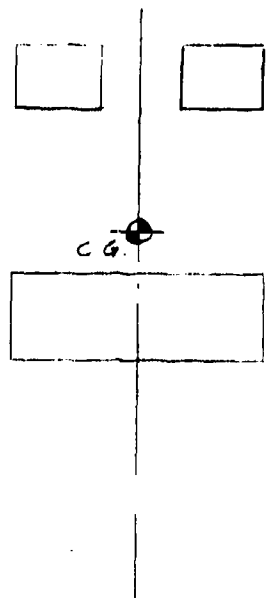

19. SPLIT (TABLE)

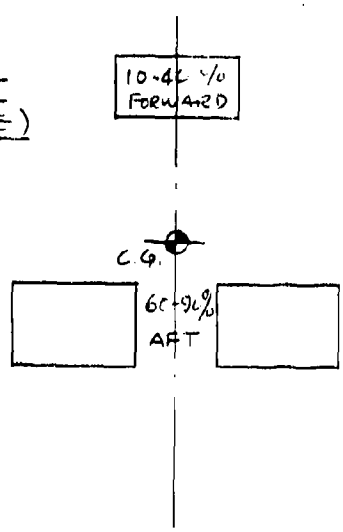

20. SPLIT

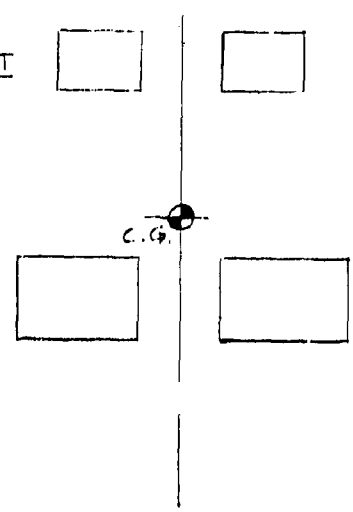

FIG. 21 FOIL ARRANGEMENTS

MONOFOILS

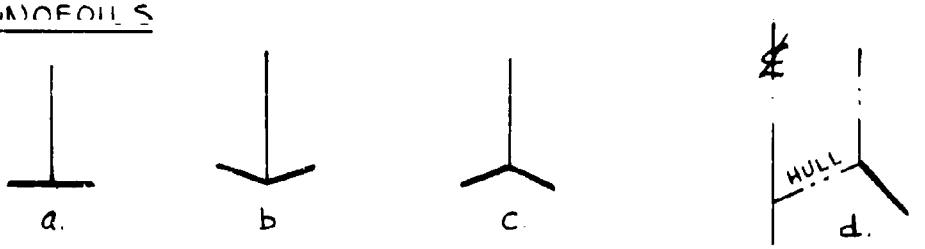

CASCADES

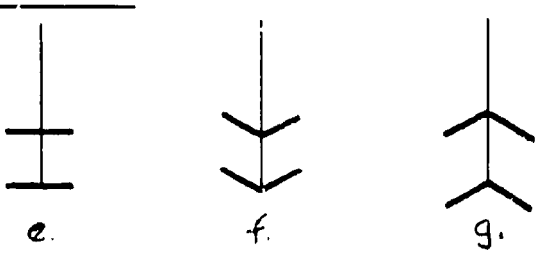

MAY BE MULTIPLE OR SINGLE STRUT (AS SHOWN)

HOOPS - HORIZONTAL FOIL MAY HAVE DIHEDRAL

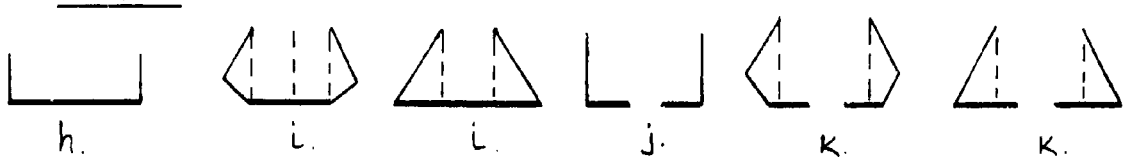

LADDERS - FOILS MAY BE OUTBOARD

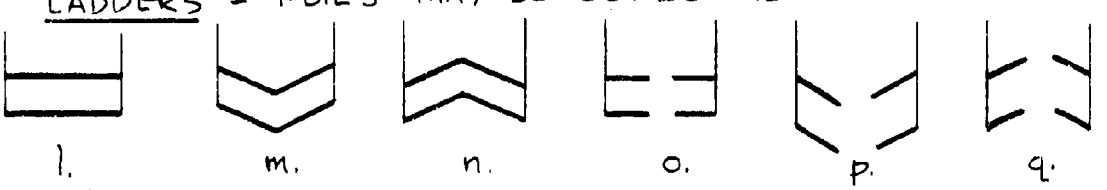

NOMENCLATURE

a. Flat monofoil
b. Positive dihedral monofoil
c. Negative dihedral monofoil
d. Cantilever monofoil
e. Cascaded flat
f. Cascaded positive dihedral
g. Cascaded negative dihedral
h. Continuous flat hoop foil
i. Continuous dihedral hoop foil
j. Split hoop foil
k. Split dihedral hoop foil
l. Continuous flat ladder foils
m. Continuous positive dihedral ladder foils
n. Continuous negative dihedral ladder foils
o. Split flat ladder foils
p. Split negative dihedral ladder foils
q. Split positive dihedral ladder foils

III. Hydrofoil Configuration Data

A. Hydrofoil Operating Principles

A hydrofoil is the marine version of the airfoil as used in water to create dynamic lift for the support of a vehicle; or as an element in a propeller type device. Subsonic airfoil section shapes perform well as hydrofoils when operating at low forward speeds. At equal Reynold's Numbers, the forces and moments created in air and water are essentially identical for these foils when the flow is completely attached. A foil operating in this condition is said to be "fully wetted" or "subcavitating".

At higher speeds, separation of the flow occurs causing changes in the forces and moments and resulting in a considerable loss of efficiency. Separation of the flow is termed "cavitation"; when the entire upper surface of a hydrofoil is completely free of attached flow, the foil is considered to be "supercavitating".

For operation at high speeds where cavitation cannot be avoided, hydrofoils specifically designed to operate in a supercavitating regime are superior to foils designed for subcavitating flow. Supercavitating hydrofoil sections are characterized by a sharp leading edge with entrance angles of about six degrees. The most common section shapes are: plane faced wedges with blunt trailing edges; the ogive, consisting of convex circular arc surfaces with sharp leading and trailing edges; circular arc concave cambered lower surface with contoured upper surface; and more complex shapes designed for increased efficiency, the best known being developed by M.P. Tulin and V.E. Johnson, Figure 22 (a) and (b).

B. Cavitation

A hydrofoil moving through the water in a subcavitating condition and at an angle of attack producing lift creates an increase in water pressure on the lower surface and a decrease on the upper surface in the same manner as an airfoil. The pressures are a function of the hydrofoil shape and: 1) velocity, 2) angle of attack, and 3) the operating depth. With increasing speed and angle of attack and decreasing depth, the pressure on the upper surface reduces until the pressure drops to the vapor pressure of the water as determined by its temperature. When this occurs, the water starts to boil or "cavitate" at the chord point where minimum pressure occurs; normally coinciding with that of maximum thickness. Further increases in speed or other factors causing additional decrease in the pressure, lead to enlargement of the cavity along the foil surface until it covers the entire surface. Still further pressure reductions cause extension of the cavity several chord lengths behind the trailing edge. The process of cavitation is

B. Cavitation (Continued)

similar to the stalling of a wing and is accompanied with a similar loss of lift. Since this occurs with increasing speeds, it has a significance similar to critical Mach effects in aerodynamics.

The aerodynamic pressure coefficient, $Cp = \frac{p-p_\infty}{q_\infty}$, which exists on the surface of an airfoil in subsonic potential flow is independent of velocity. The same coefficient in hydrodynamics is independent of velocity up to the point of cavitation inception, where flow separation occurs. In the zone of separation, the pressure coefficient has reached the lowest attainable value for cavitation and is defined as $Cp_{min} = \frac{p_v-p_\infty}{q_\infty}$, where p_v is the vapor pressure of the liquid, p_∞ is the static pressure of the liquid at at the operating depth, and q is the dynamic pressure. In hydrodynamics, the negative of the pressure coefficient is used and defined as the cavitation number: $\sigma_v = \frac{p_\infty - p_v}{q_\infty}$.

Figures 22 (a) and (b) show the shapes and equations for four supercavitating hydrofoils.

The effect of the cavitation number on the flow pattern about a hydrofoil is schematically illustrated in Figure 22 (c). The patterns shown are not static but are a typical average of a dynamic situation. At zero speed, $\sigma = \infty$; as speed increases, σ decreases, eventually reaching cavitation conditions. When cavitation occurs, the value of σ is known as the incipient cavitation number, being equal to the negative of Cp_{min}; $\sigma_i = -Cp_{min}$. As σ continues to decrease, the cavity size spreads over the foil surface and goes through a phase which creates foil erosion due to cavitation. When the cavity lengthens to a collapse point such that the pressure pulses created by the cavity collapse clear the trailing edge of the foil, the erosion phase ceases. In this condition, however, the eddies and the re-entrant jet which exist at the downstream end of the cavity may impinge upon the foil trailing edge and cause severe buffeting and foil vibration. Upon further reduction of σ, the cavity lengthens downstream such that the re-entrant jet is dissipated before it reaches the trailing edge of the foil, Figure 22 (c). In that condition, the flow is said to be supercavitating. Thus, cavities associated with supercavitating flows are relatively long, usually well over two chord lengths, and are filled with either liquid vapor or foreign gas, or a mixture of both. Flows in which the cavity is filled with atmospheric air have come to be called "ventilated" or "vented" flows. The term "Supercavitating" applies to all cases of sufficiently long cavities, regardless of whether they are filled with water vapor or air.

C. Ventilation

Naturally ventilated flows frequently occur during hydrofoil operation due to the proximity of the lifting and supporting devices to the free water surface. Natural ventilation is the passage of atmospheric air into the low pressure regions on the upper surface of the hydrofoil, taking a path along the low pressure side of a surface piercing strut, or along the blunt trailing edge of a surface piercing strut or foil. Natural ventilation occurs only after cavitation has been established and develops abruptly to its full state.

Where the foil is operating under partial cavitation conditions, ie. not supercavitating, ventilation can result in the immediate loss of 75 percent of lift, dropping the supported vehicle into the water. Natural ventilation occurs at high speeds, in rough water and during unporting and turning maneuvers. Once ventilation has been established, it tends to continue even though conditions become less favorable. Unfortunately, the onset of natural ventilation cannot be predicted easily from theory or model tests, and suitably simple scaling laws for ventilation onset are not available.

Forced or controlled ventilation is accomplished by artificially supplying air under pressure to that portion of the hydrofoil where the cavity is desired. In this case, established cavitation is not necessary. When the cavity size is changed by using forced air, the cavitation number will change and result in changes in the lift and drag.

For a foil that is operating under supercavitating conditions, ventilation will have little effect on the lift and drag. For ventilation, the cavitation number is computed by using the air pressure in the cavity, p_c, in place of the vapor pressure, p_v. The characteristics of optimum ventilated foils and supercavitating foils are identical if the cavitation number is the same.

D. Aircraft Applications

Since cavitation and ventilation cannot be avoided for aircraft applications due to operation at the water surface and at high speeds, hydrofoils for aircraft use should be designed to be supercavitating and readily ventilated. By using this approach, the lift and drag on the foil will remain smooth and continuous, and are essential conditions for successful hydrofoil aircraft operation.

E. Lift, Drag and Moment of Hydrofoils with Zero Sweep and Zero Dihedral at Infinite Depth

The lift, drag and moment characteristics of hydrofoils are dependent on the same factors of shape, attitude, velocity and fluid

E. Lift, Drag and Moment of Hydrofoils with Zero Sweep and Zero Dihedral at Infinite Depth (Continued)

density that affect airfoils, but in addition are dependent upon depth and cavitation number. With these additional parameters, the amount of data required to catalog hydrofoil characteristics becomes exceedingly large. In order to avoid the use of a great number of charts, the approach taken in this study is to show the characteristics of typical hydrofoils favored for aircraft use, as well as the effects of these various factors on performance. Furthermore, the volume of experimental data in the hydrofoil field is far from adequate, thereby inhibiting any comprehensive compilation of systematic data.

Figures 23 and 24 show the variation of lift, drag, and moment coefficients and the L/D ratio with angle of attack for subcavitating and supercavitating flows. The data were taken from several sources and were combined in the figures to compare the characteristics of the different types of foils.

Figure 23 shows the subcavitating characteristics of a conventional airfoil (NACA 66_1-012), a subcavitating hydrofoil (DTMB Series HF-1), and six degree wedge (optimum for supercavitation) with a blunt trailing edge. The lift curve slopes of the wedge appear to be higher than the other two by a small amount, but the data did not extend sufficiently over the range of aspect ratios and maximum lifts to permit a through comparison. The wedge apparently produces lift with characteristics similar to foils designed for subcavitating flow. The drag of the NACA 66_1-012 foil is considerably less than the wedge at those low angles of attack where the L/D of the NACA foil approaches a maximum. At higher angles of attack, the drag of the NACA foil exceeds that of the wedge, while the L/D diminishes rapidly, and if extended, might drop below the values for the wedge. Moment data is provided and is of primary significance in the structural design of the foil and strut.

Figure 24 shows the supercavitating characteristics of the six degree wedge, the NACA 66_1-012 airfoil, and the Johnson 5 term supercavitating hydrofoil. In supercavitating flow, the Johnson foil shows slightly higher lift than the wedge and the NACA foil lift degrades almost immediately, developing at most only 25 percent of the lift of the other two foils. The inferiority of a foil designed for fully wetted operation under supercavitating conditions is clearly shown here. It is interesting to note that maximum L/D values for supercavitating foils are reached in the first four degrees of angle of attack from zero lift, too near zero lift for sustained aircraft operation. Since normal trim angles would be in the range of about four to twelve degrees above the zero lift angle, normal supercavitating foil operation would center around that portion of the curve producing 50 to 75 percent of maximum L/D. These lower L/D and consequently higher drag values would be occuring at

E. Lift, Drag and Moment of Hydrofoils with Zero Sweep and Zero Dihedral at Infinite Depth (Continued)

unporting which is the critical phase of the take-of from a performance and controllability standpoint. The high L/D associated with the low angles of attack would occur at the high speed end where it is not as critical.

F. Calculation of Cavitation Inception

Figure 25 (a) is a nomograph for the calculation of the speed at which cavitation begins. Data is presented for a two dimensional foil operating in sea water at a temperature of 55°F, and requires knowledge of the inception cavitation number for that foil. The values obtained are low in comparison to the three dimensional case. However, no known work has been published covering the three dimensional case or the effect of temperature variations on lift and drag. Vapor pressure variation with water temperature is presented in Figure 25 (b).

G. Effects of Cavitation Number on Foil Performance

Figures 26, 27, and 28 show the variations of C_L, C_D and L/D with cavitation number for the NACA 66_1-012 airfoil. The horizontal portions of the curves are regions where cavitation does not exist. When cavitation begins there is a rapid decrease in L/D ratio, even though Figure 26 shows an increase in lift with small amounts of cavitation at angles of attack greater than three degrees. At cavitation, the increase in drag is proportionately greater than the increase in lift. Further reduction in the cavitation number causes the drag coefficient to peak and then decrease. The lift coefficient, however, decreases rapidly with cavitation number and the reduction in drag coefficient merely causes a reduction in the slope of the L/D ratio curves.

Figures 29 through 40 show the variations of C_L, C_D, C_M and L/D with cavitation number for a six degree wedge hydrofoil with blunt trailing edge at aspect ratios of one, two and four. The lift, drag and moment plots show lines of constant cavity length, given in chord lengths of x/c. The lift plots show that the lift starts to decrease when the cavity size equals one chord length. The drag changes approximately in proportion to the lift with the result that the L/D ratios tend to remain constant or increase slightly. Aspect ratio does not affect lift and drag appreciably, although a slight improvement of L/D ratio does occur with increasing aspect ratio.

H. Effect of Depth of Submergence on Foil Performance

The effect of depth of submergence on the lift curve slope of subcavitating hydrofoils of various aspect ratios is shown in Figure 41. The lift curve slope decreases as the foil approaches the surface, with the most marked reduction occurring within one chord length of the water surface. The effect on foils of aspect ratios less than ten is essentially the same.

For supercavitating foils, the effect of depth on the effective angle of attack due to camber also decreases rapidly within one chord length of the water surface, as shown in Figure 42. The variation of lift and drag coefficients due to submergence within one chord length of the surface are given in Figure 43. It is shown that for the Tulin-Burkart (cambered) foil, the lift and drag do not vary. However, the flat plate lift does increase slightly as the foil approaches the surface, with the drag remaining essentially constant. Figures 44 (a) and (b) show that the increase in lift coefficient near the surface is slightly higher for higher aspect ratios.

I. Effect of Leading Edge Sweep and Taper on Foil Performance

The most significant effects of leading edge sweep on a hydrofoil are a delay in cavitation inception and decreased lift, L/D ratios, and lift curve slopes. Sweep is highly advantageous for subcavitating systems attempting to achieve maximum speeds. Conversely, sweep has a detrimental effect on supercavitating designs due to cavitation delay and loss of lift. Taper ratio has negligible effect on cavitation speed and force characteristics.

Figure 45 is based on analysis and shows the effects of sweep and aspect ratio on the lift curve slope of subcavitating hydrofoils. The lift curve slope reduces as aspect ratio becomes smaller and sweep increases.

Figure 46 presents the physical characteristics of four hydrofoils of various sweep angles and taper ratios but of equal area. All have the NACA 65A006 airfoil section parallel to the free stream velocity and were constructed of heat treated chrome-vanadium steel having a modulus of elasticity of approximately 30 million. The hydrodynamic characteristics of these foils are given in Figures 47 through 54.

Figure 47 shows the angular deflection of the swept-back hydrofoils and the resulting reduction in maximum lift loading capability of the 60 degree sweep foil due to twist.

Figure 48 (a) through 51 (c) present the lift, drag and L/D ratio data for the four foils.

Figure 52 shows the increase of cavitation inception speed with sweep at various coefficients of lift.

I. Effect of Leading Edge Sweep and Taper on Foil Performance (Continued)

Figure 53 shows the decrease in lift drag ratio with sweep at various coefficients of lift.

Figure 54 shows that taper ratio has a slight effect upon L/D ratios.

J. Effect of Dihedral on Foil Performance

Dihedral is an important design parameter for aircraft application, since the hydrofoil in this case should invariably be of the surface piercing type.

The surface piercing hydrofoil has a natural venting path and, therefore, tends to vent readily. Prior to full ventilation, forces produced by the six degree wedge are shown in Figure 55 (a) by the lines labeled fully attached (base vented). As speed or angle of attack are increased, flow separation occurs on the upper surface and full ventilation is achieved. The lift forces produced are reduced considerably and are given by the line labeled fully ventilated. The drag forces are given in Figure 55 (b).

A factor which bears mention is the change of aspect ratio with immersion of a surface piercing foil. Since aspect ratio affects lift and drag, the relationship of immersion to aspect ratio should be given consideration when designing a surface piercing foil system.

K. Effect of Hydrofoil Leading Edge Angle in Supercavitating Flow

The value of L/D increases as the included angle of the hydrofoil leading edge decreases, thereby requiring the entrance angle to be the minimum permitted by structural considerations. A small included angle will allow operation at lower angles of attack and consequently higher L/D's for any given bottom shape. Near the leading edge, the pressures due to angle of attack are predominant for high angles of attack and will establish the critical structural design conditions. Design pressures over the first four to five percent of the chord are thus independent of camber and bottom shape. A reduction in these pressures could be achieved by sacrificing leading edge sharpness, but this entails a loss in foil L/D and cavity inception characteristics. The leading edge profile should be maintained as sharp as structurally feasible.

Figure 56 shows chordwise bending stresses on the sharp leading edge of a foil operating at 12 degrees angle of attack which

K. Effect of Hydrofoil Leading Edge Angle in Supercavitating Flow (Continued)

subjects it to a loading of approximately "q" ($\frac{1}{2}\rho v^2$) psf. It is clear that a high strength leading edge material must be considered if reasonably small wedge angles and therefore maximum L/D's are to be realized. The loading of "q" psf and corresponding angle of attack of about 12 degrees are reasonable values for structural design. This loading at an ultimate stress of 200,000 psi requires a leading edge wedge angle of 3.1 degrees for a maximum vehicle speed of 100 knots, and 6.2 degrees for a maximum vehicle speed of 200 knots.

L. Effect of Trailing Edge Flaps on Hydrofoil Performance

The L/D values of various hydrofoils designed for supercavitating flow are all very similar when plotted versus angle of attack. However, when plotted versus C_L, the peak values of L/D occur at different values of C_L depending upon the bottom shape of the foil. For wedges with flat bottoms, the maximum L/D occurs at a very low C_L. As camber increases and as the bottom shape becomes more optimum, for example the Johnson 5 to 1 foil, the maximum L/D occurs at progressively higher values of C_L. The advantage of the cambered design is that high lift is obtained at maximum L/D values. Such profiles would be ideal for optimizing conditions at the critical point of hump speed and unporting, where drag is at a peak. Their disadvantage, however, lies in the fact that cambered hydrofoils must be operated at angles of attack of about four degrees above zero lift to obtain optimum L/D values. This narrow range is impractical for aircraft application since comparitively large trim angles will be realized during heave, pitch and unporting. As a result, the advantages of a sophisticated foil such as the Johnson are diminished, and the wedge shape becomes more attractive. The penalty paid for using the wedge is a smaller value of C_L compared to the Johnson type at equal values of L/D.

A wedge can be made to perform similarly to a cambered foil by the use of a trailing edge flap. In this way, the advantages of both foils can be realized. For a supercavitating foil, experiments have indicated that trailing edge flaps are an effective way of maintaining lift at speeds below cruising. At a fixed foil incidence angle, the flap permits lift to be maintained at lower speeds and with less drag than would be possible by increasing the foil incidence without the aid of the flap. Furthermore, a combination of incidence control and flap deflection provides even higher lift forces than with flap alone. On an aircraft, incidence control is obtained simply through changing the pitch of the aircraft.

L. Effect of Trailing Edge Flaps on Hydrofoil Performance (continued)

Figure 57 (a) and (b) provide lift and drag coefficient data for a naturally ventilated six degree wedge hydrofoil with a 25 percent chord trailing edge flap. As can be seen, both lift and drag respond proportionally to flap deflection.

By progressing from the lower left to the upper right of the C_L/C_D versus C_L plot, figure 58 (c) shows that the L/D ratio can be improved with flap deflection.

Figure 59 provides data for establishing the minimum angles of attack required to maintain a fully developed cavity in smooth and rough water. This should assist in determining the lower limit of angle of attack.

While of interest for cruise range water vehicles and large seaplanes, the added structural and mechanical complexity of flapped hydrofoils must be weighed against their operational advantages.

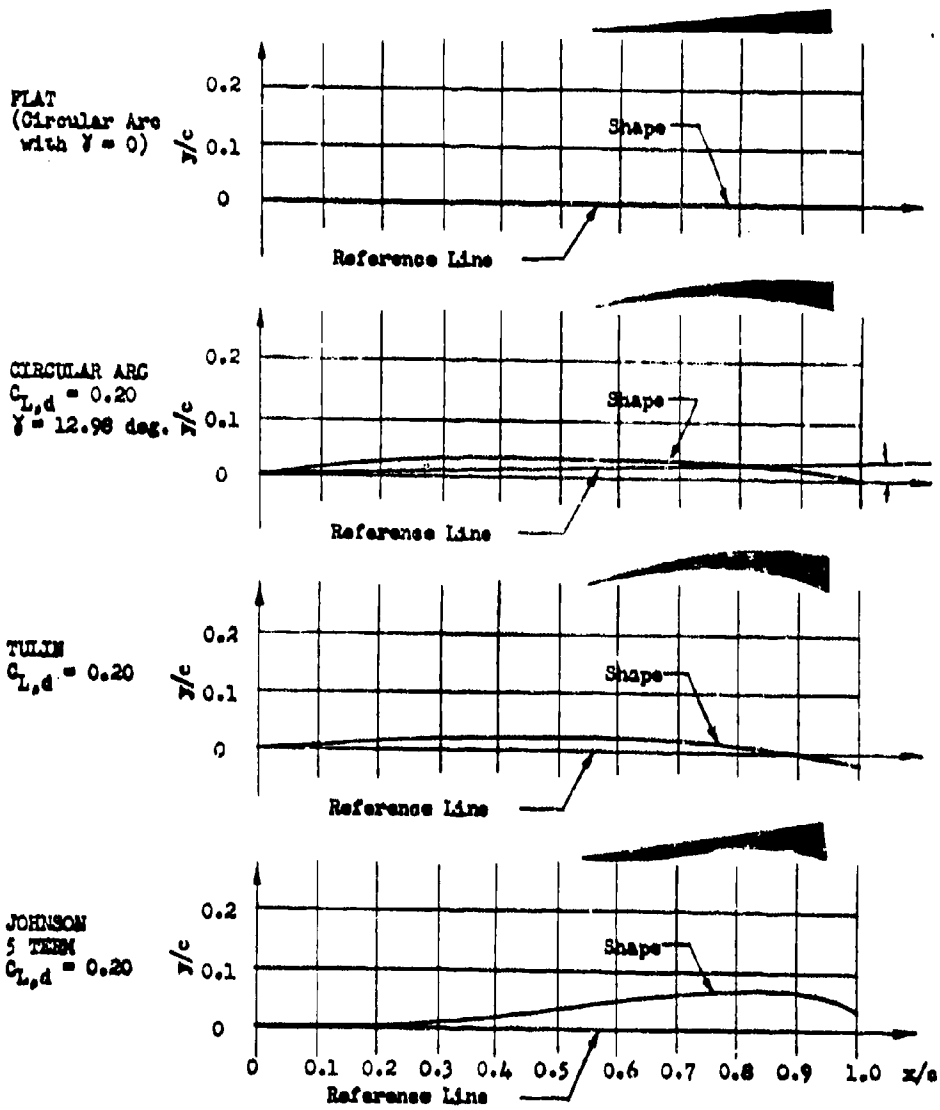

FIG. 22 (a)

SUPERCAVITATING HYDROFOIL BOTTOM SHAPES

Free stream direction coincides with Reference Axes for α = 0.

Ref: Grumman Rept. PB 161759 Fig. II.1

Fig. 22 (b)

BOTTOM SHAPE, LIFT AND DRAG EXPRESSIONS FOR
TWO DIMENSIONAL SUPERCAVITATING HYDROFOILS
AT INFINITE DEPTH AND WITH ZERO FRICTION DRAG

BOTTOM SHAPE	EQUATIONS
FLAT	$y = 0$
CIRCULAR ARC	$\left[x - (c/2)\right]^2 + \left[y + R\cos(\gamma/2)\right]^2 = R^2$; $\gamma = \left[(32)/(9\pi)\right] c_{L,d}$
TULIN	$(y/c) = \left[(4c_{L,d})/(5\pi)\right]\left[(x/c) + (8/3)(x/c)^{3/2} - \tfrac{1}{2}(x/c)^2\right]$
JOHNSON 5 TERM	$(y/c) = \left[(6c_{L,d})/(1575\pi)\right]\left[210\,(x/c) - 2240\,(x/c)^{3/2} + 12600\,(x/c)^2 + \right.$ $\left. - 30912\,(x/c)^{5/2} + 35840\,(x/c)^3 - 15360\,(x/c)^{7/2}\right]$

BOTTOM SHAPE	C_L	C_D	A_1	L/D $\alpha = 0$
FLAT	$(\pi/2)\alpha$	$(\pi/2)(\alpha)^2$	0	$\pi/(2c_L)$
CIRCULAR ARC	$(\pi/2)\left[\alpha + (16/16)A_1\right]$	$(\pi/2)\left[\alpha + (A_1/2)\right]^2$	$(\gamma/2) = \left[16/(9\pi)\right] c_{L,d}$	$(16/16)\left[\pi/(2c_{L,d})\right]$
TULIN	$(\pi/2)\left[\alpha + (5/4)A_1\right]$	$(\pi/2)\left[\alpha + (A_1/2)\right]^2$	$\left[8/(5\pi)\right] c_{L,d}$	$(25/8)\left[\pi/(2c_{L,d})\right]$
JOHNSON 5 TERM	$(\pi/2)\left[\alpha + (5/3)A_1\right]$	$(\pi/2)\left[\alpha + (A_1/2)\right]^2$	$\left[6/(5\pi)\right] c_{L,d}$	$(100/9)\left[\pi/(2c_{L,d})\right]$

Ref: Grumman Rept. PB 161759 Table II.1

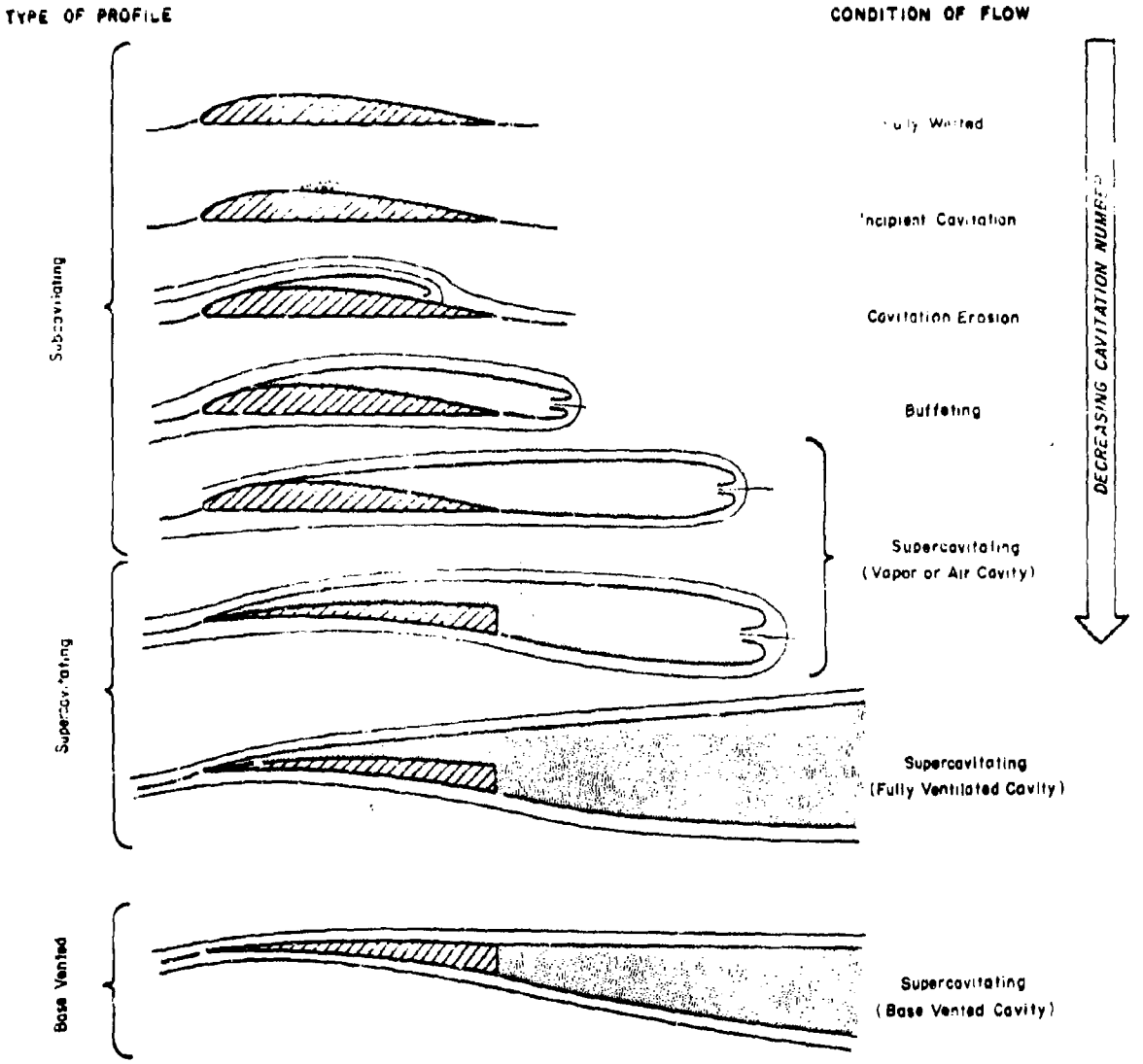

Fig. 22 (c)

- The Effect of Cavitation and Ventilation on the Hydrofoil Flow Pattern.

Ref: Hydronautics Tech. Rept. 001-7 Fig. 1

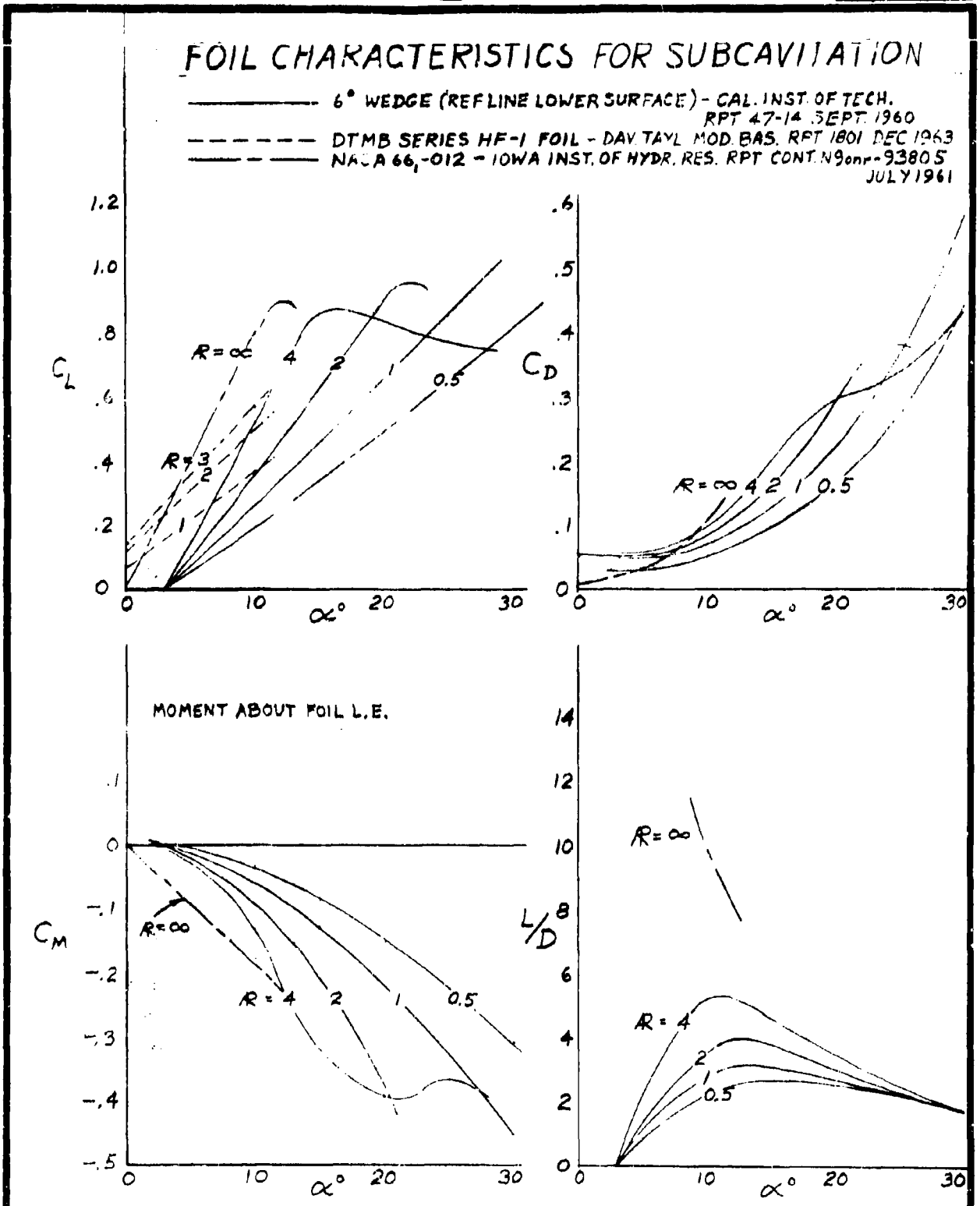
FOIL CHARACTERISTICS FOR SUBCAVITATION
6° WEDGE (REF LINE LOWER SURFACE) - CAL. INST. OF TECH. RPT 47-14 SEPT 1960
DTMB SERIES HF-1 FOIL - DAV. TAYL. MOD. BAS. RPT 1801 DEC 1963
NACA 66,-012 - IOWA INST. OF HYDR. RES. RPT CONT. N9onr-93805 JULY 1961
C_L
C_D
C_M
L/D
AR = ∞
AR = 4
AR = 3
AR = 2
AR = 1
AR = 0.5
MOMENT ABOUT FOIL L.E.
α°

Fig. 23

FOIL CHARACTERISTICS FOR SUPERCAVITATION

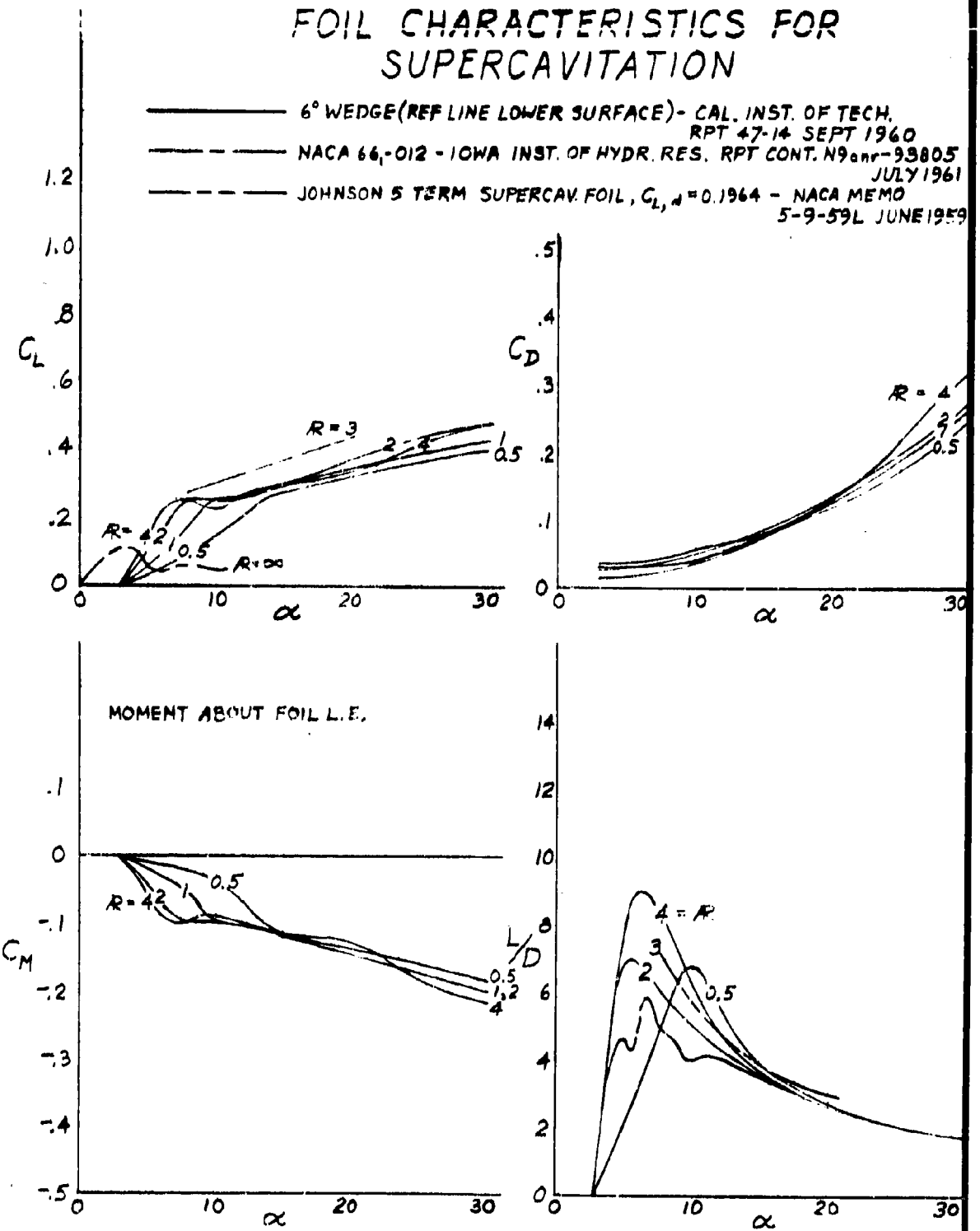

Fig. 24

MODEL _____
CONT _____

THURSTON AIRCRAFT CORPORATION
SANFORD, MAINE

REPORT NO. 6912
DATE _____

Nomograph Showing the Relationship of Depth of Submergence, Cavitation Index, and Speed of Incipient Cavitation for any Body

TWO DIMENSIONAL

Ref: Davidson Lab (SIT) Tech. Mem. 133 Fig. 8

Note: This chart applies to sea water at 55°F

To estimate the speed of incipient cavitation for a body, lay a straightedge on the given h and σ ; the resultant cavitation speed is the intercept on the U_i scale

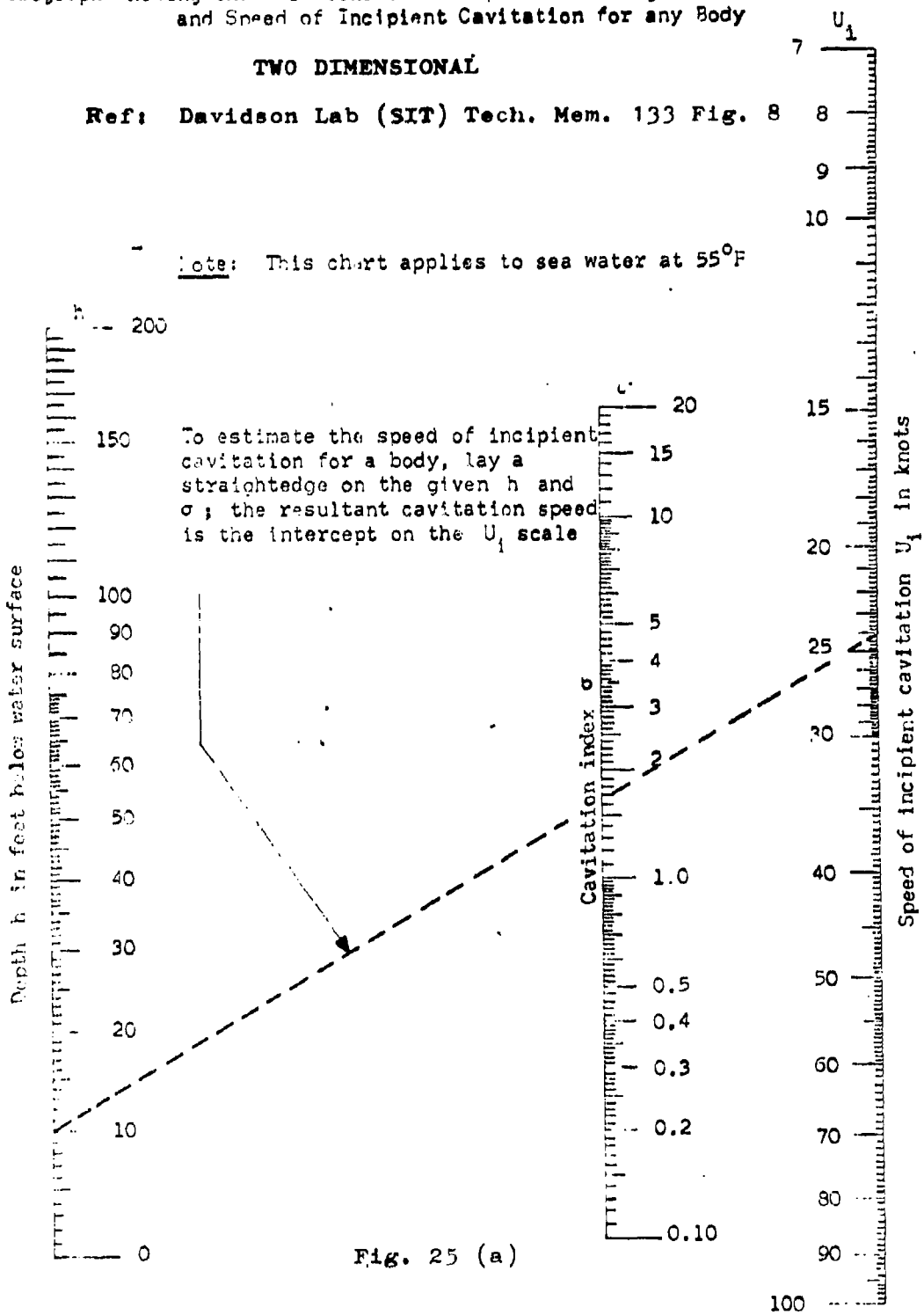

Fig. 25 (a)

VARIATION OF VAPOR PRESSURE WITH WATER TEMPERATURE FOR SEA WATER

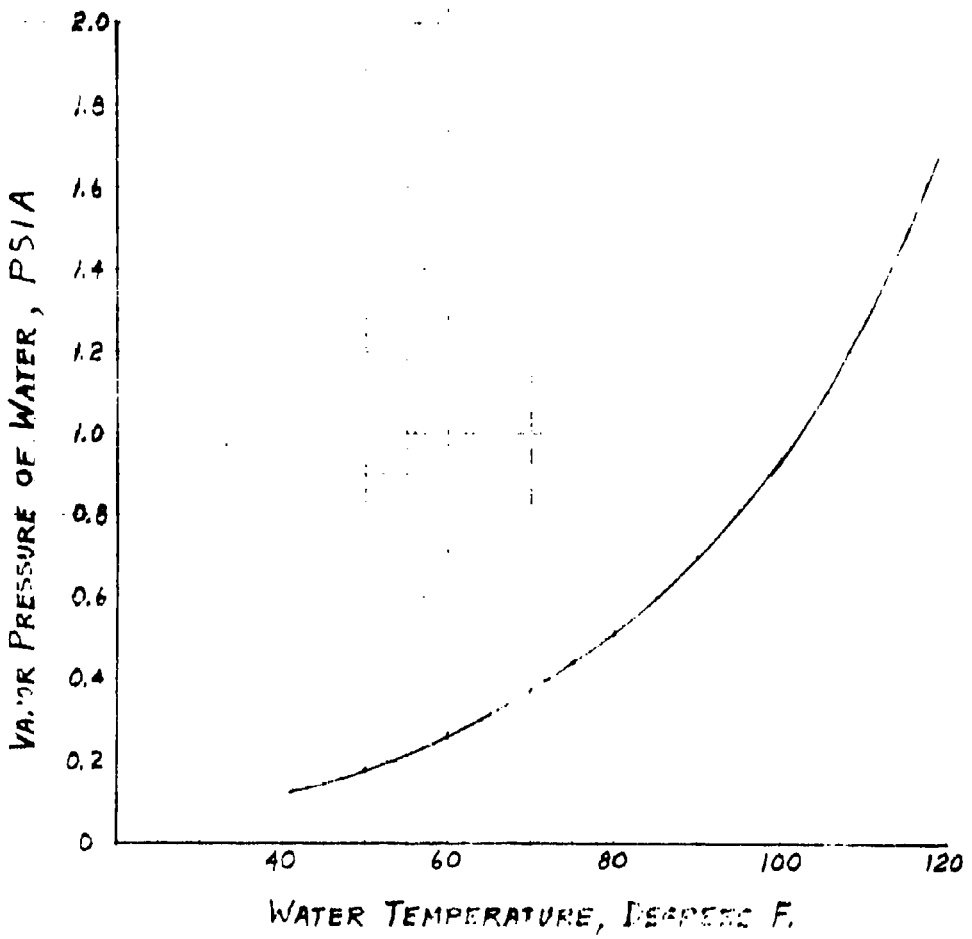

Fig. 25 (b)

Ref: Grumman Rept. PB 161759 Fig. I.8

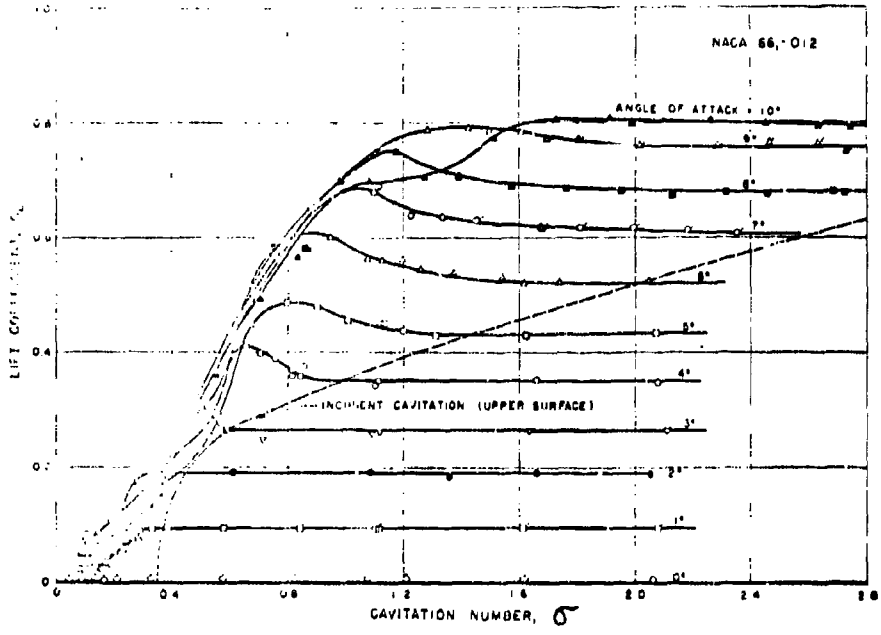

Fig. 26 - Lift coefficient as a function of cavitation number at constant angle of attack for the NACA 66_1-012 hydrofoil. Each angle of attack represents one test run.

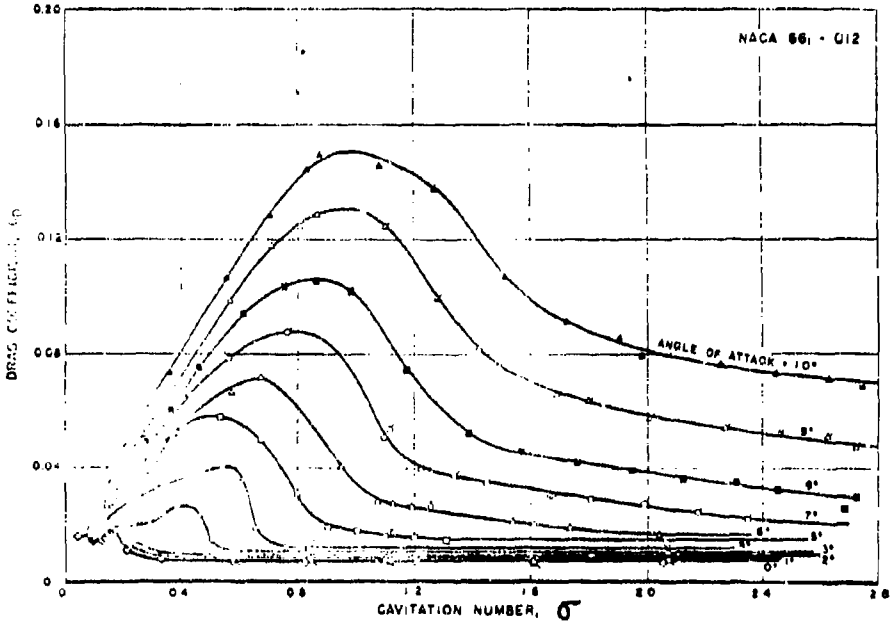

Fig. 27- Drag coefficient as a function of cavitation number at constant angle of attack for the NACA 66_1-012 hydrofoil. Each angle of attack represents one test run.

Ref. Cal Tech Rept. 47-7 Figs. 7 and 8

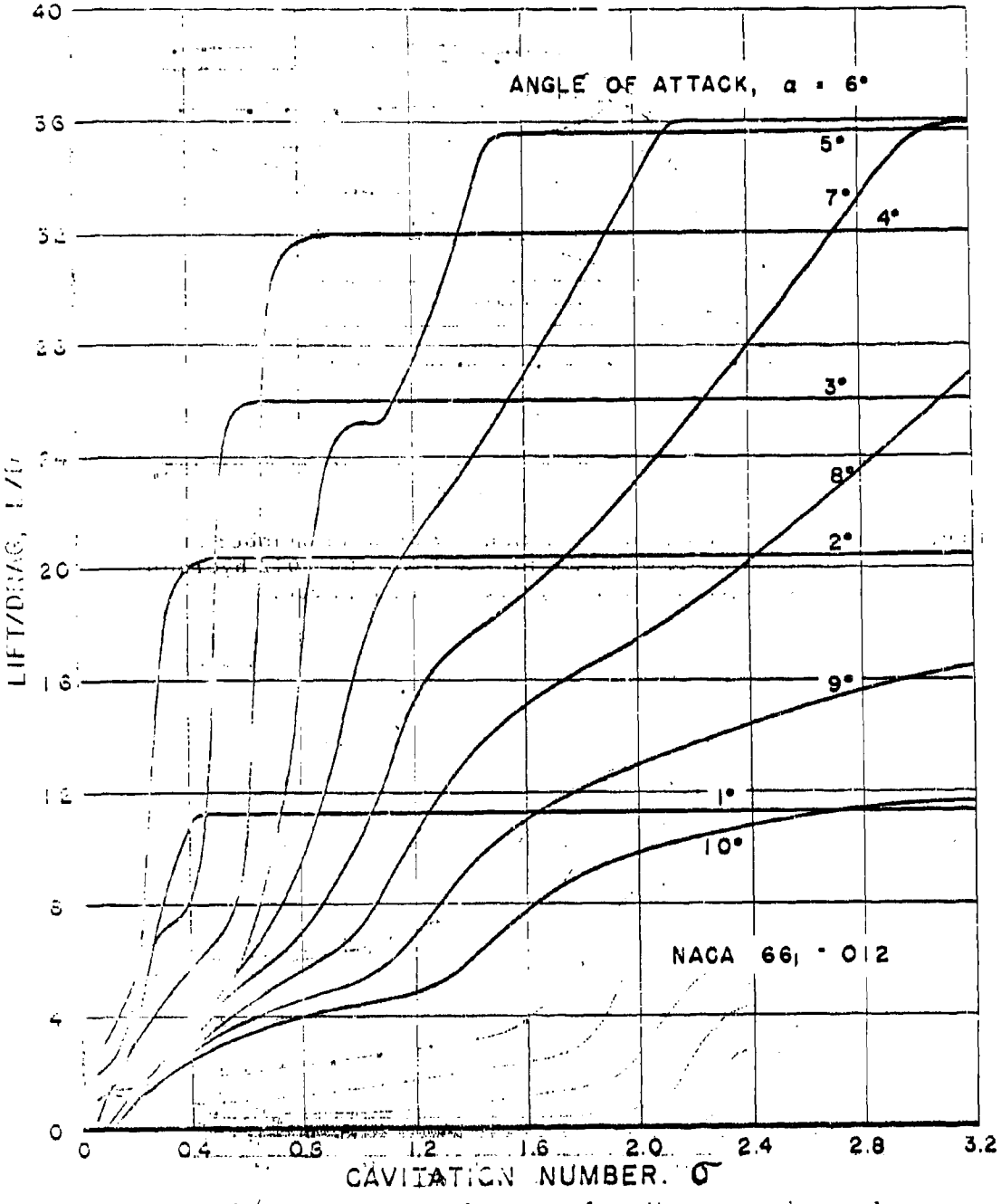

Fig. 28 - Lift/drag ratio as a function cavitation number and angle of attack for the NACA 66_1-012 hydrofoil.

Ref: Cal Tech Rept. 47-7 Fig. 11

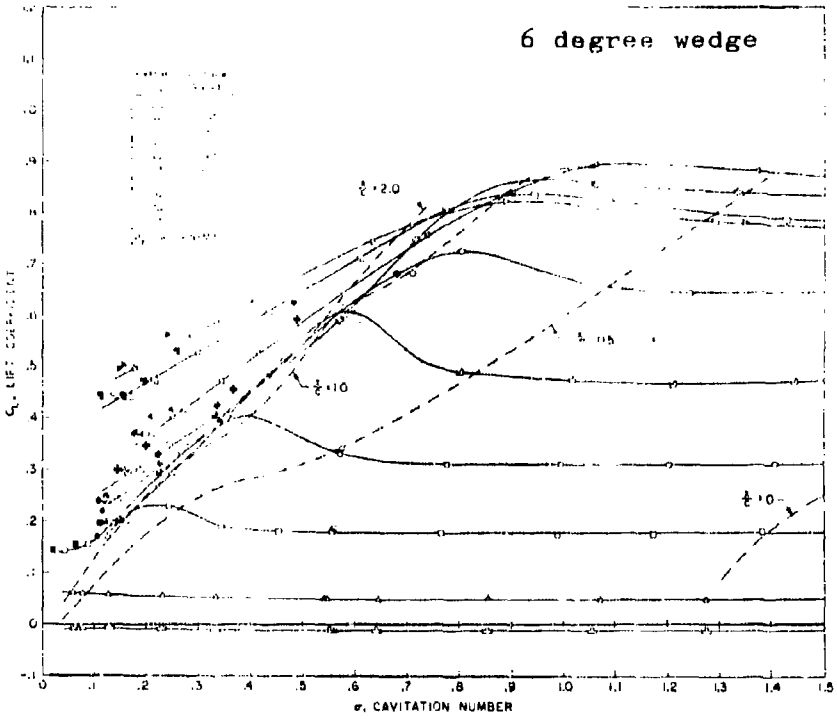

Fig. 29 Lift Coefficient as a Function of Cavitation Number at Constant Angle of Attack, AR = 4.0.

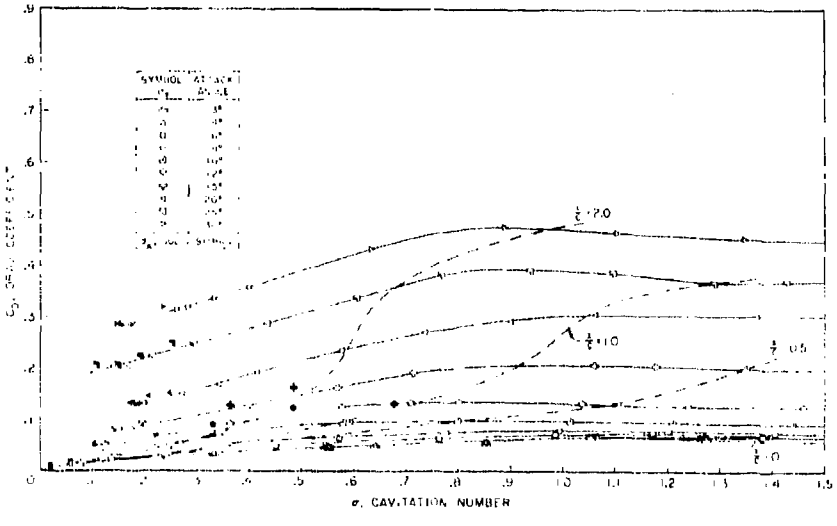

Fig. 30 Drag Coefficient as a Function of Cavitation Number at Constant Angle of Attack, AR = 4.0.

Ref: Cal Tech Rept 47-14 Fig. 8 and 9

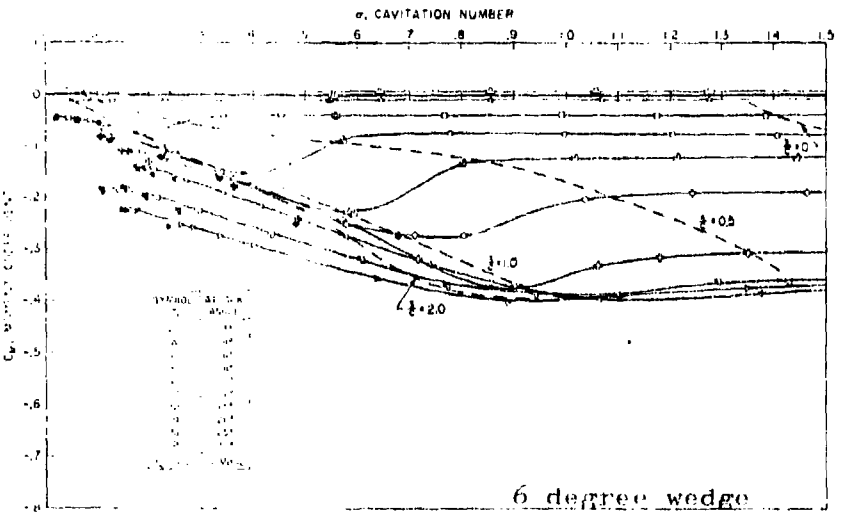

Fig. 31 Moment Coefficient as a Function of Cavitation Number at Constant Angle of Attack, AR = 4.0.

Moment about foil leading edge.

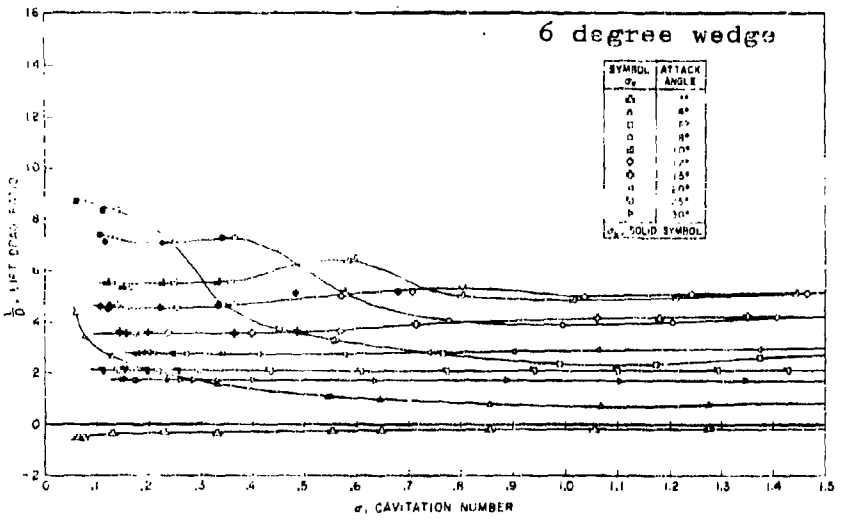

Fig. 32 Lift-Drag Ratio as a Function of Cavitation Number at Constant Angle of Attack, AR = 4.0.

Ref: Cal Tech Rept 47-14 Fig. 10 and 11

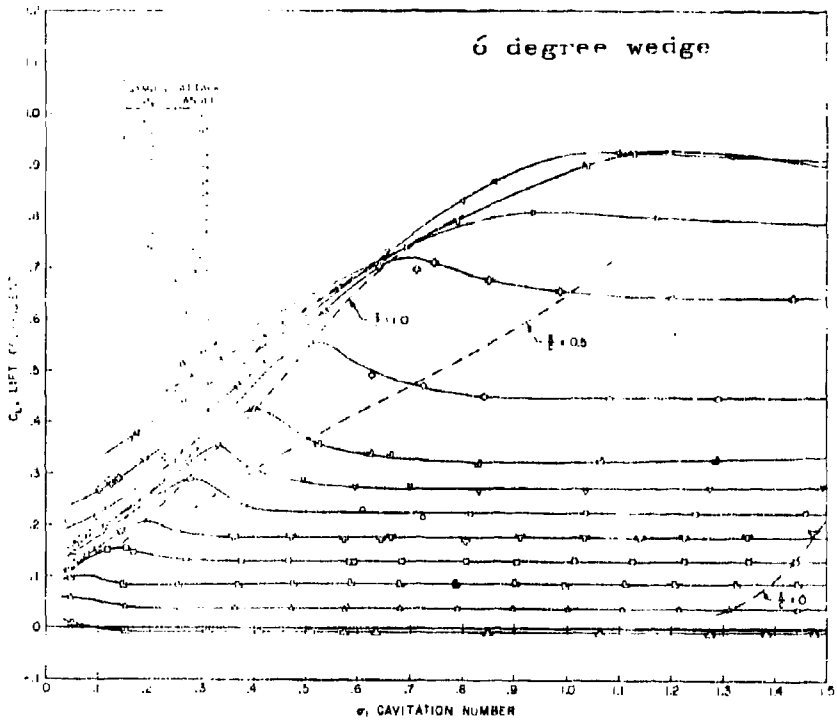

Fig. 33 Lift Coefficient as a Function of Cavitation Number at Constant Angle of Attack, AR = 2.0.

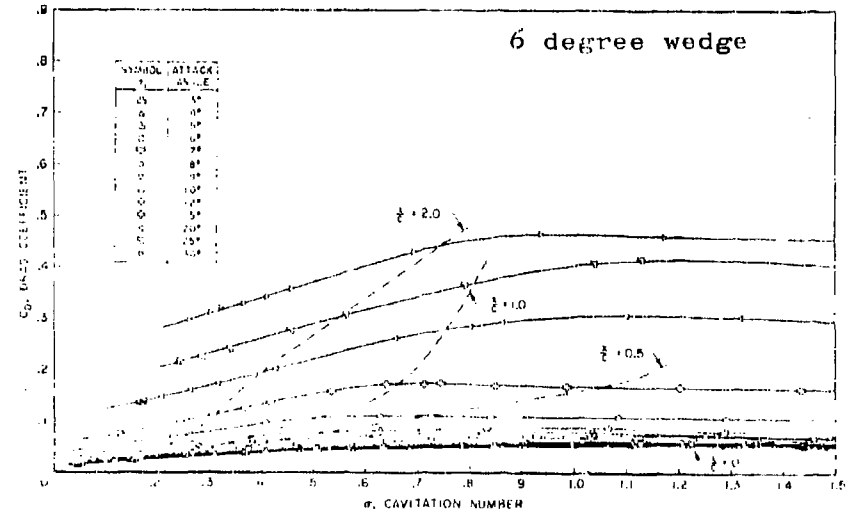

Fig. 34 Drag Coefficient as a Function of Cavitation Number at Constant Angle of Attack, AR = 2.0.

Ref: Cal Tech Rept 47-14 Fig. 12 and 13

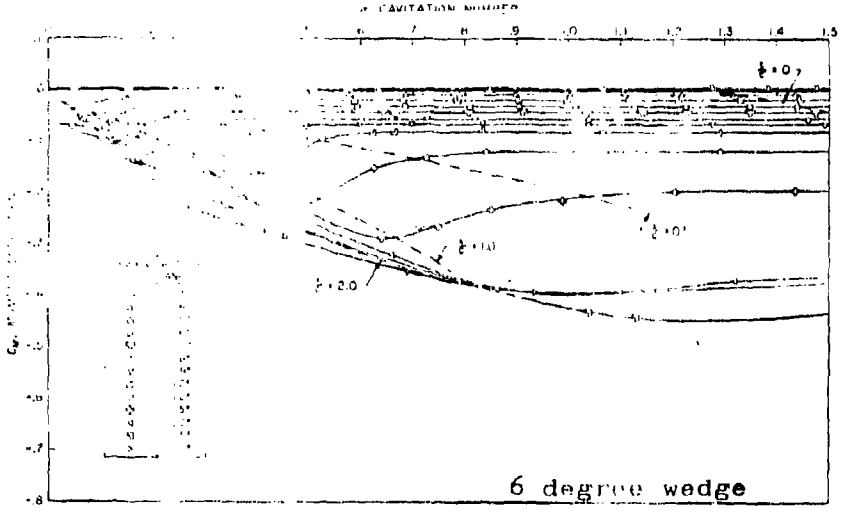

Fig. 35 Moment Coefficient as a Function of Cavitation Number at Constant Angle of Attack, AR = 2.0.
Moment about foil leading edge.

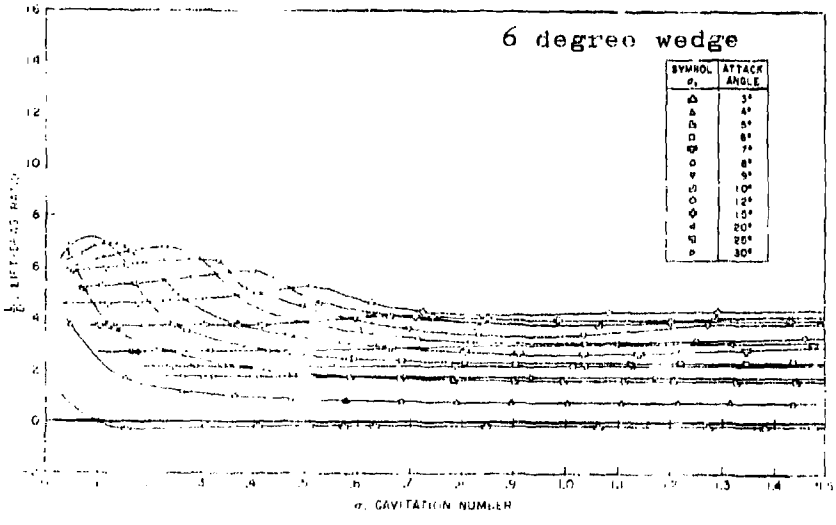

Fig. 36 Lift-Drag Ratio as a Function of Cavitation Number at Constant Angle of Attack, AR = 2.0

Ref: Cal Tech Rept 47-14 Fig. 14 and 15

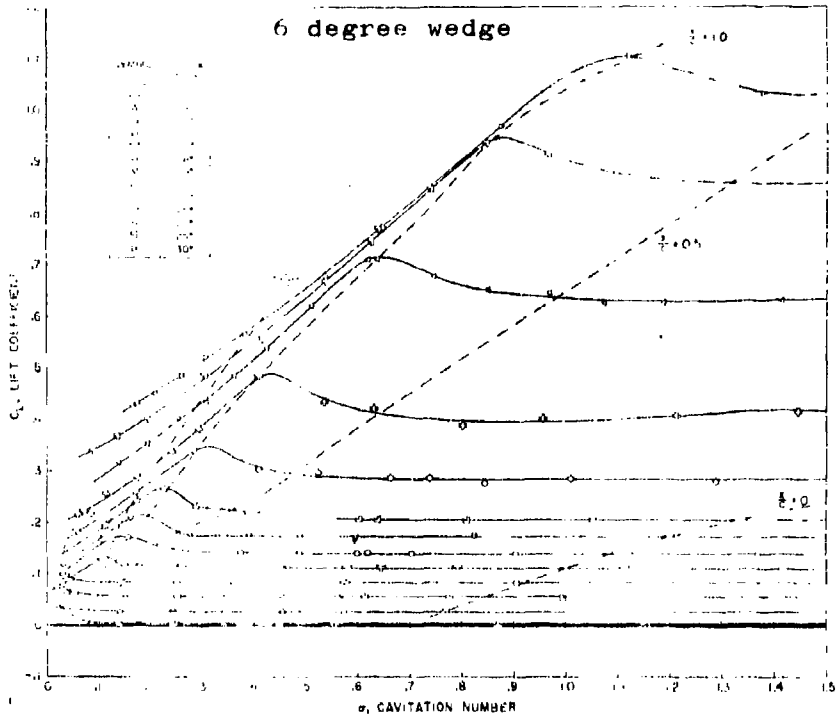

Fig. 37 Lift Coefficient as a Function of Cavitation Number at Constant Angle of Attack, AR = 1.0.

Ref: Cal Tech Rept 47-14 Fig. 16 and 17

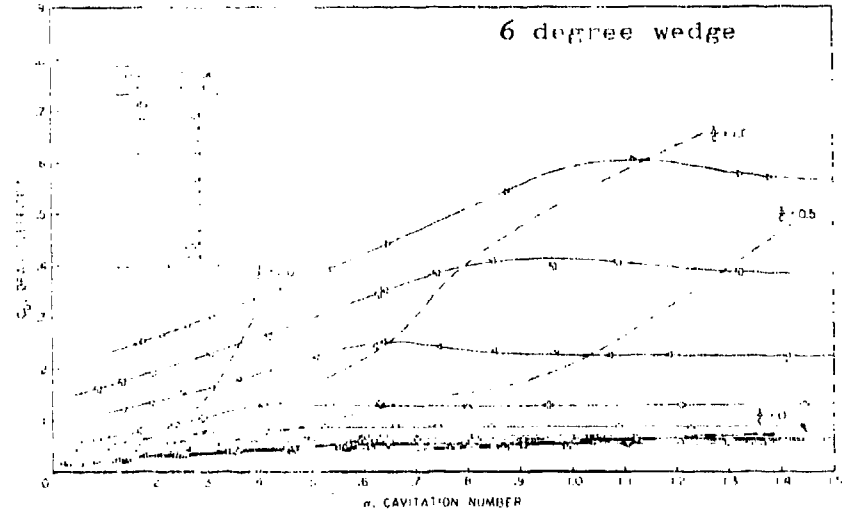

Fig. 38 Drag Coefficient as a Function of Cavitation Number at Constant Angle of Attack, AR = 1.0.

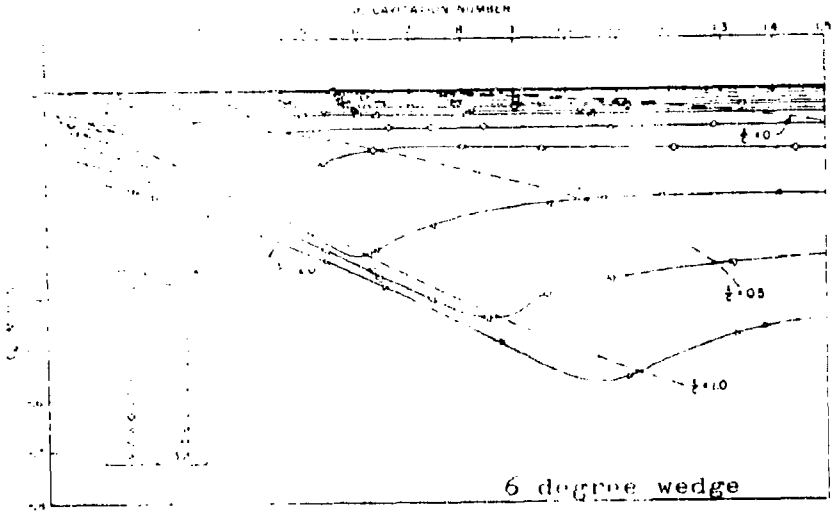

Fig. 39 Moment Coefficient as a Function of Cavitation Number at Constant Angle of Attack, AR = 1.0.

Moment about foil leading edge.

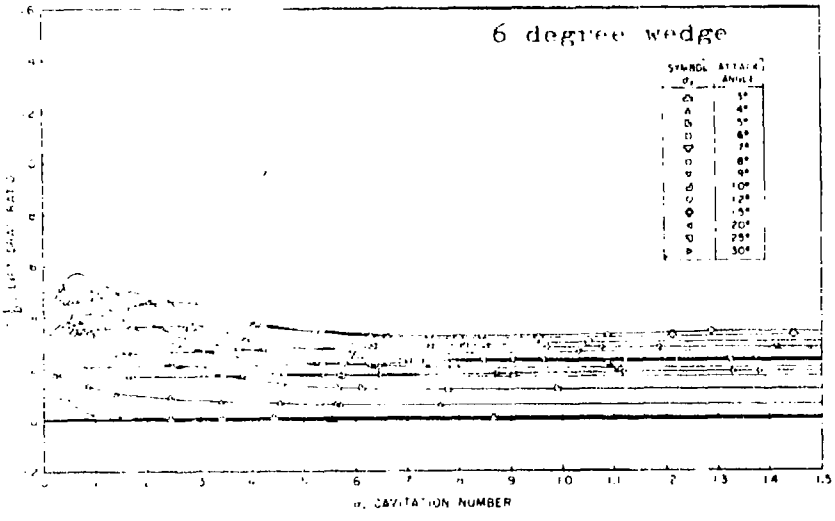

Fig. 40 Lift-Drag Ratio as a Function of Cavitation Number at Constant Angle of Attack, AR = 1.0.

Ref: Cal Tech Rept 47-14 Fig. 18 and 19

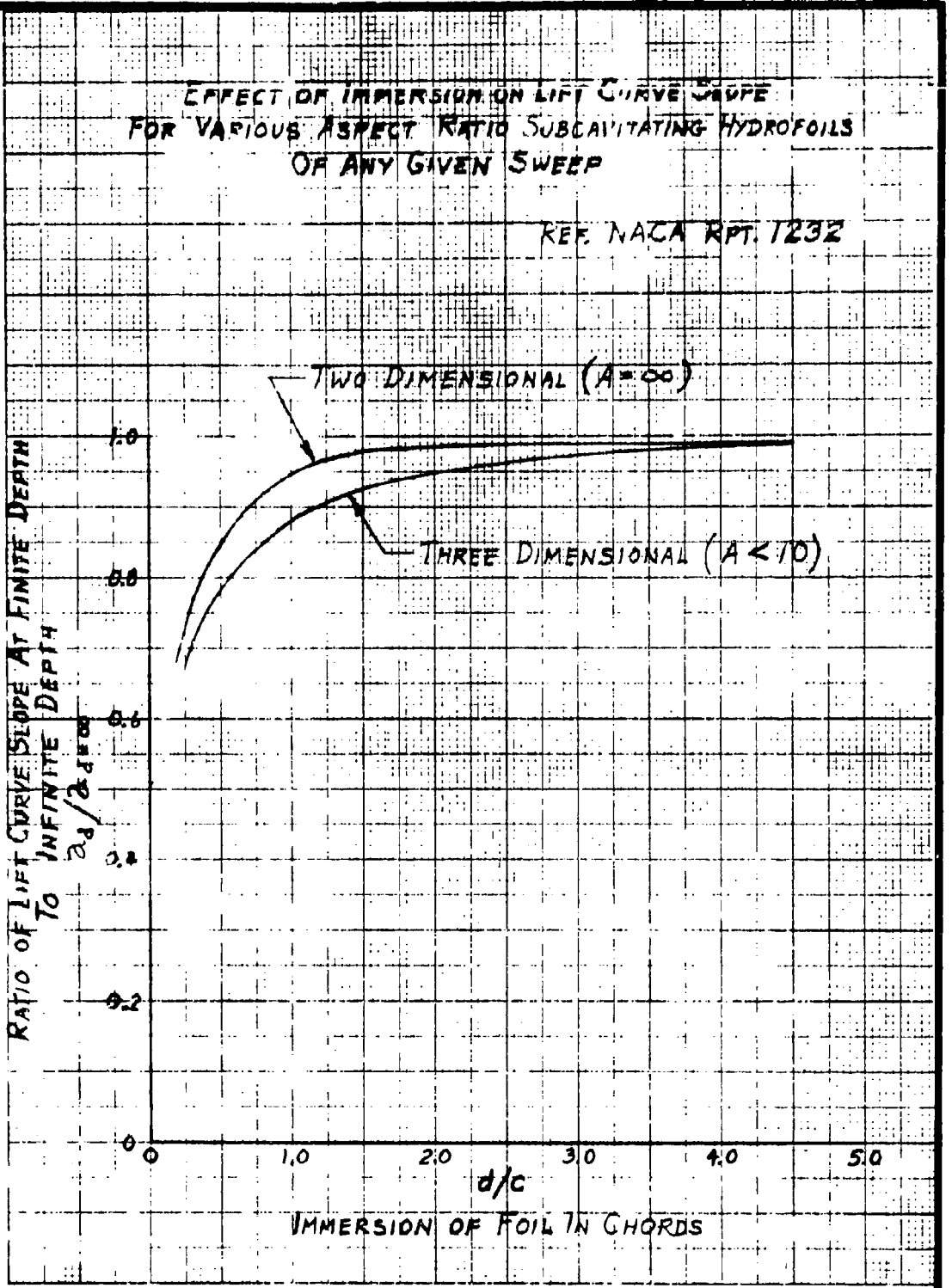

Fig. 41

Ref: Grumman Rept. PB 161759 Fig.I.4

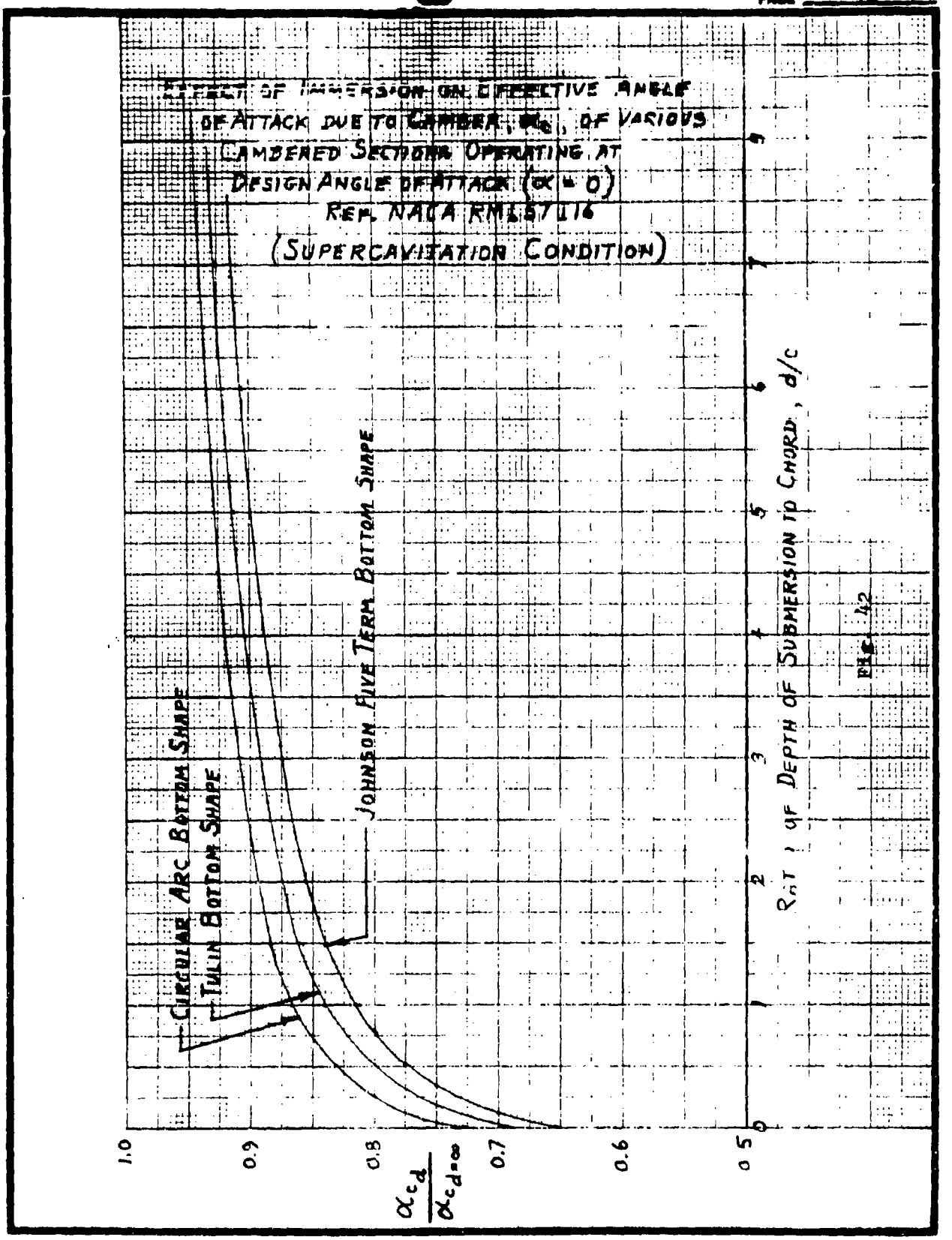
EFFECT OF IMMERSION ON EFFECTIVE ANGLE OF ATTACK DUE TO CAMBER, α_{c_d}, OF VARIOUS CAMBERED SECTIONS OPERATING AT DESIGN ANGLE OF ATTACK ($\alpha = 0$)
REF. NACA RM L57I16
(SUPERCAVITATION CONDITION)
JOHNSON FIVE TERM BOTTOM SHAPE
CIRCULAR ARC BOTTOM SHAPE
TULIN BOTTOM SHAPE
RATIO OF DEPTH OF SUBMERSION TO CHORD, d/c
$\frac{\alpha_{c_d}}{\alpha_{c_{d=\infty}}}$
1.0
0.9
0.8
0.7
0.6
0.5
0
1
2
3
4
5
6
7
FIG. 42

Effect of Depth of Submergence on Supercavitating Hydrofoil Performance

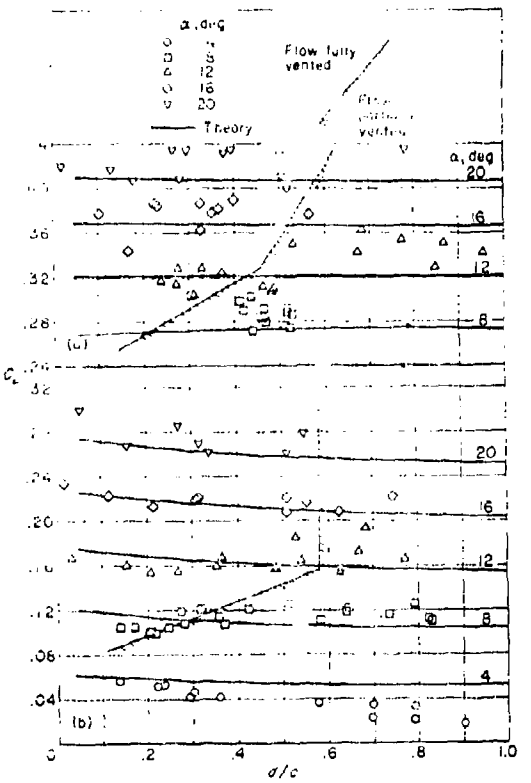

(a) Tulin-Burkart; $C_{L,a}=0.392$.
(b) Flat.

Comparison of theoretical lift coefficients with experimental data reported in reference 10 on aspect-ratio-1 flat and Tulin-Burkart sections. $\sigma \approx 0$.

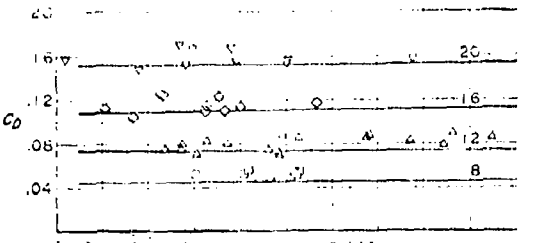

(a) Tulin-Burkart; $C_{L,a}=0.392$.

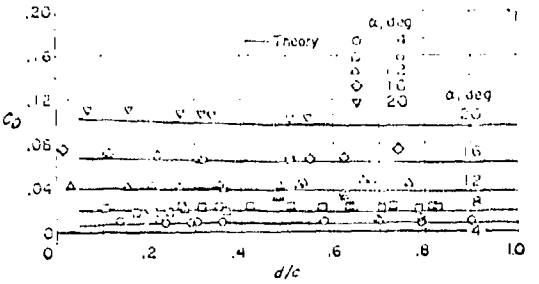

(b) Flat.

Comparison of theoretical drag coefficients with the experimental data reported in reference 18 on aspect-ratio-1 flat and Tulin-Burkart sections. $\sigma \approx 0$.

Fig. 43

Ref: NASA Tech. Rept. R-93 Fig. 46 and 50

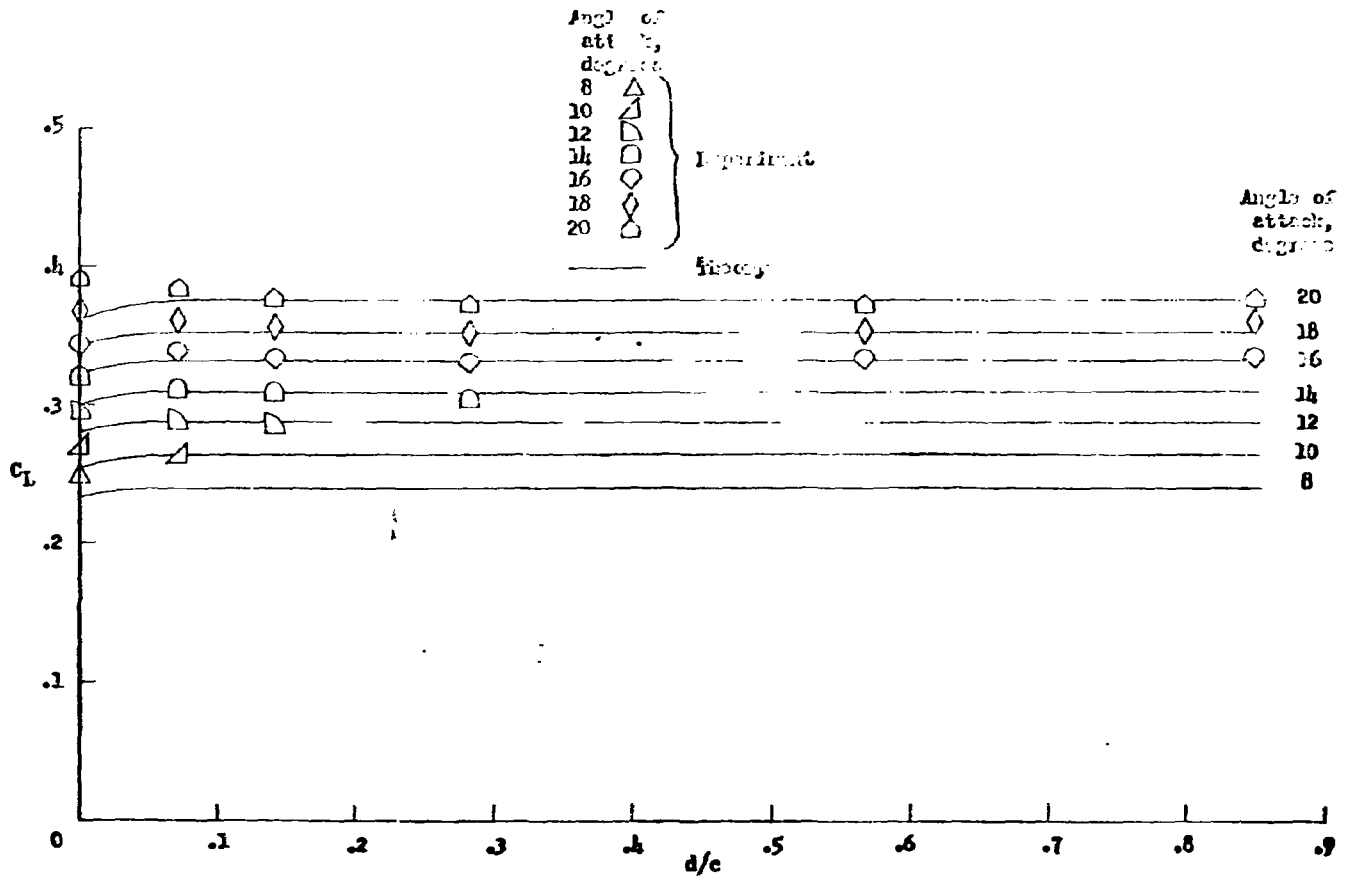

Fig. 44 (a) Aspect ratio 1 hydrofoil

Johnson 5 term foil under supercavitating conditions, $\sigma = 0$.
Comparison of theoretical and experimental lift coefficients with depth of submergence.

Ref: NASA Memo 5-9-59L Fig. 18

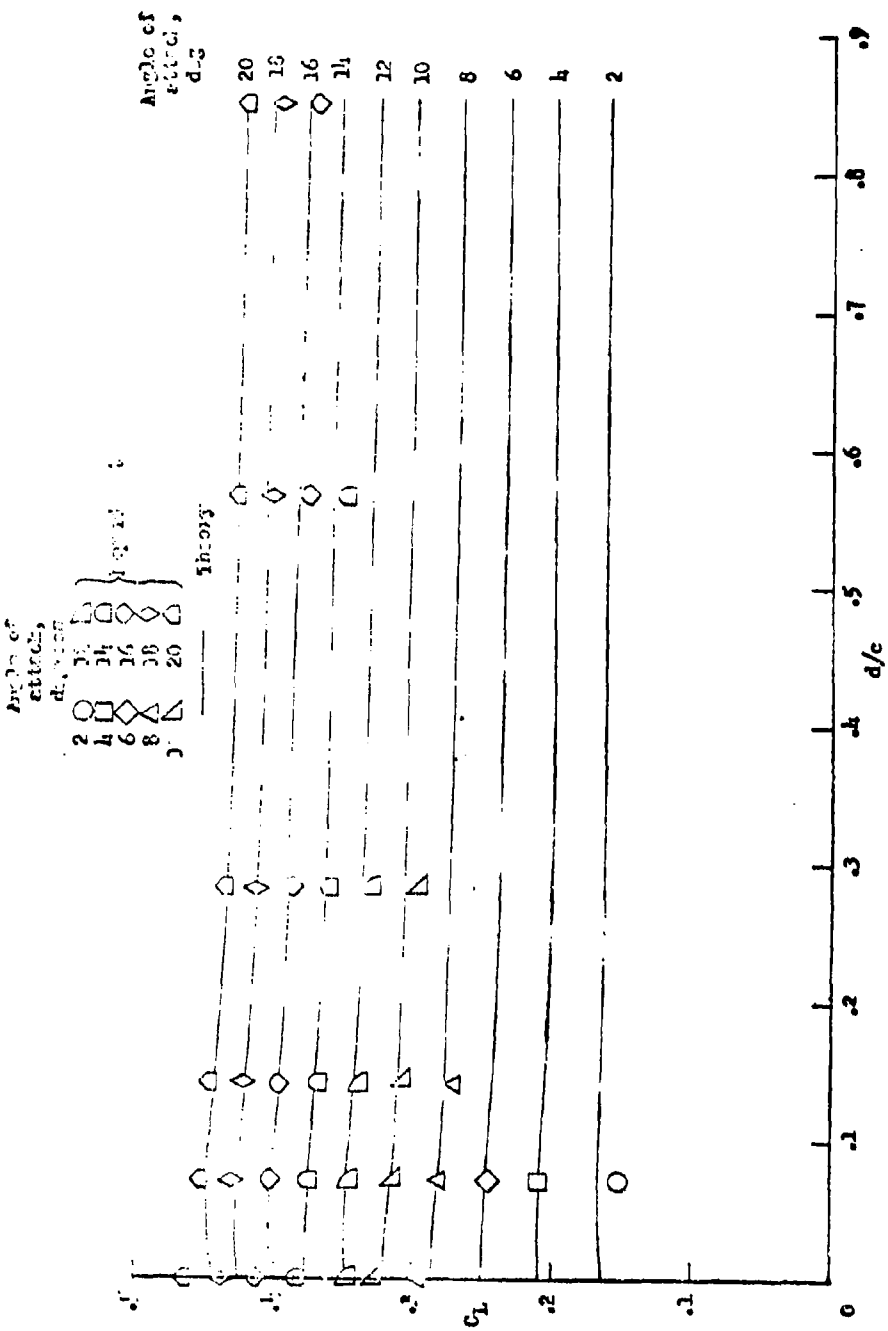

Fig. 44(b) Aspect-ratio-3 hydrofoil.

Johnson 5 term foil under supercavitating conditions, $\sigma = 0$.

Comparison of theoretical and experimental lift coefficients with depth of submergence

Ref: NASA Memo 5-9-59L Fig. 13

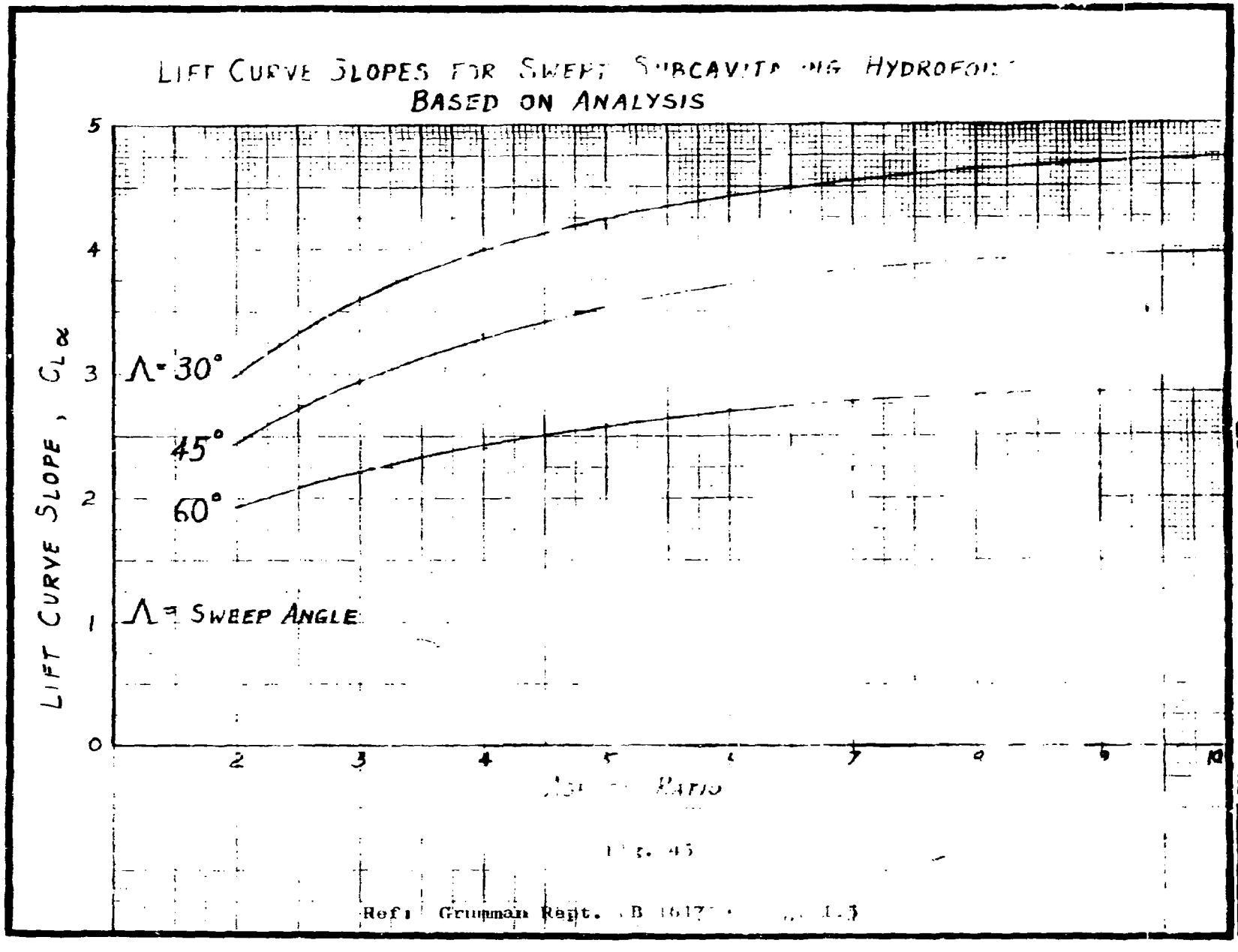

Fig. 45

Ref: Grumman Rept. No. IB 1617 ... 1.3

Ref:
NACA RM L52J10

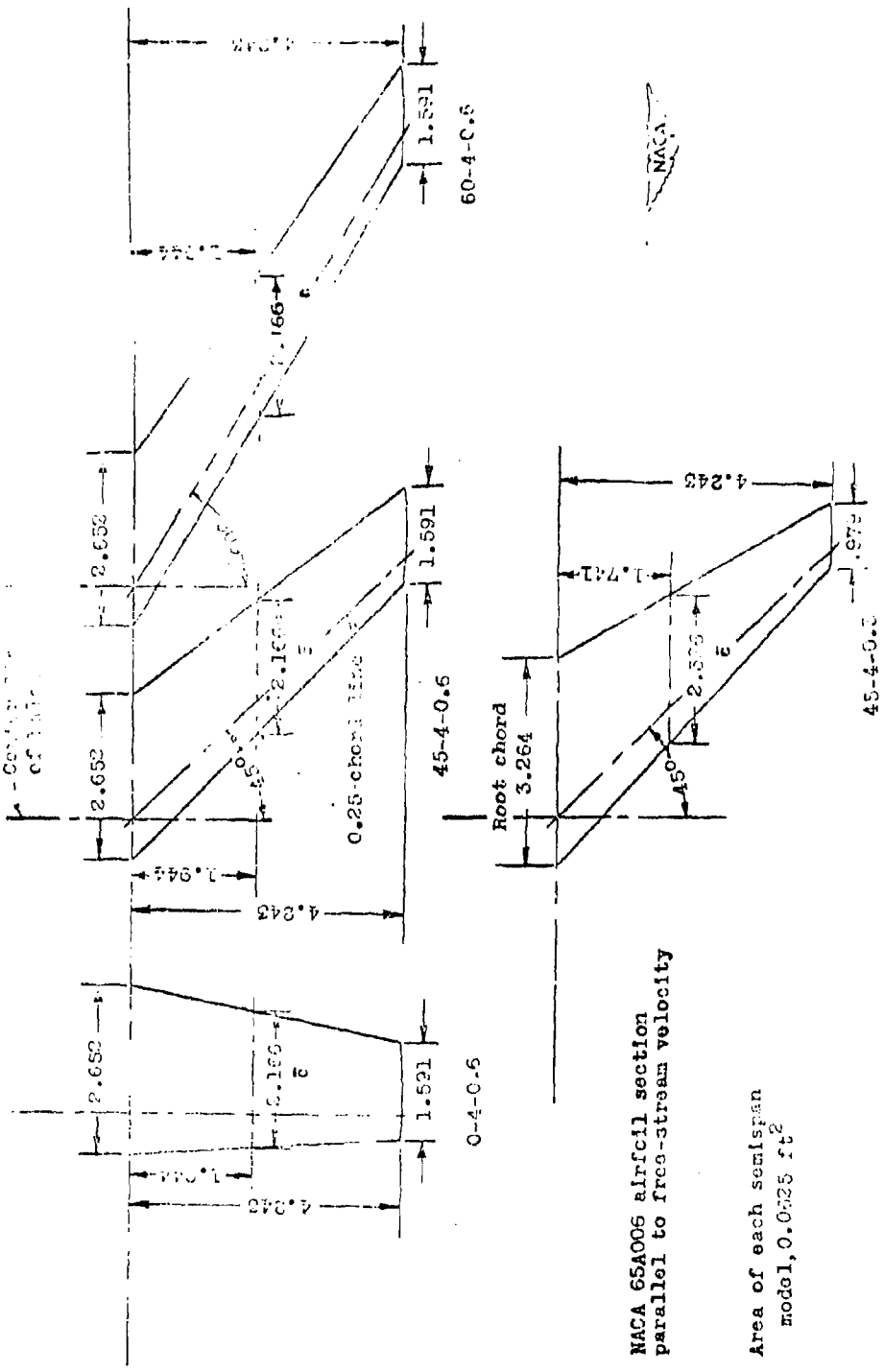

Fig. 4 - Dimensions of semispan [illegible]. All dimensions are in inches.

Ref:
NACA TN 1476

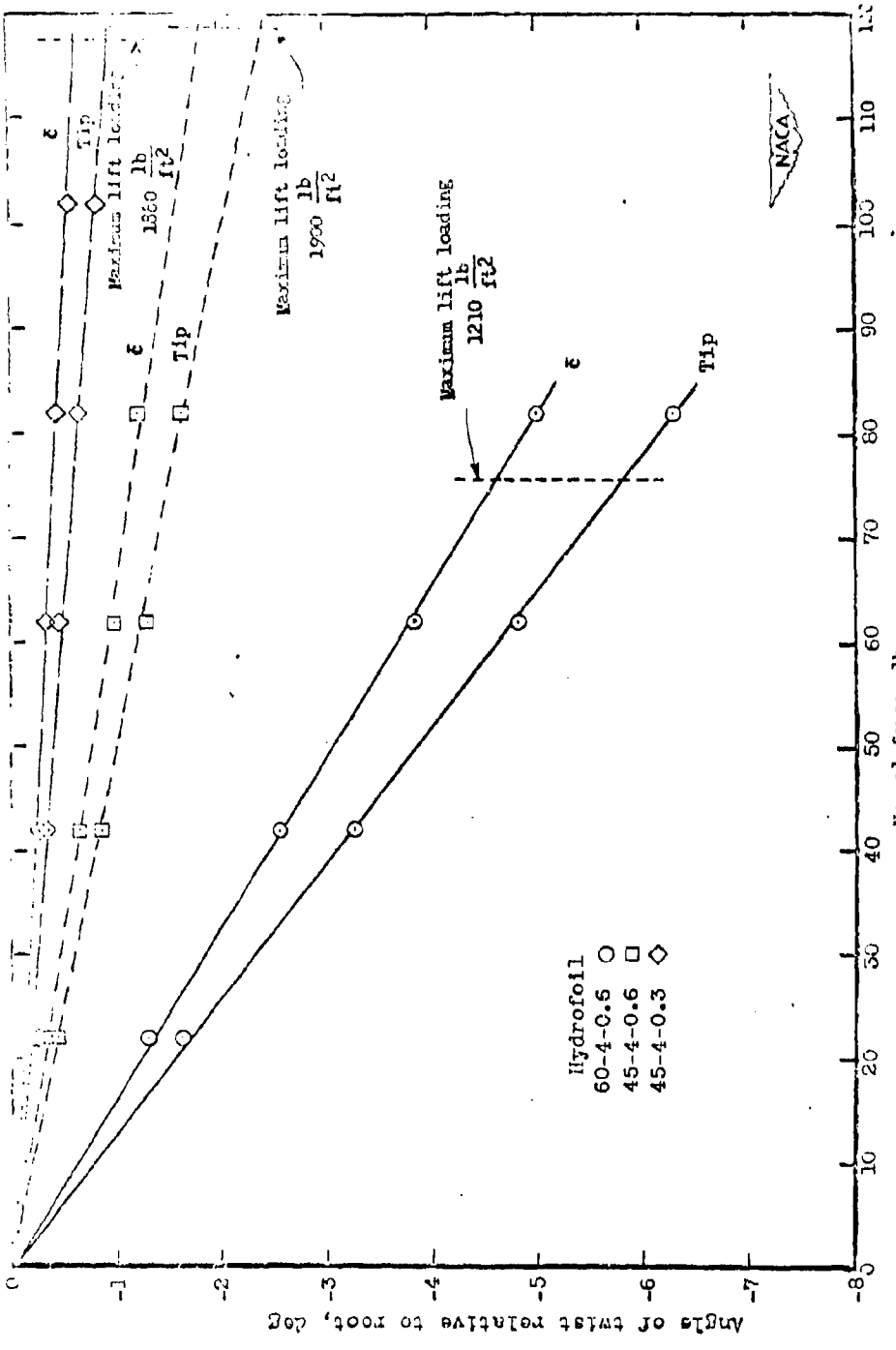

Fig. 47 - Angular deflection of sweptback hydrofoils due to load.

Ref: NACA RM L52J10

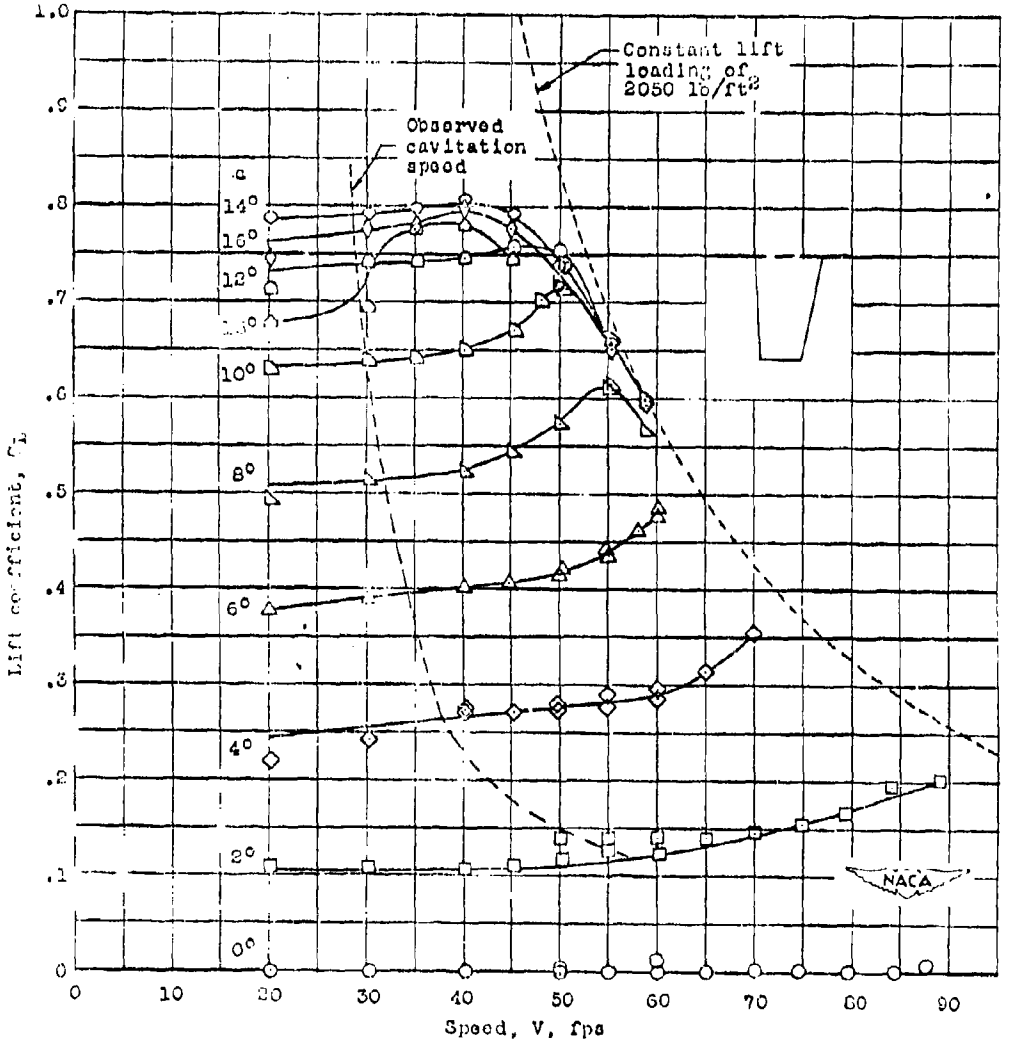

Fig. 48 (a) Lift coefficient.

- Variation with speed of hydrodynamic characteristics of 0-4-0.6 hydrofoil.

Ref:
NACA RM L52J10

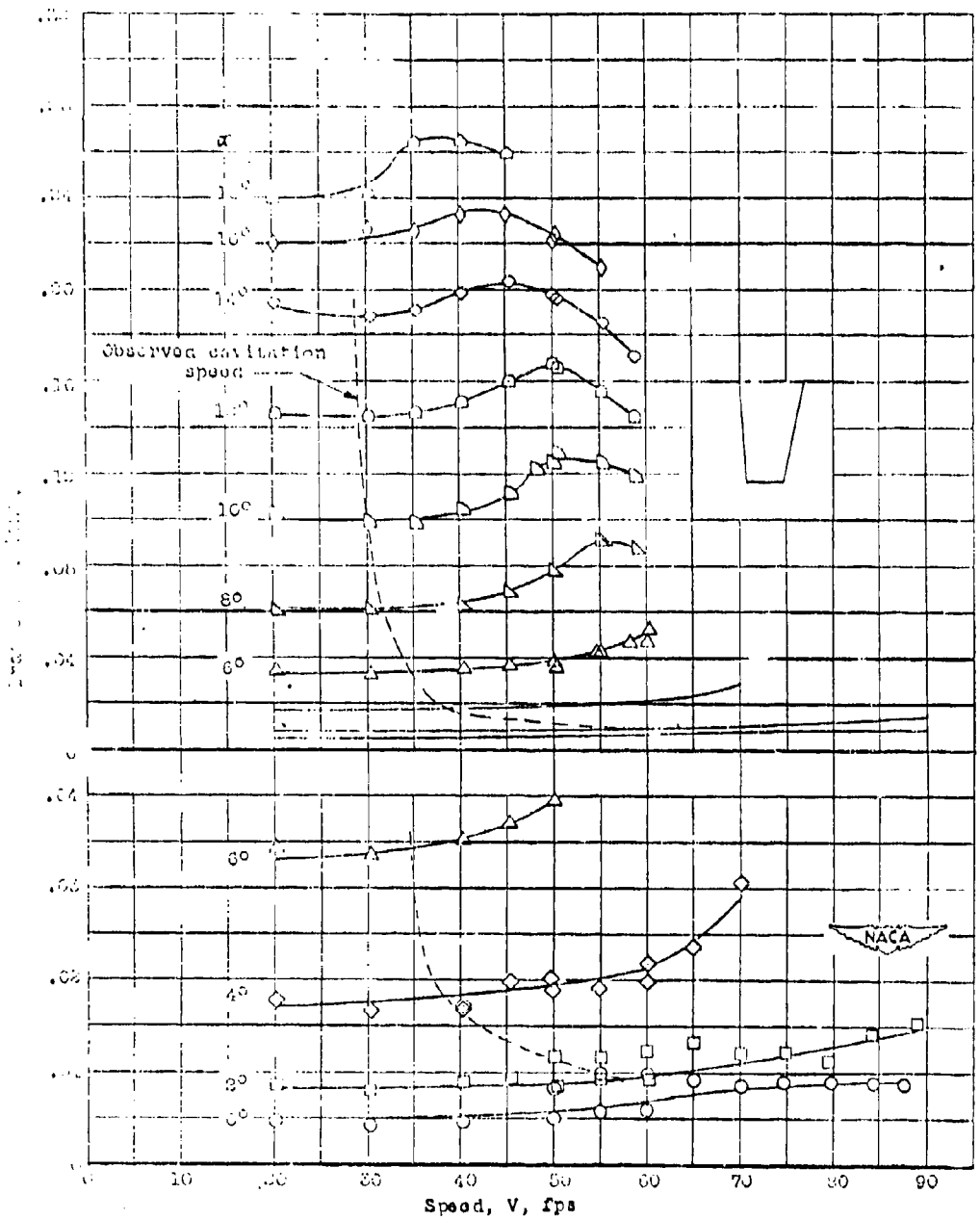

Fig. 48(b) Drag coefficient.

Ref: NACA RM L52J16

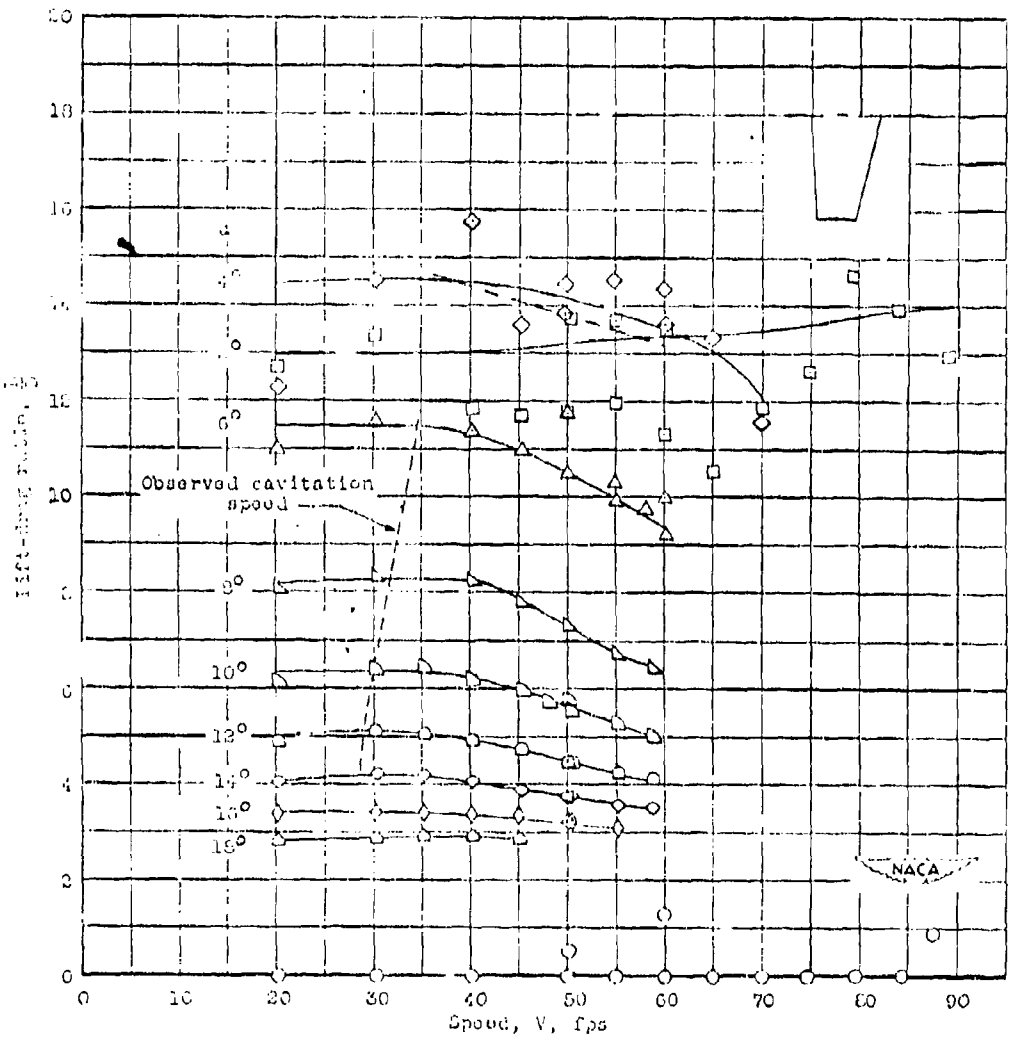

Fig. 48 (c) Lift-drag ratio.

Ref: NACA RM L52J10

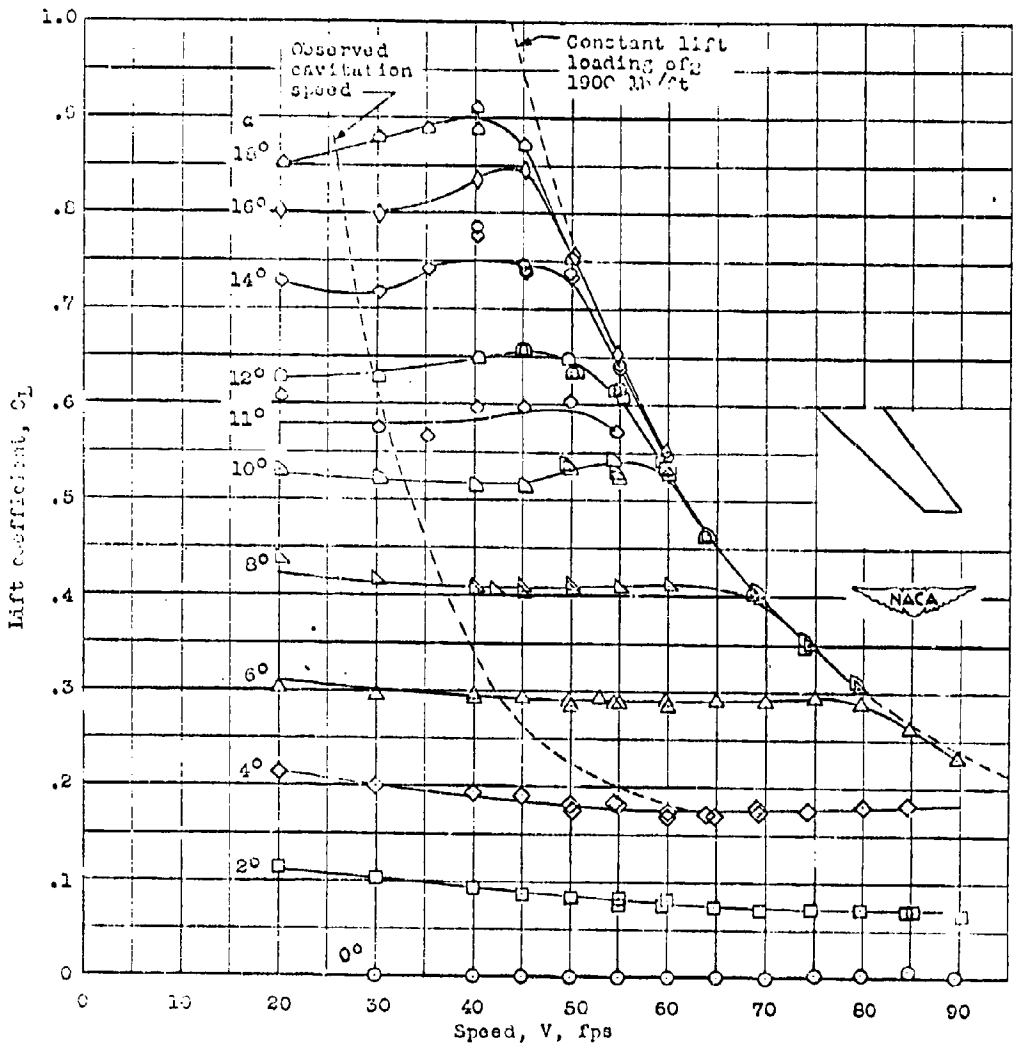

Fig.49 (a) Lift coefficient.

- Variation with speed of hydrodynamic characteristics of 4--4-0.6 hydrofoil.

Ref:
NACA RM L52J10

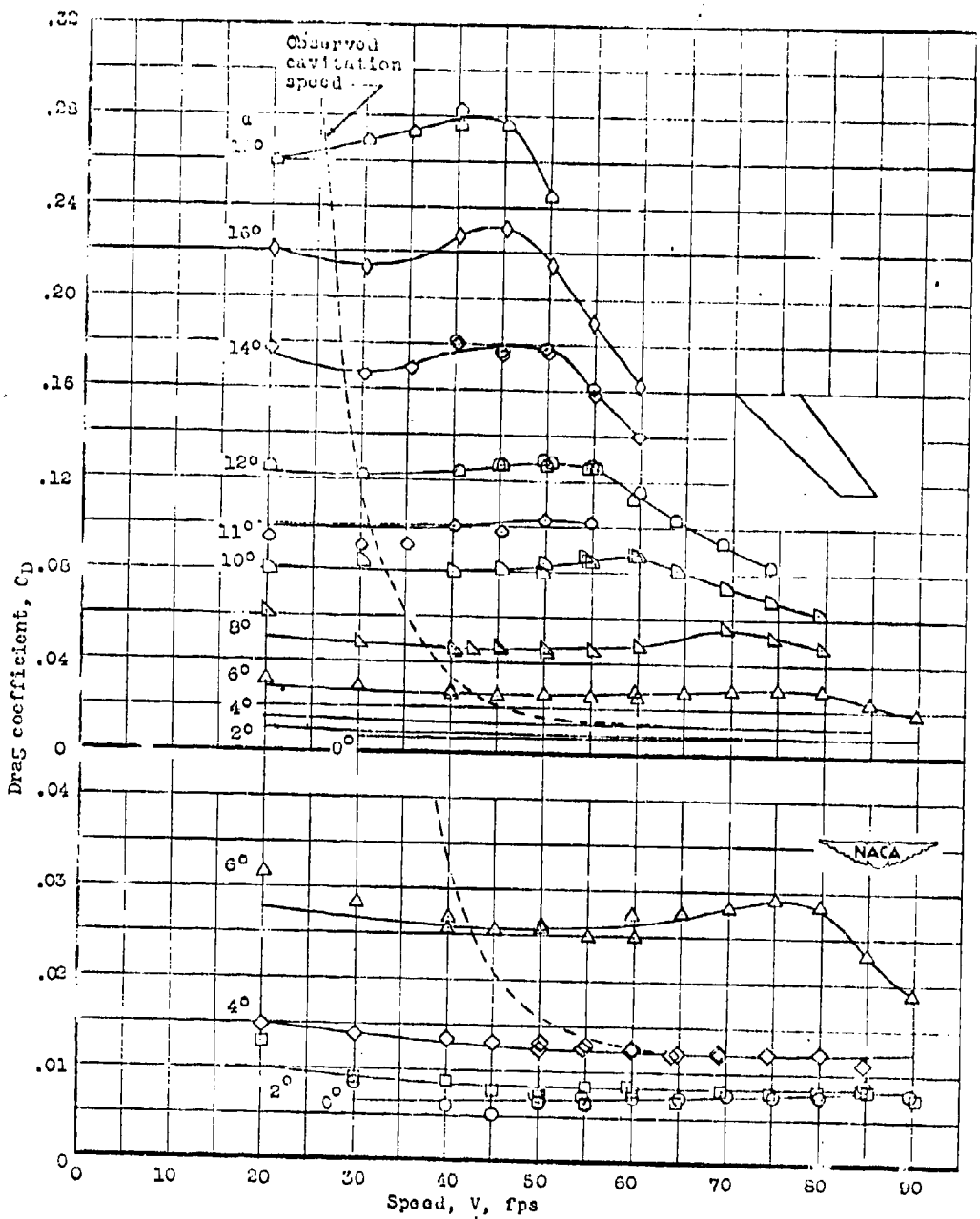

Fig. 49 (b) Drag coefficient.

Ref: NACA RM L52J10

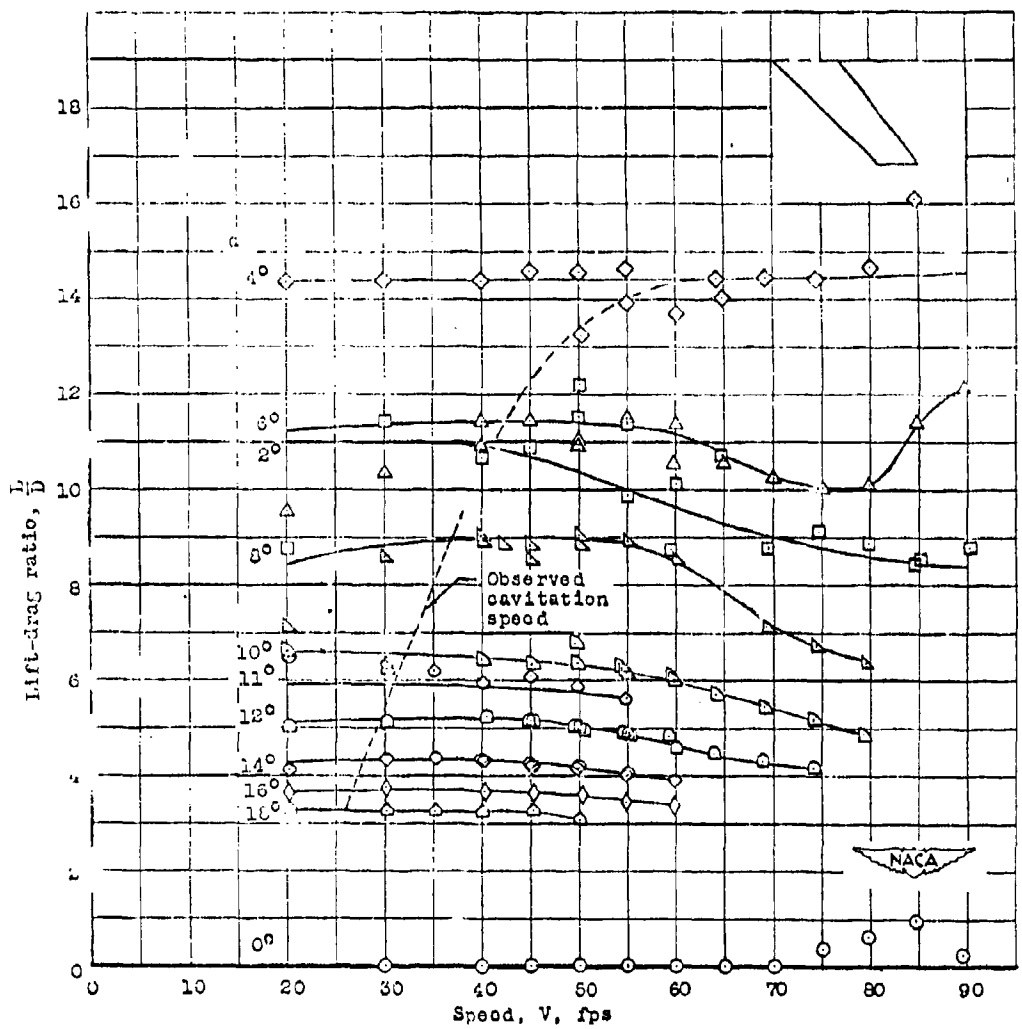

Fig. 49 (c) Lift-drag ratio.

Ref:

NACA RM L52J10

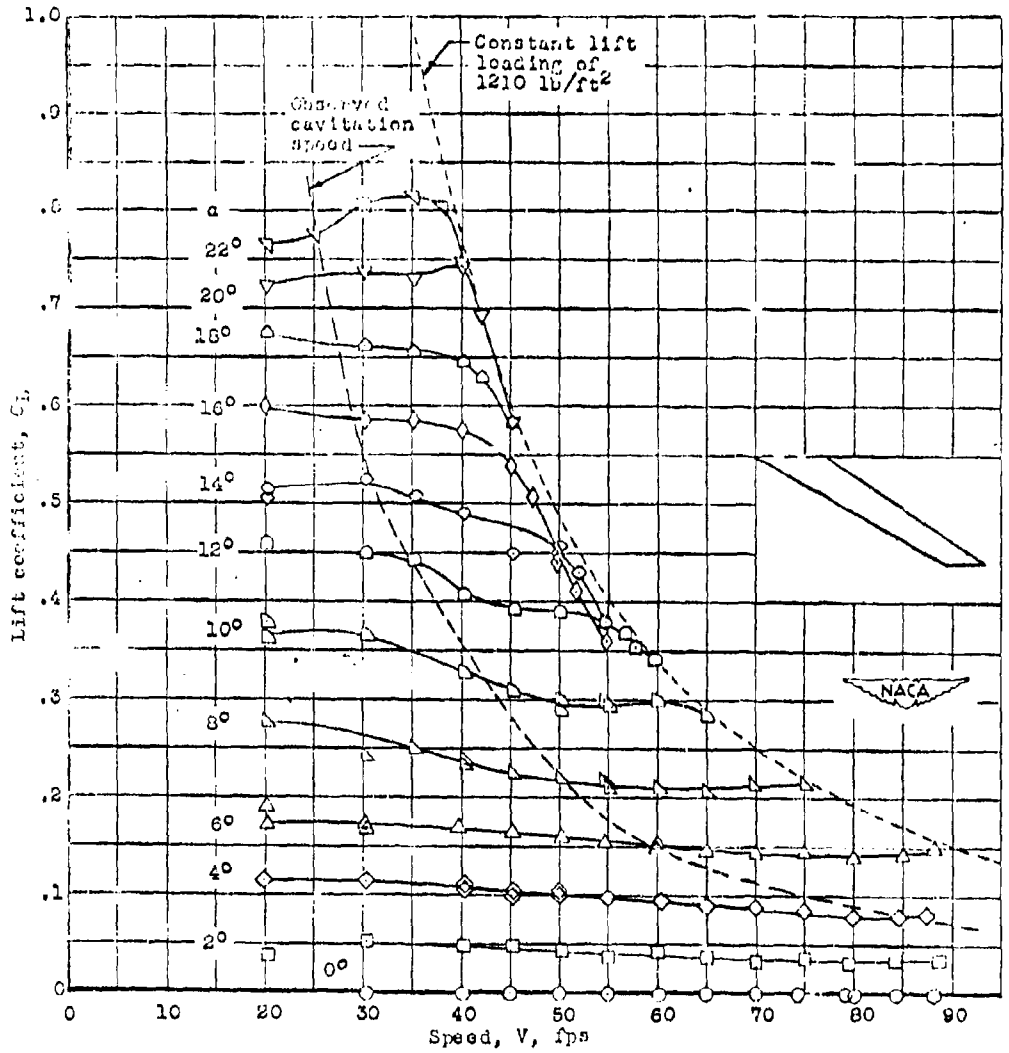

Fig. 50 (a) Lift coefficient.

- Variation with speed of hydrodynamic characteristics of 60-4-0.6 hydrofoil.

Ref: NACA RM L52J10

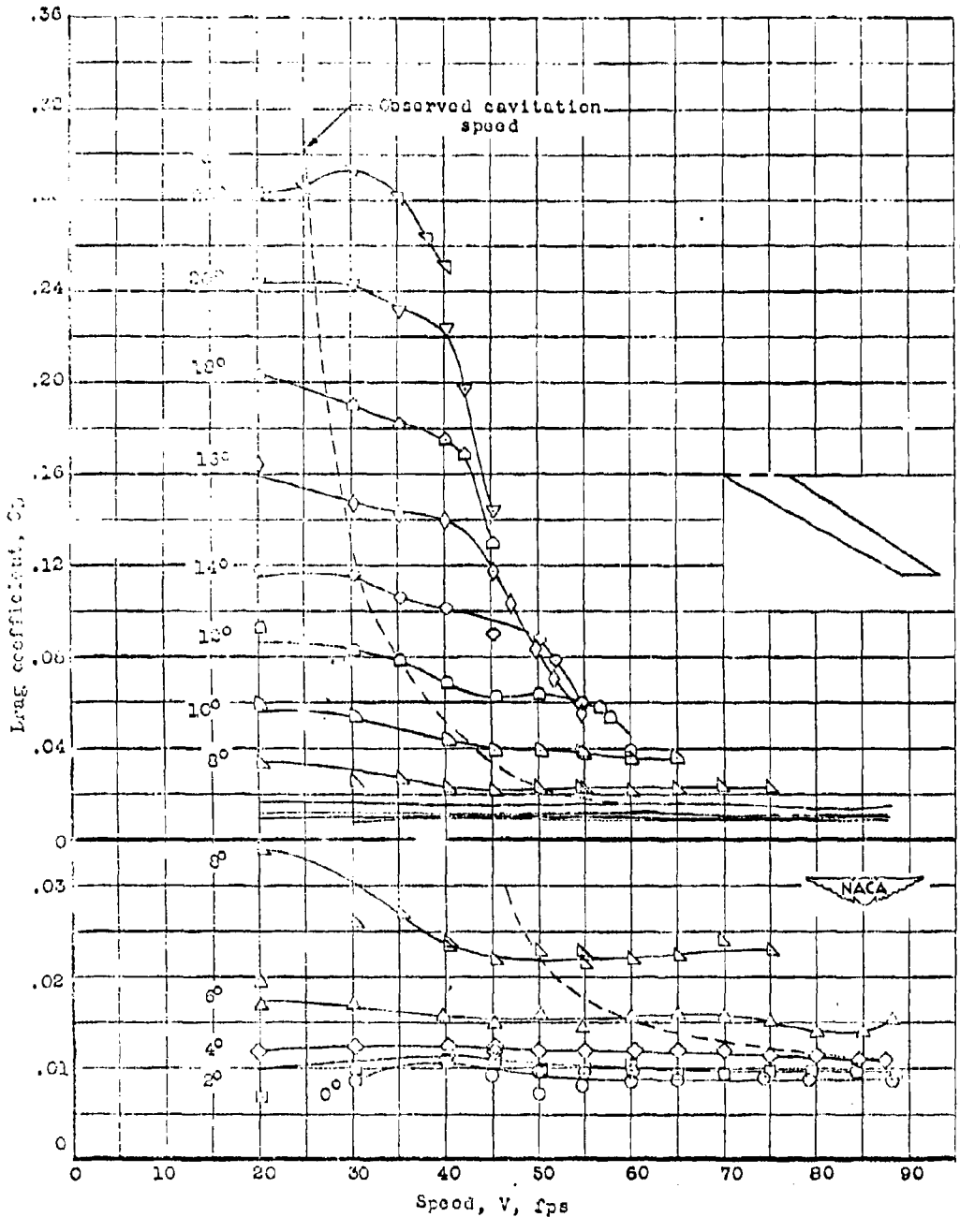

Fig. 50 (b) Drag coefficient.

Ref:
NACA RM L52J10

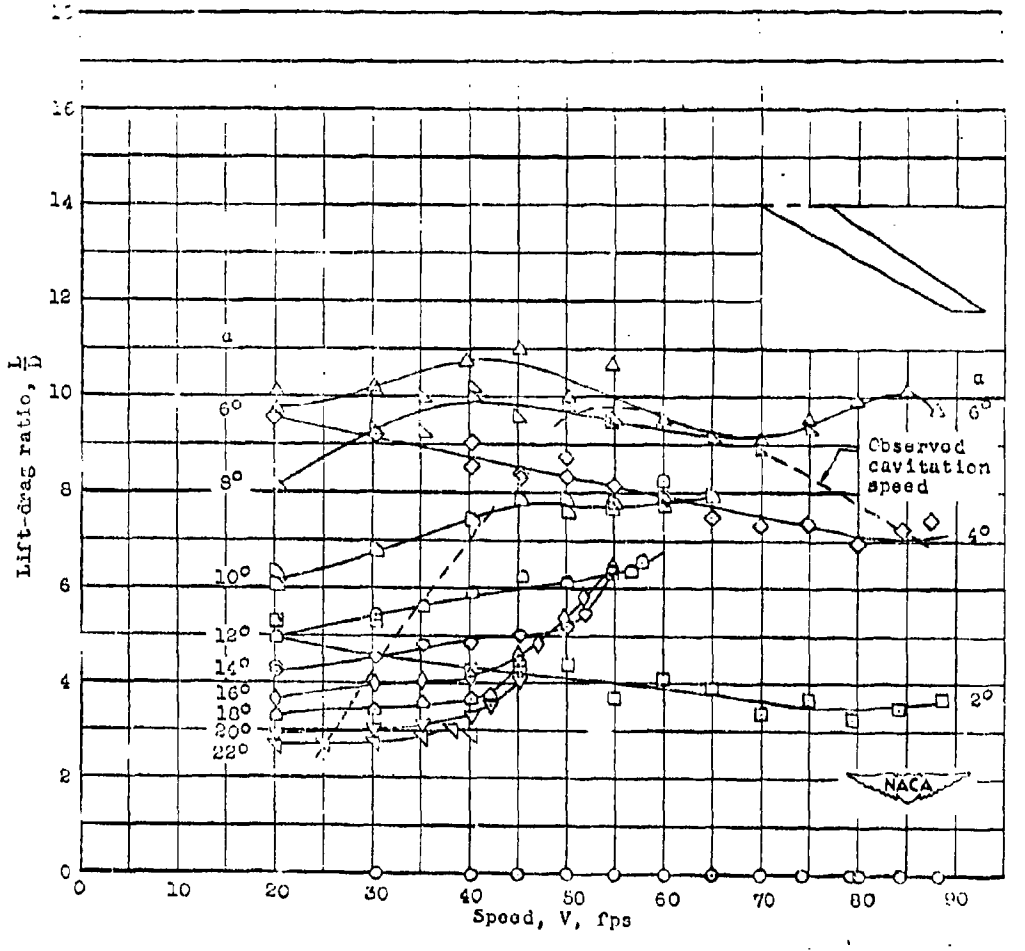

Fig. 50(c) Lift-drag ratio.

Ref: NACA RM L52J10

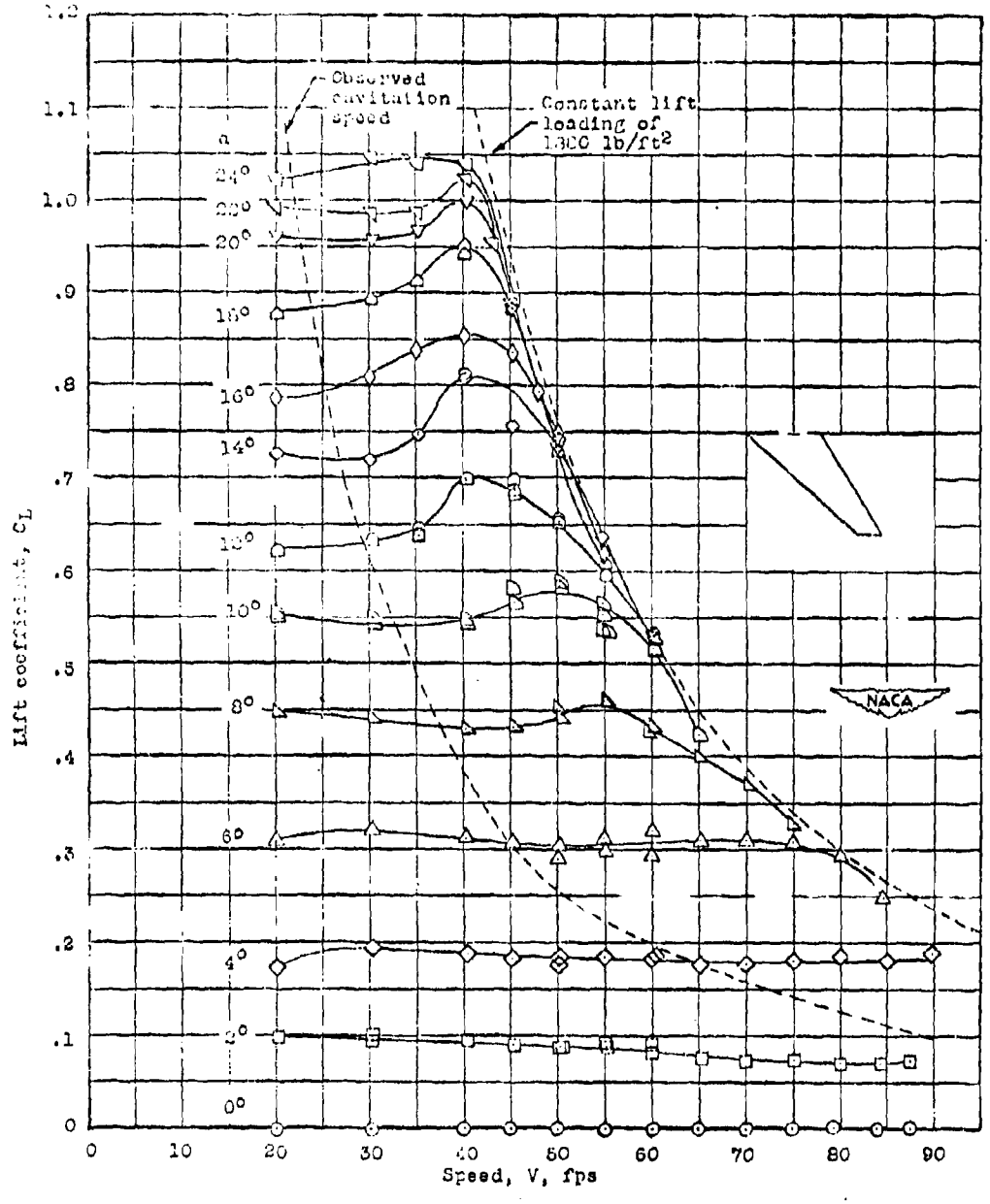

Fig. 51 (a) Lift coefficient.

- Variation with speed of hydrodynamic characteristics of 45-4-0.3 hydrofoil.

Ref:
NACA RM L52J10

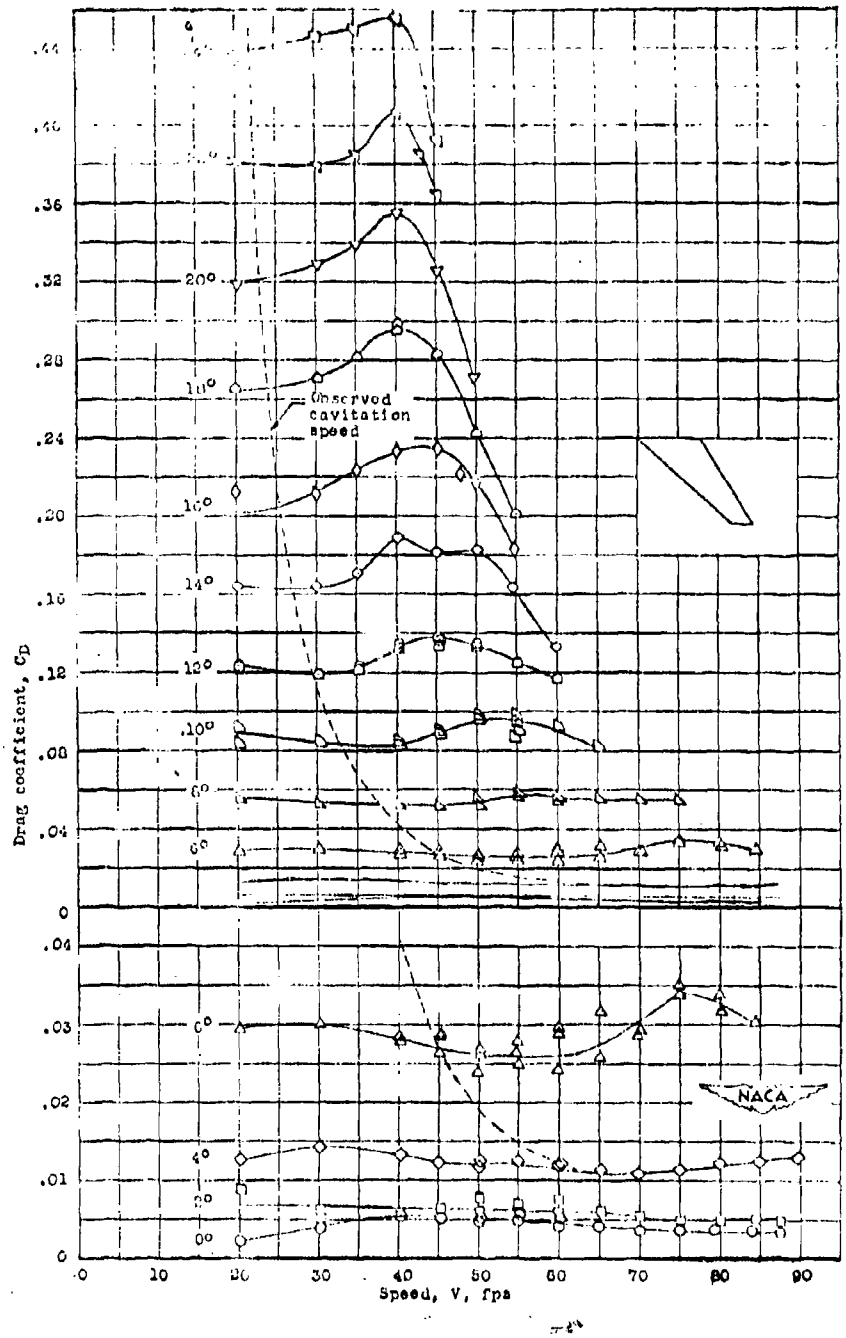

Fig. 51(b) Drag coefficient.

Ref: NACA RM L50J10

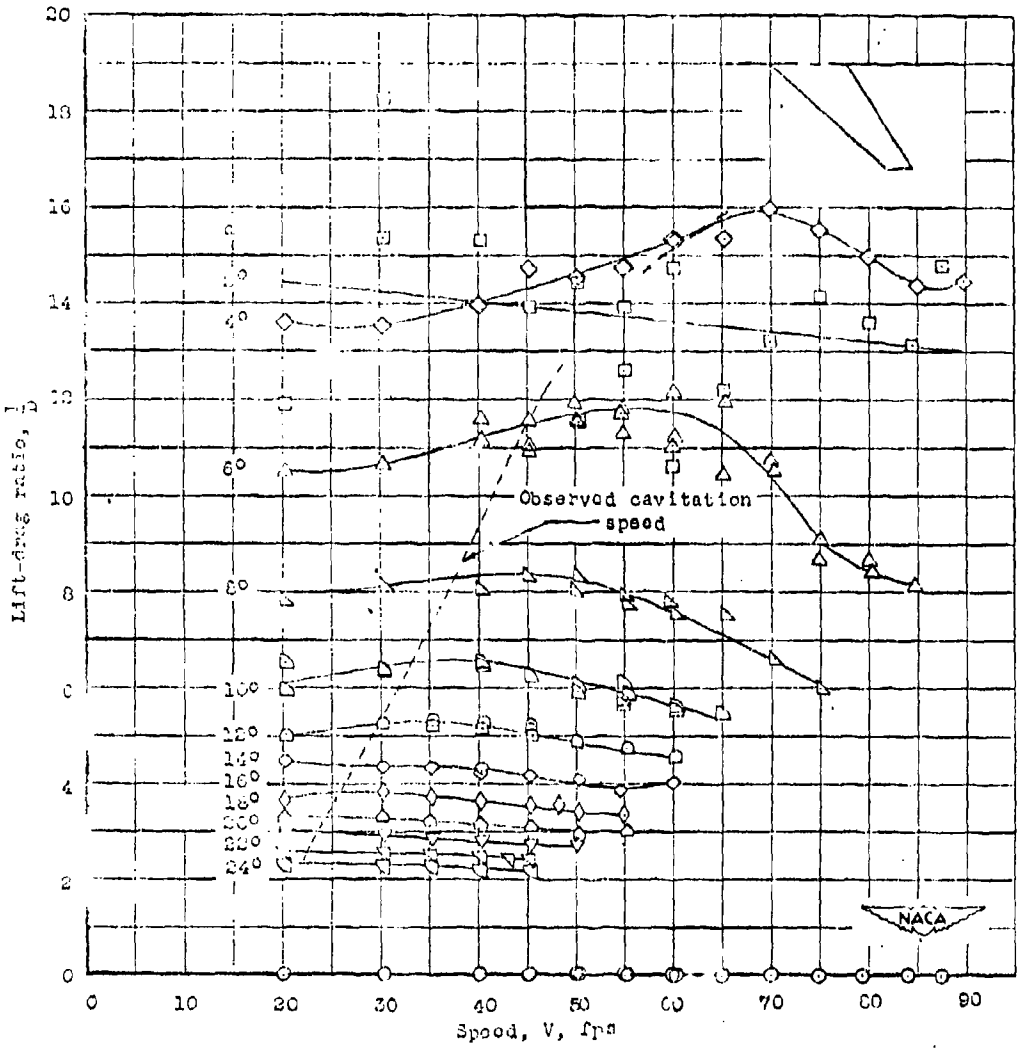

Fig. 51(c) Lift-drag ratio.

Ref:
NACA RM L52J16

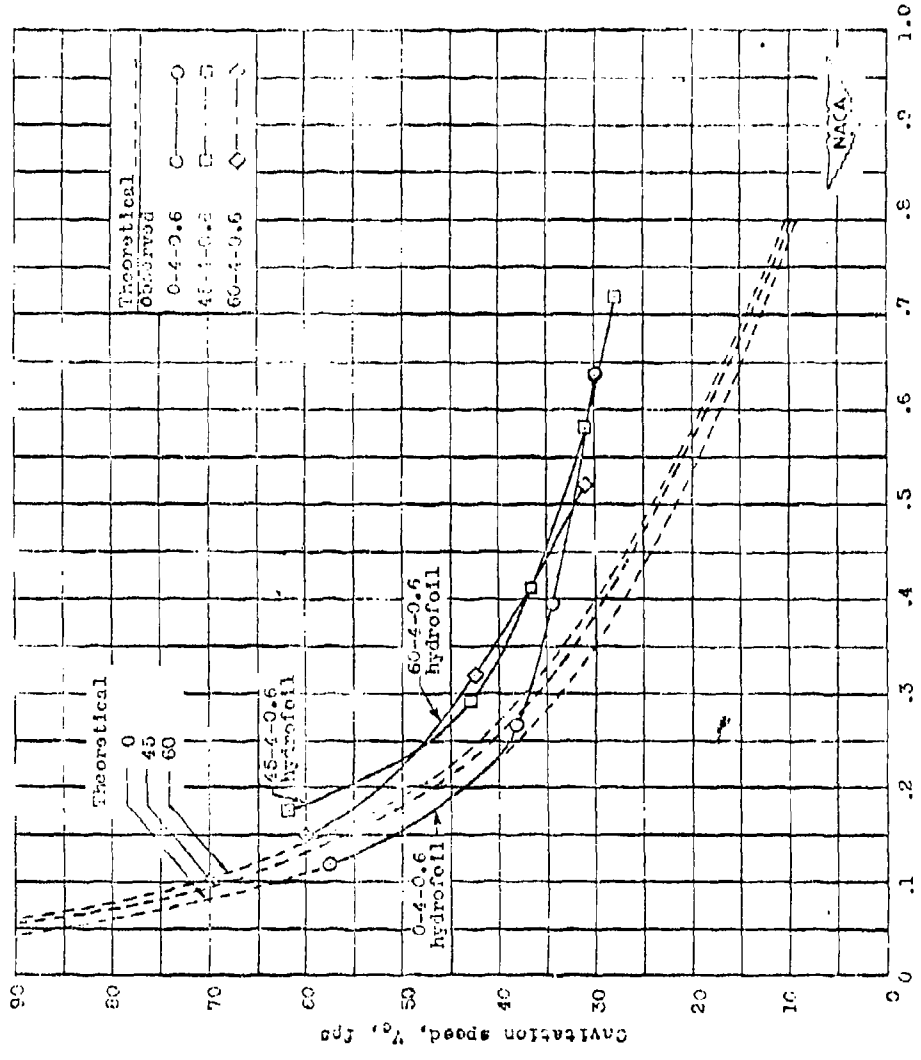

Fig. 52 - Effect of sweep on cavitation speed.

Ref:
NACA RM L52J10

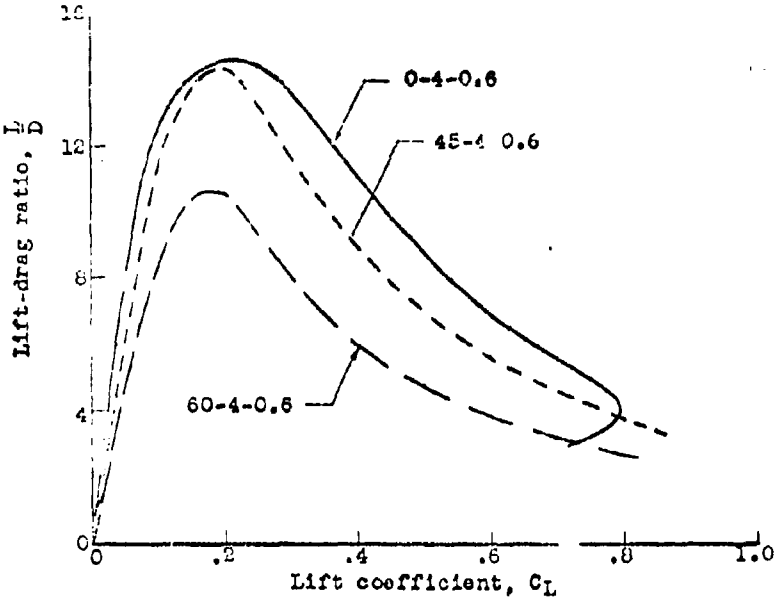

(a) Speed, 30 feet per second.

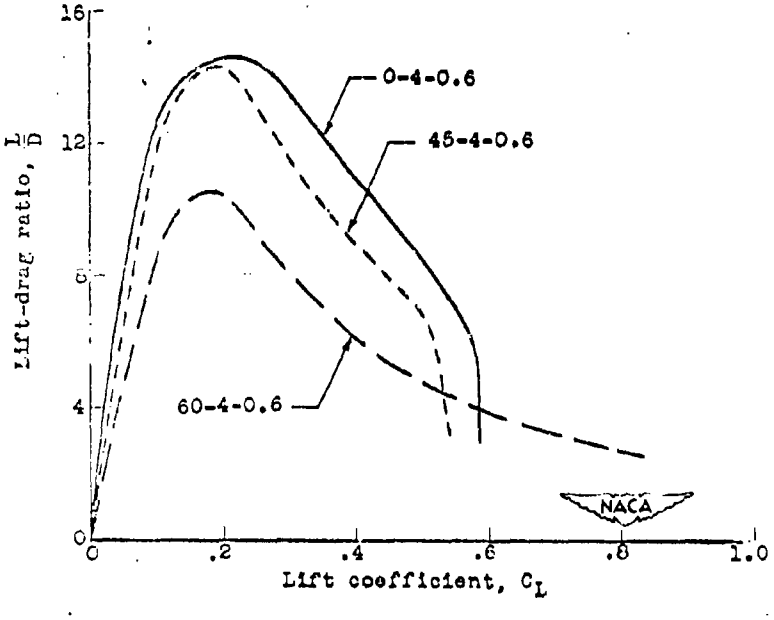

Speed, 60 feet per second.

Fig. 53 Effect of sweep on lift-drag ratio.

Ref NACA RM L52J10

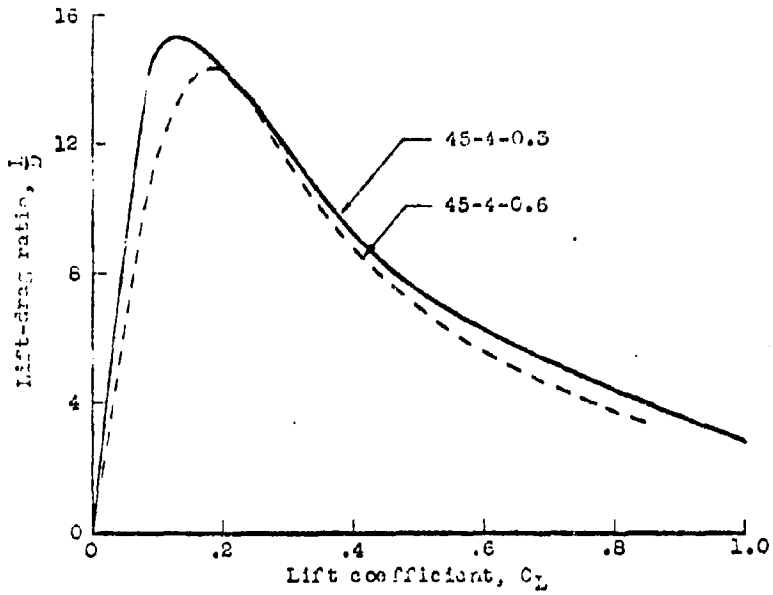

(a) Speed, V, 30 feet per second.

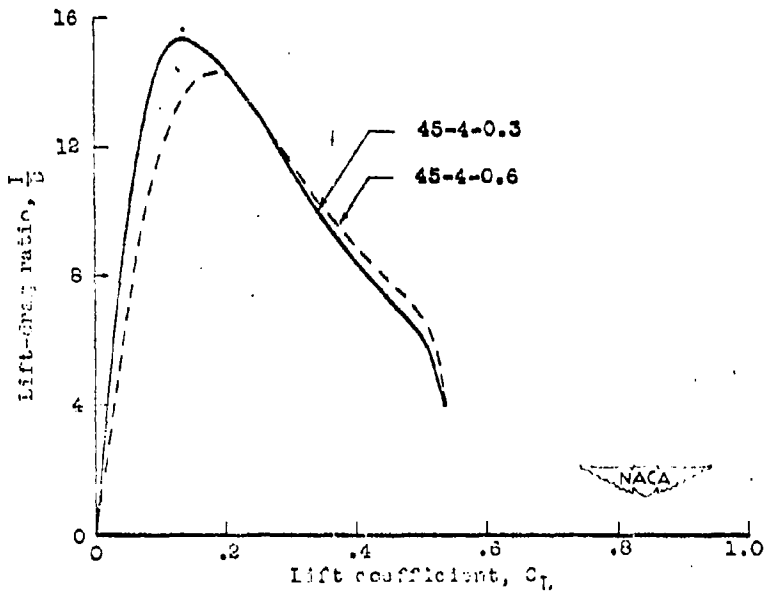

Speed, V, 60 feet per second.

Fig. 54 - Effect of taper on lift-drag ratio.

LIFT CHARACTERISTICS

6 degree wedge

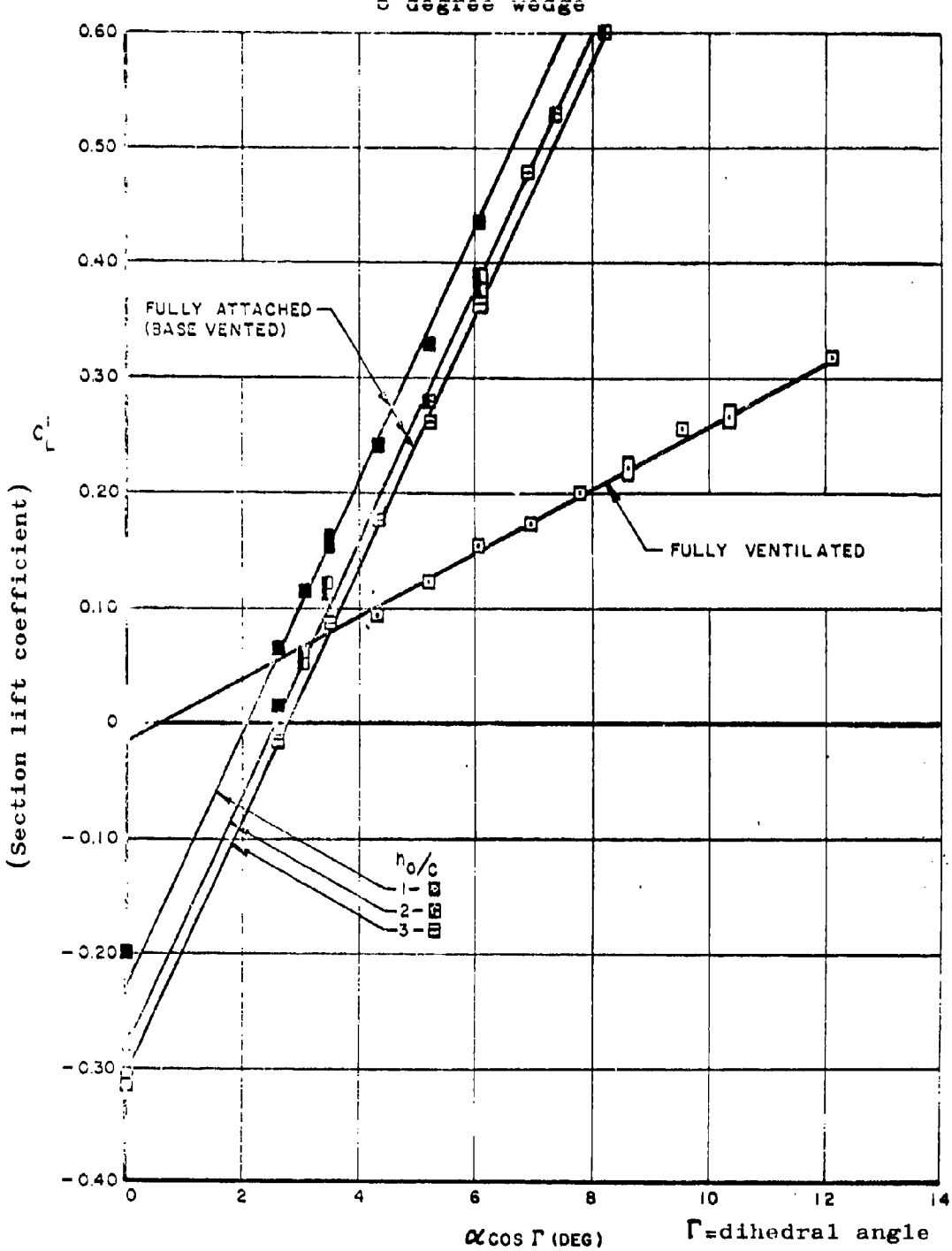

Fig. 55 (a)

Ref: Davidson Lab (SIT) Rept 952 Fig. 2

DRAG CHARACTERISTICS (FULLY VENTILATED)

6 degree wedge

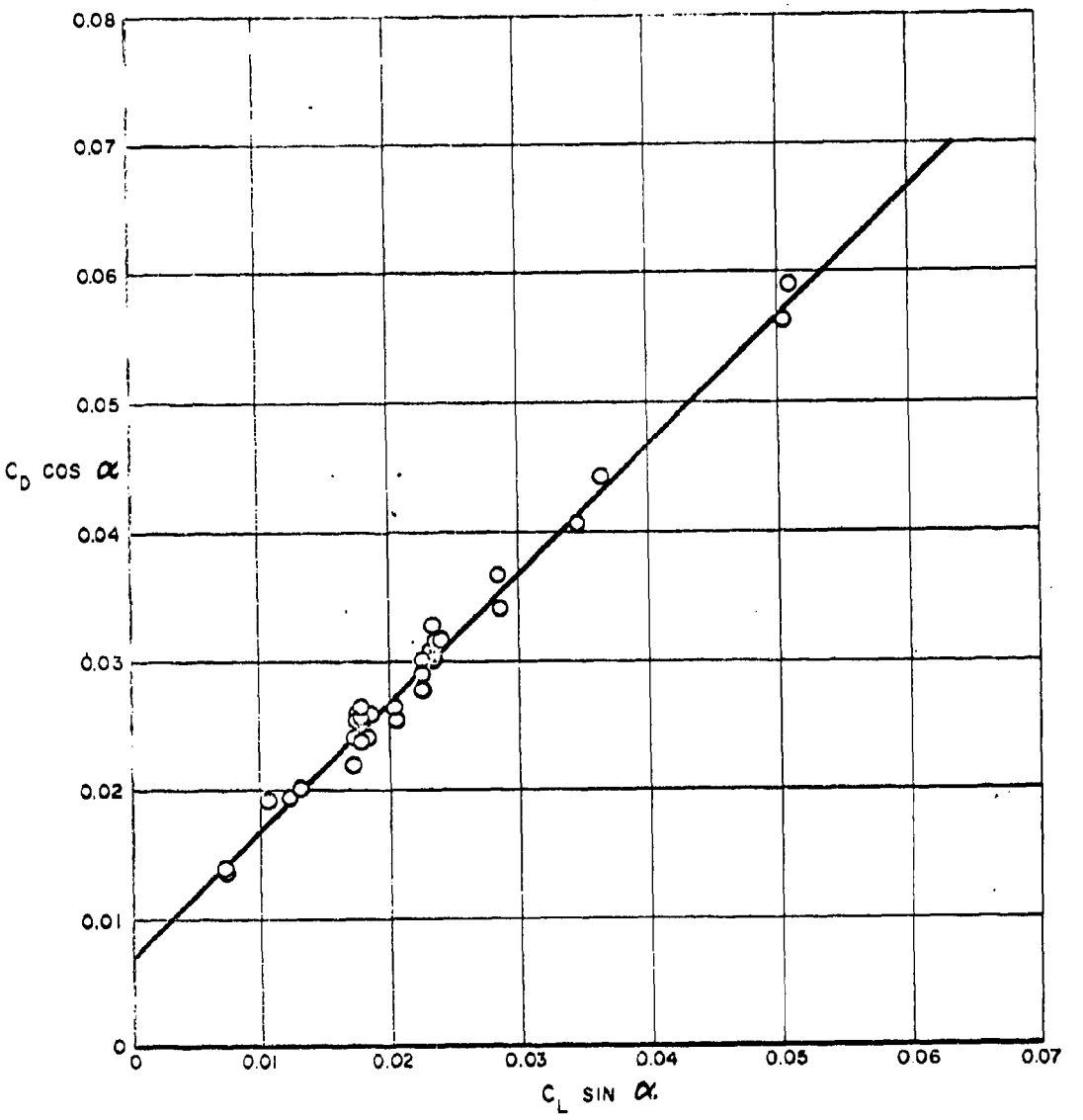

Fig. 55 (b)

Ref: Davidson Lab (SIT) Rept. 952 Fig. 3

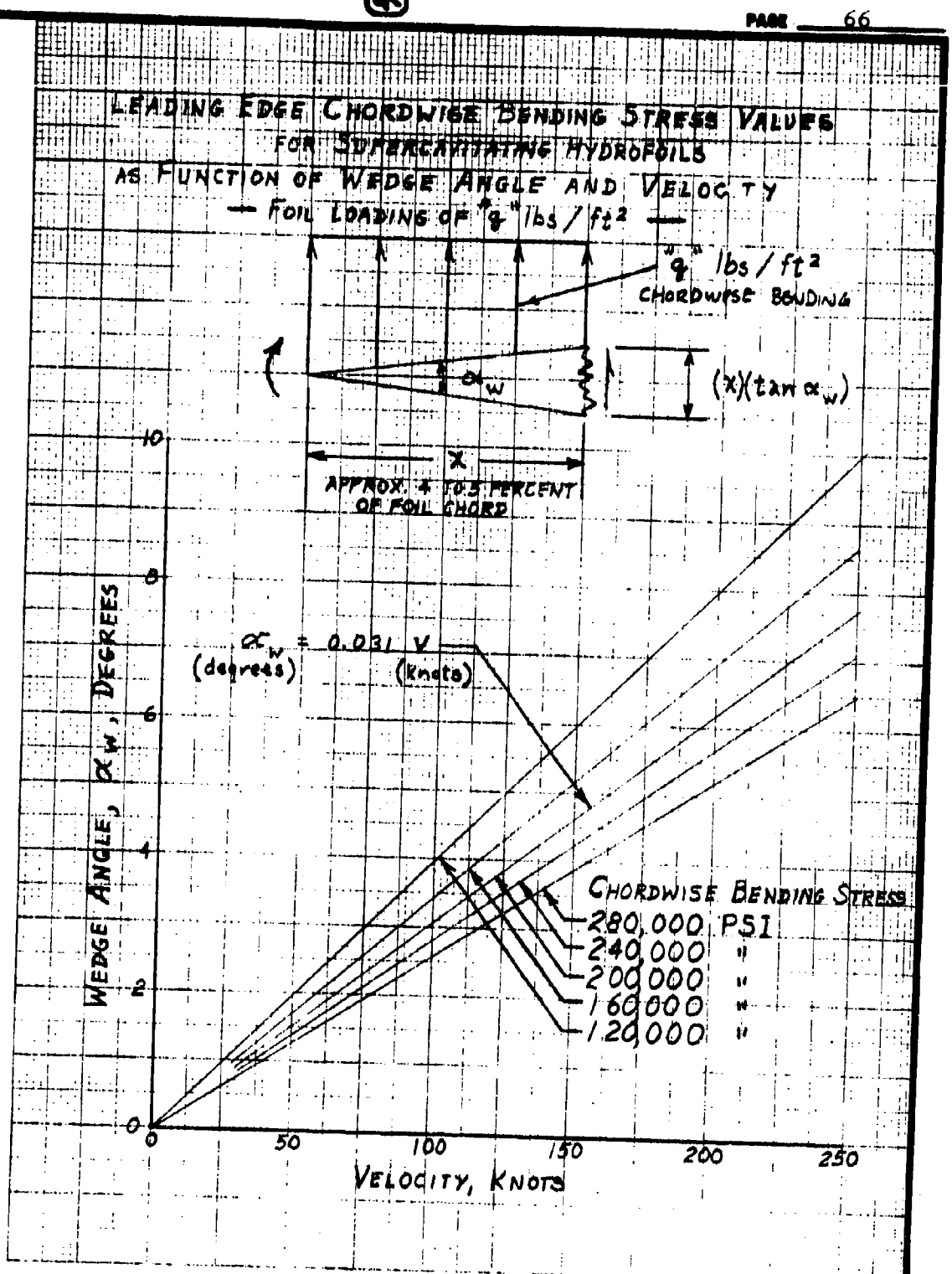

Fig. 56

Ref: Grumman Rept. PB 161759 Fig. II.59

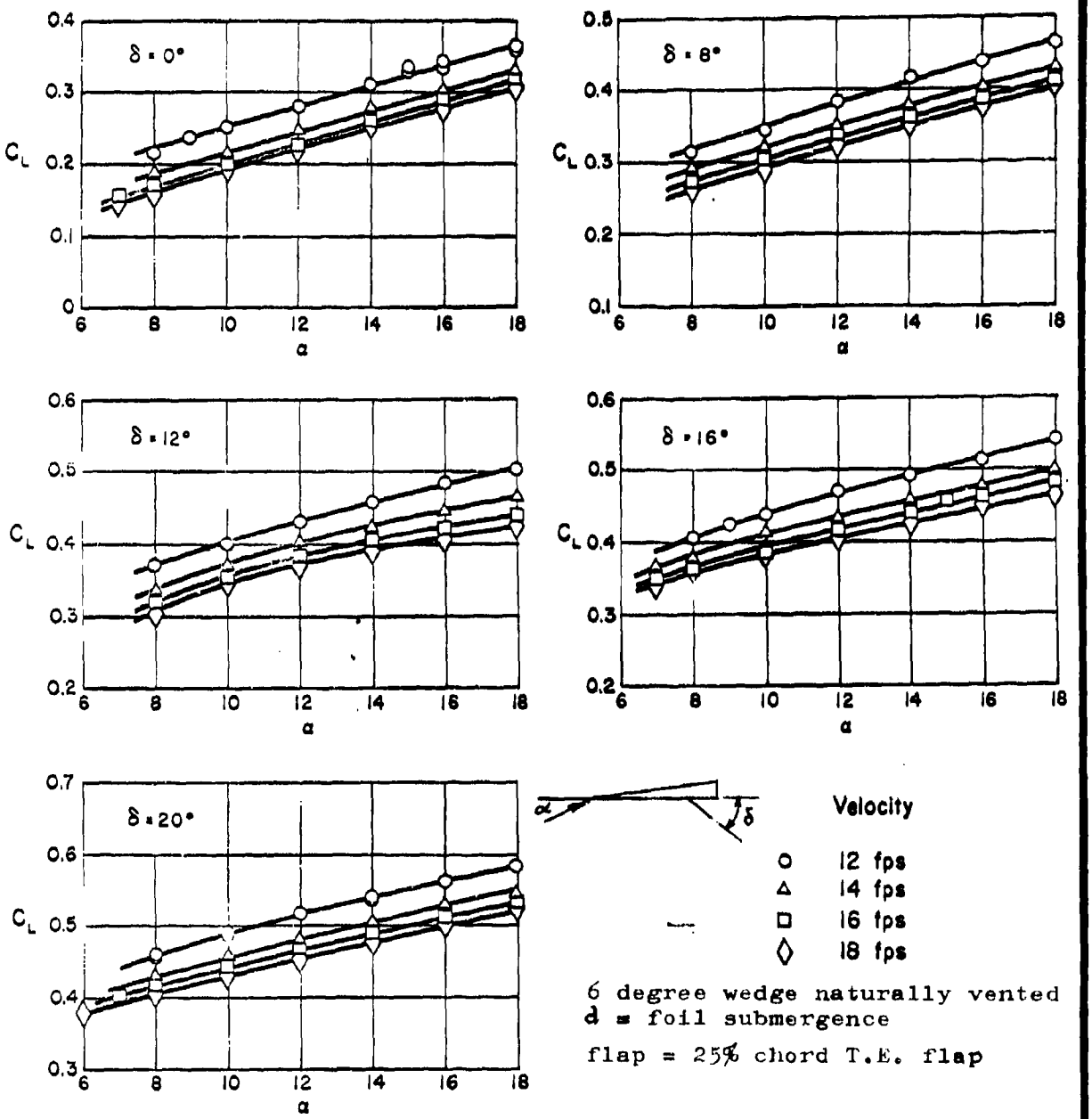

Fig. 57 (a) Variation of Steady Lift Coefficient with Angle of Attack, AR = 2, d/c = 1

Ref: U. of Minnesota St. Anthony Falls Rept 68, Fig. 2

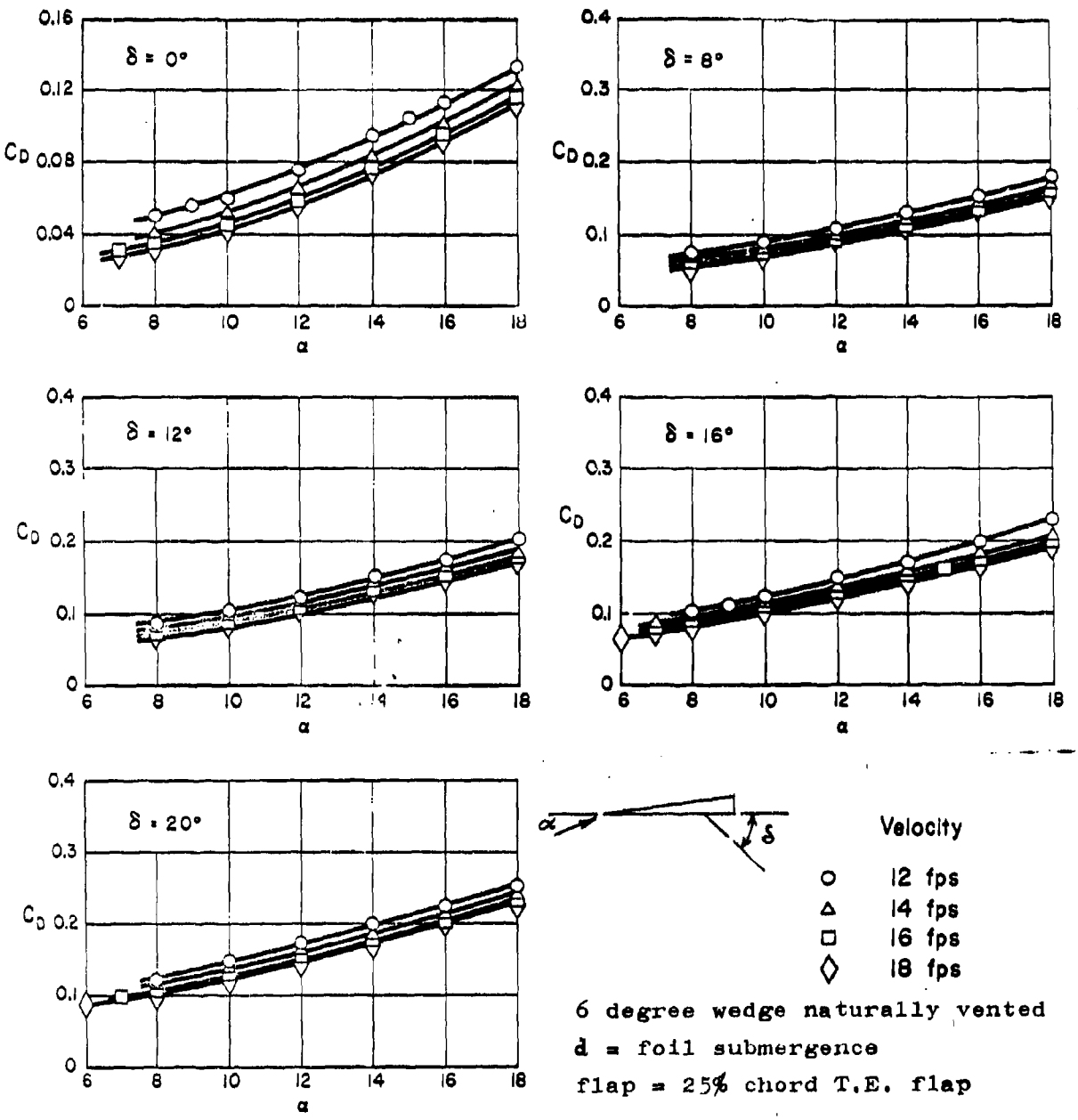

Fig. 57 (b) Variation of Steady Drag Coefficient with Angle of Attack, AR = 2, d/c = 1

Ref: U. of Minnesota St. Anthony Falls Rept. 68 Fig. 3

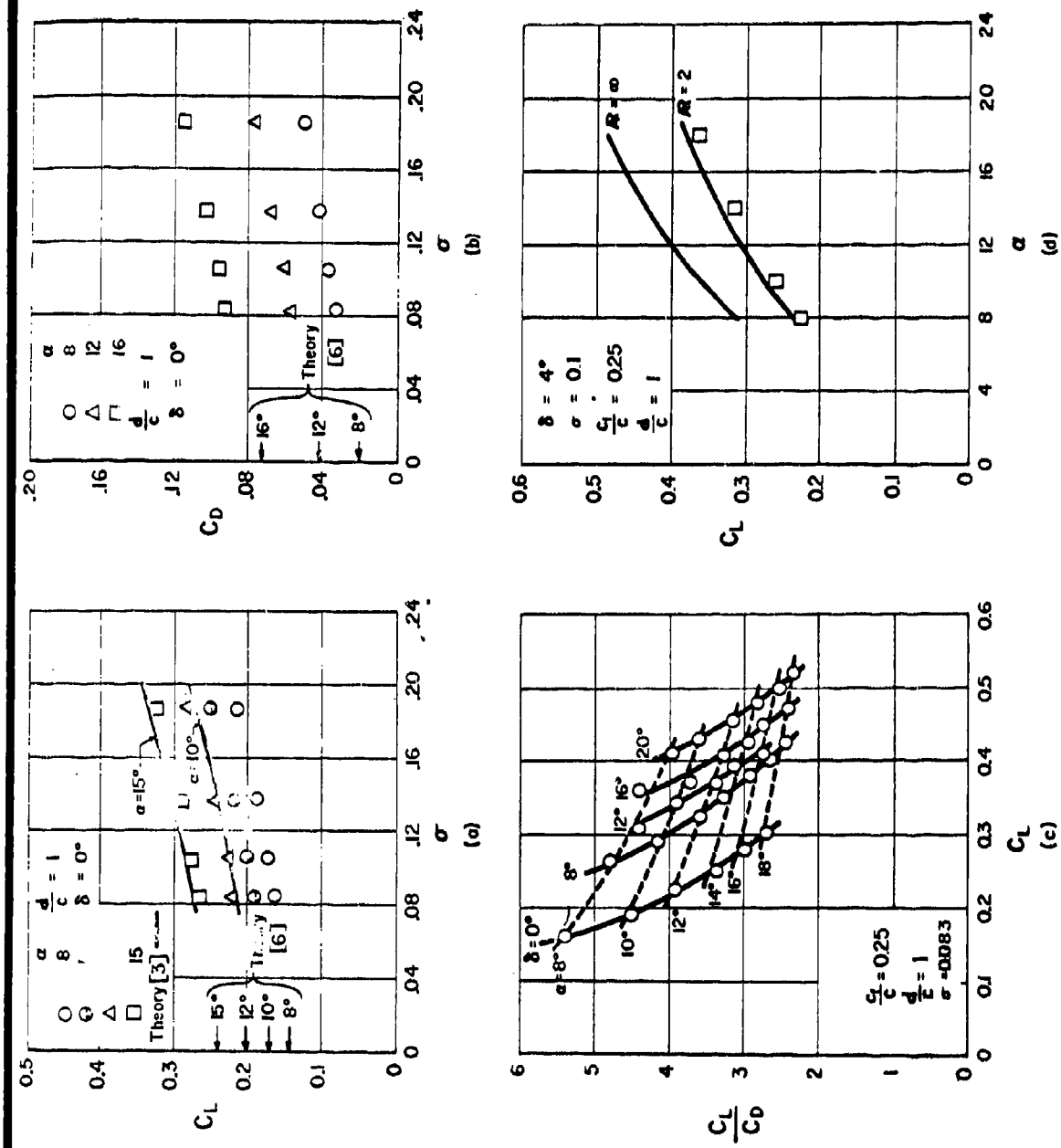

Fig. 58 - Comparison of Steady Force Data with Theory for AR = 2 foil

6 degree wedge naturally vented
d = foil submergence
flap = 25% chord T.E. flap

Ref: U. of Minnesota St. Anthony Falls Rept. 68 Fig. 9

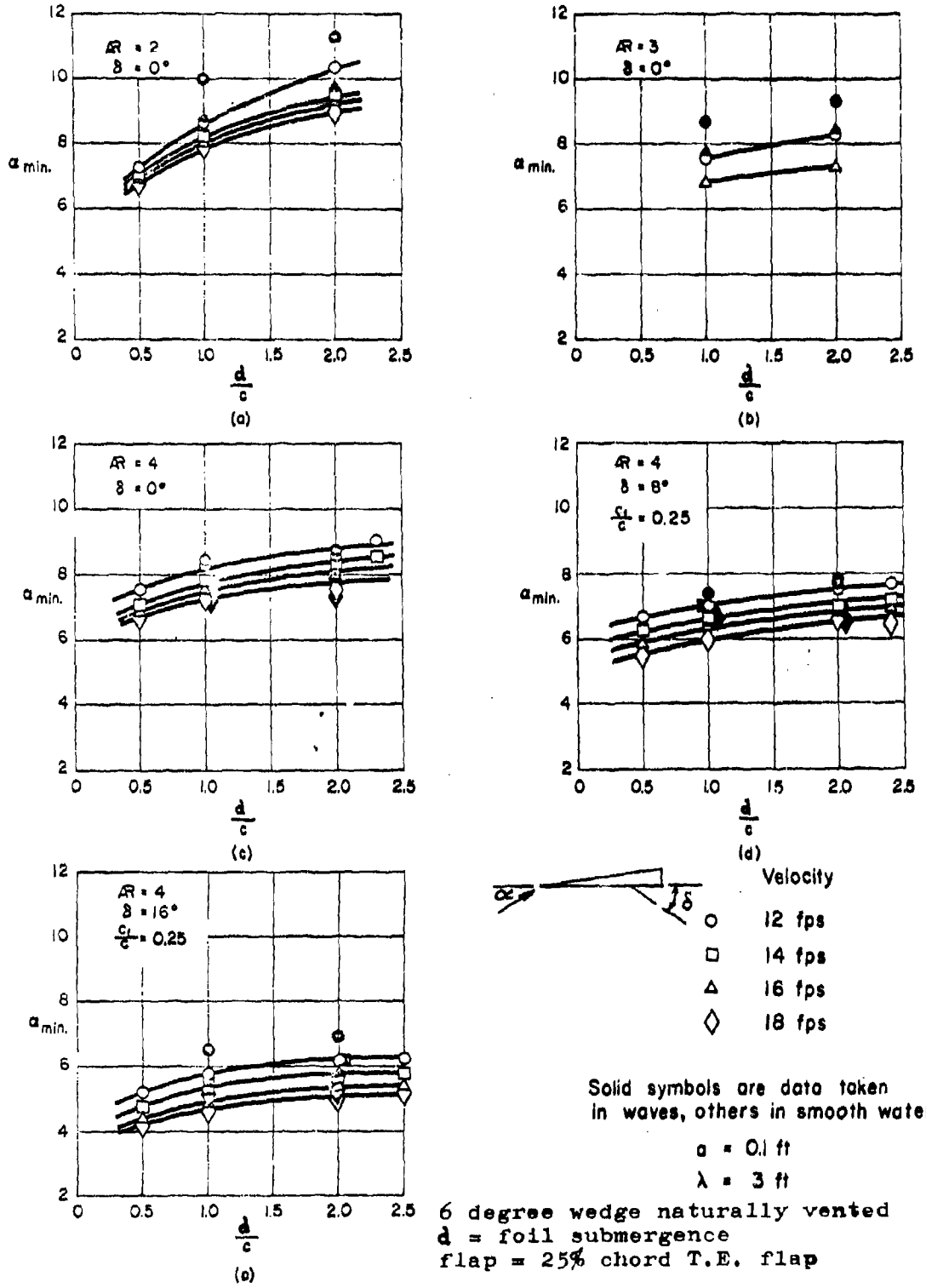

Fig. 59 - Minimum Angle of Attack Required to Maintain a Fully Developed Cavity in Smooth and Rough Water

IV. Strut Configuration Data

A. Design factors affecting strut selection

Selection of a strut to support the airplane on the hydrofoil will depend upon the following factors:

1. Airplane gross weight
2. Aerodynamic lift curve
3. Take off thrust
4. Hydrodynamic drag of entire airplane including estimated foil system drag
5. Hump and lift off speeds
6. Lift and drag characteristics of foil for all operating conditions
7. Type of hydrofoil system

The strut must be designed to achieve structural soundness within acceptable performance boundaries. The main considerations for strut design are: low side forces, low drag, provision for venting the hydrofoil, adequate structural rigidity, and resistance to flutter.

B. Drag

Drag is most critical in the region of hump speed, where the unporting phase of take off begins. If sufficient excess thrust exists at hump speed to provide necessary longitudinal acceleration, strut drag requirements will be reduced in importance.

C. Side Forces

Strut side forces must be kept as low as possible to minimize highly undesirable aircraft rolling and yawing moments. For this reason, struts should be made from hydrofoil profile shapes that develop as little lift as possible. The most effective configuration is a supercavitating strut having a relatively large leading edge wedge angle, flat sides with relatively high thickness ratio, and a blunt trailing edge. The blunt trailing edge provides early separation and a path for ventilating air to the foil. The relatively blunt leading edge induces early cavitation and a cavity wide enough to completely surround the strut. Any yawing of the strut should then provide strut clearance from the cavity boundry. Under these conditions, the side loads on the strut are minimal. The actual configuration must take drag into consideration, while the final design will be a compromise between drag, side forces, and structural rigidity.

D. Typical Strut Cross-Section Shapes

Figure 60 shows two typical struts; one a streamlined subcavitating shape with a blunt trailing edge and the other a rectangular supercavitating cross-section with a wedge leading edge.

E. Subcavitating Struts

Figures 61 through 67 apply to struts that are fully wetted, ie. cavitation is absent. They provide a breakdown of the various drag components and spray height. This data permits calculation of the total strut drag and the spray height for a non-yawed condition. Side force can be approximated by using the subcavitating lift data for the DTMB series HF-1 foil from Figure 23 for the appropriate aspect ratio.

The drag of a subcavitating strut can be divided into profile drag, wave drag and spray drag:

1. Profile Drag; Applies to a section in two dimensional flow and is the total drag for fully submerged struts (pre-hump speed). This term is the sum of shear and viscous pressure forces.

2. Wave Drag and Spray Drag; For surface piercing struts (post-hump), wave and spray drag are two additional surface effect drag terms.

Figure 61 presents the profile drag for three NACA airfoils (with varying thickness and size) plus one ogive section, versus Reynolds Number. A comparison is also made with the skin friction drag of a flat plate surface. Figure 62 shows the ogive strut data in more detail. Figure 63 provides wave drag versus Froude Number, and shows this factor becomes insignificant at higher speeds (for example, above approximately 20 feet per second for a strut with a one foot chord). Figure 64 presents spray drag data for struts of varying thickness ratios. Figure 65 is a plot of the residual drag for a typical strut, defined as the total drag minus the profile drag; or in other terms, the spray drag plus the wave drag.

For speeds greater than 20 feet per second, where the wave drag diminishes, the residual drag is approximately equal to the spray drag. This is the region of interest for a seaplane, since unporting will occur at speeds above 20 feet per second. Figure 66 shows the direct influence of thickness ratio on profile drag, while Figure 67 provides spray height information versus speed.

F. Supercavitating Struts

For supercavitating struts, Figure 68 presents drag coefficients for varying leading edge angles; the leading edge of the wedge is the only portion of the strut in contact with the water. The cavity left behind provides the boundary wall which limits the size of the strut. Any size or shape strut can be introduced inside the cavity without affecting the drag or side force. Figure 69 provides the cavity width, while Figure 70 presents cavity length information. The effect of strut yaw (with the strut remaining inside the cavity boundry) must be considered when selecting leading edge angle.

With this data, it is possible to select a strut configuration providing the desired performance and structural strength. This is a preliminary step toward testing the system for further refinement.

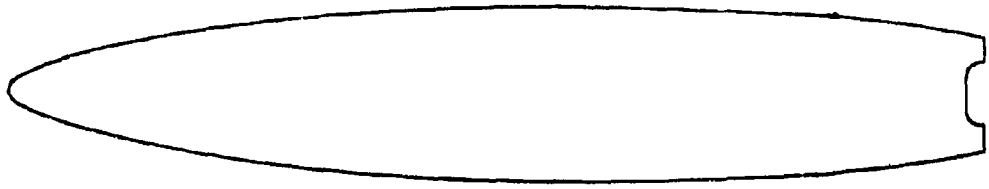

Subcavitating Strut

Ref: Thurston Aircraft Corp. Strut No.2
TAC Report No. 6702-3 Feb 1967 Fig. 3

Supercavitating Strut

Fig. 60

STRUT PROFILE DRAG COEFFICIENTS

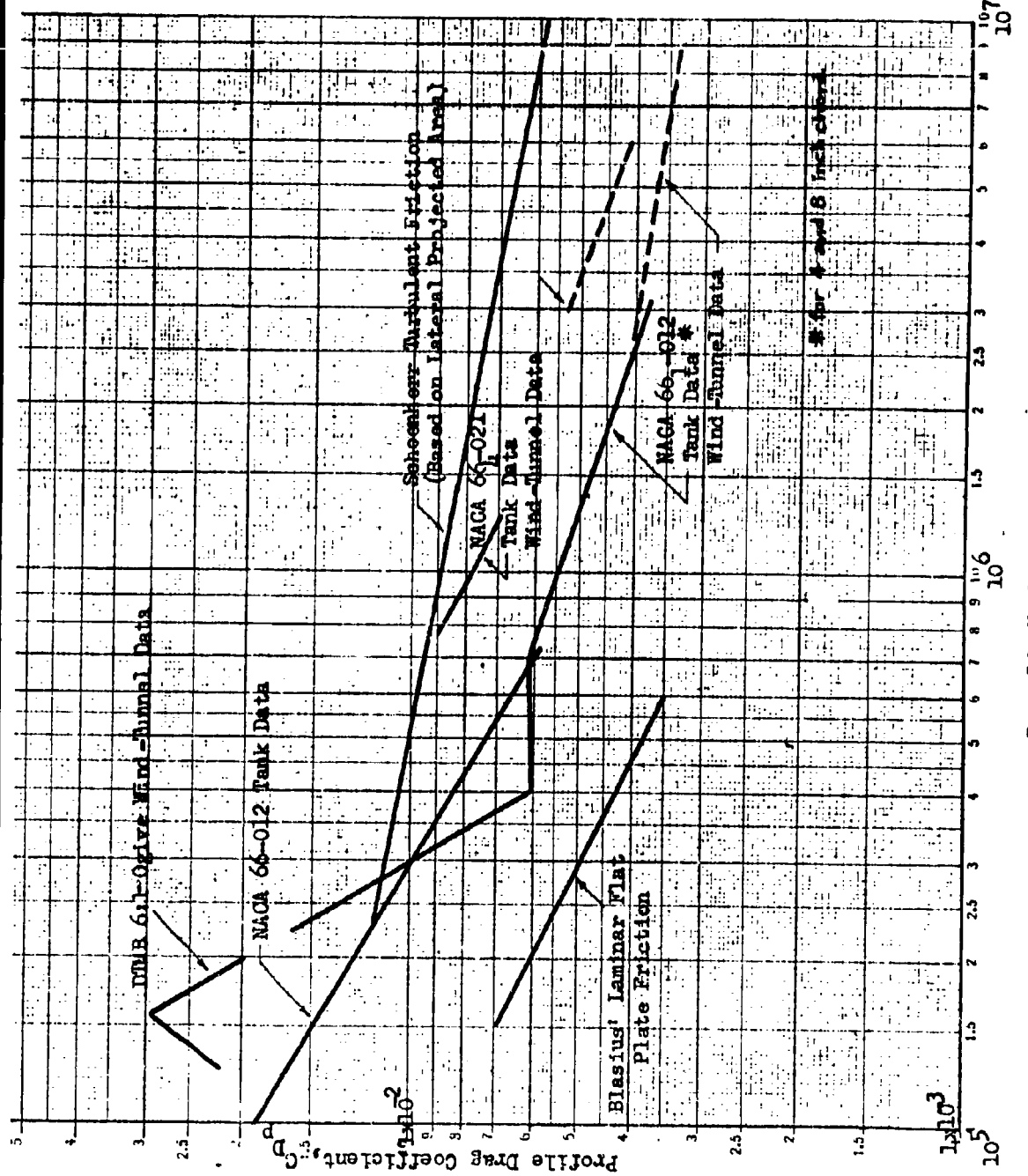

Fig. 61

Ref: Davidson Lab (SIT) Rept R-596 Fig. 2

PROFILE DRAG COEFFICIENT FROM DTMB WIND-TUNNEL TEST OF AN OGIVE STRUT HAVING A CHORD OF 11.90 IN. AND A THICKNESS OF 2 IN. AT ZERO YAW

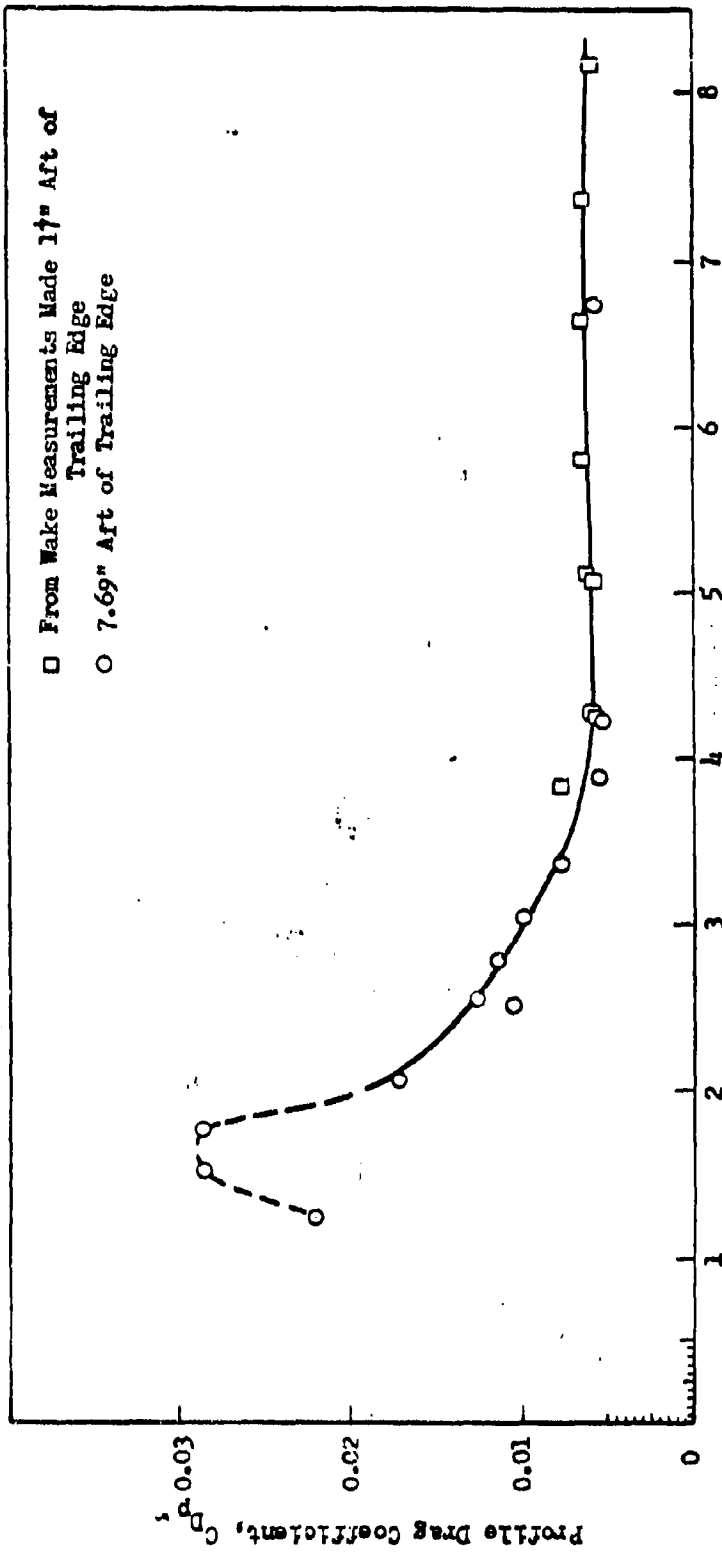

Fig. 62

Ref: Davidson Lab (SIT) Rept R-596 Fig. 5

VARIATION OF THEORETICAL WAVE DRAG COEFFICIENT
AT HIGH FROUDE NUMBERS FOR SLENDER STRUTS HAVING
DOUBLE-SYMMETRIC CIRCULAR ARC SECTIONS

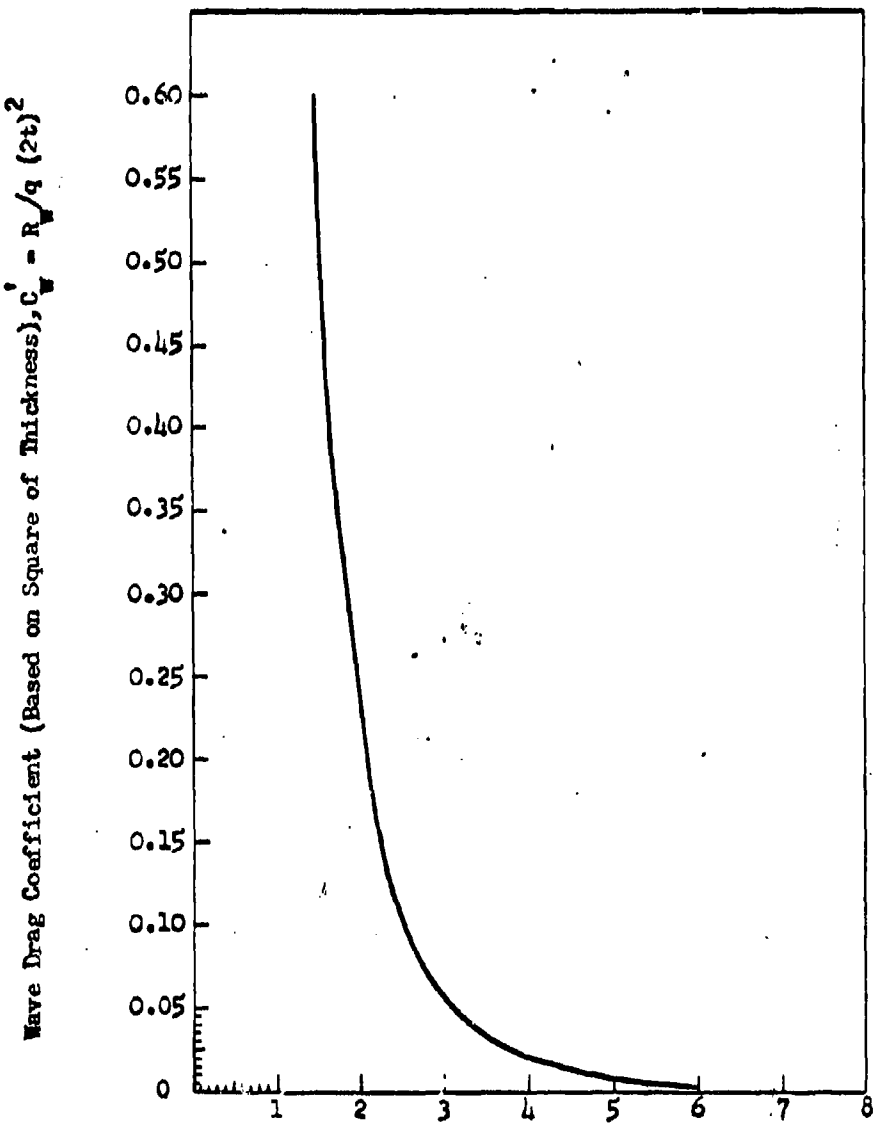

Fig. 63

Ref: Davidson Lab (SIT) Rept R-596 Fig. 1

RESULTS OF GRAPHICAL DETERMINATIONS
OF SPRAY DRAG FROM VARIOUS SOURCES

Reference: Kaplan P., Stevens Inst. of Techn.
Letter Report No. LR-488, 1953
and
Davidson Lab (SIT) Rept R-596 Fig. 4

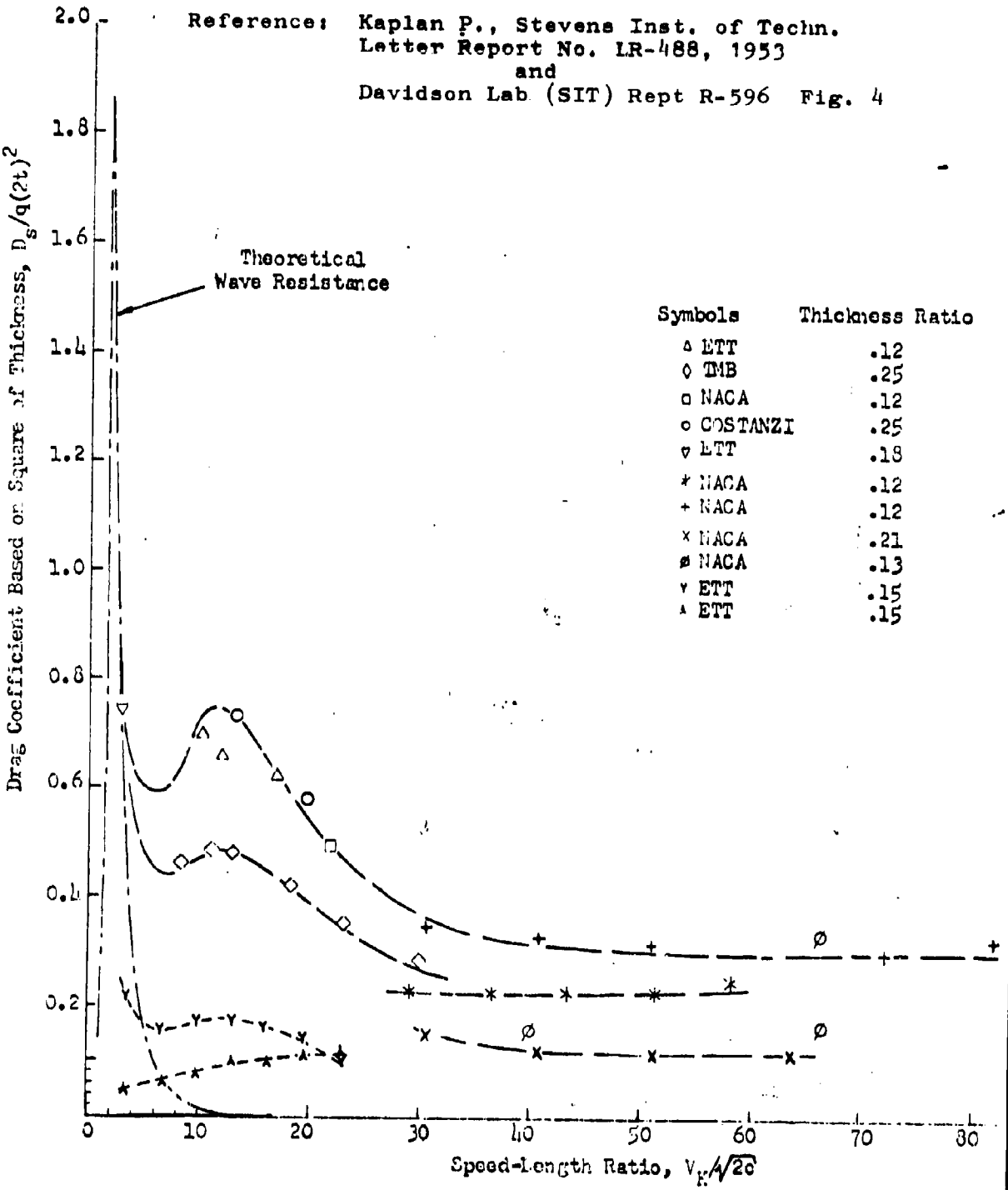

Fig. 64

FIG. 65 TYPICAL STRUT RESIDUAL DRAG COEFFICIENT

NOTE: (1) RESIDUAL DRAG = TOTAL DRAG - PROFILE DRAG

(2) FOR $F > 3$ ($V > 20$ for $c = 1$ foot) RESIDUAL DRAG $\approx$ SPRAY DRAG

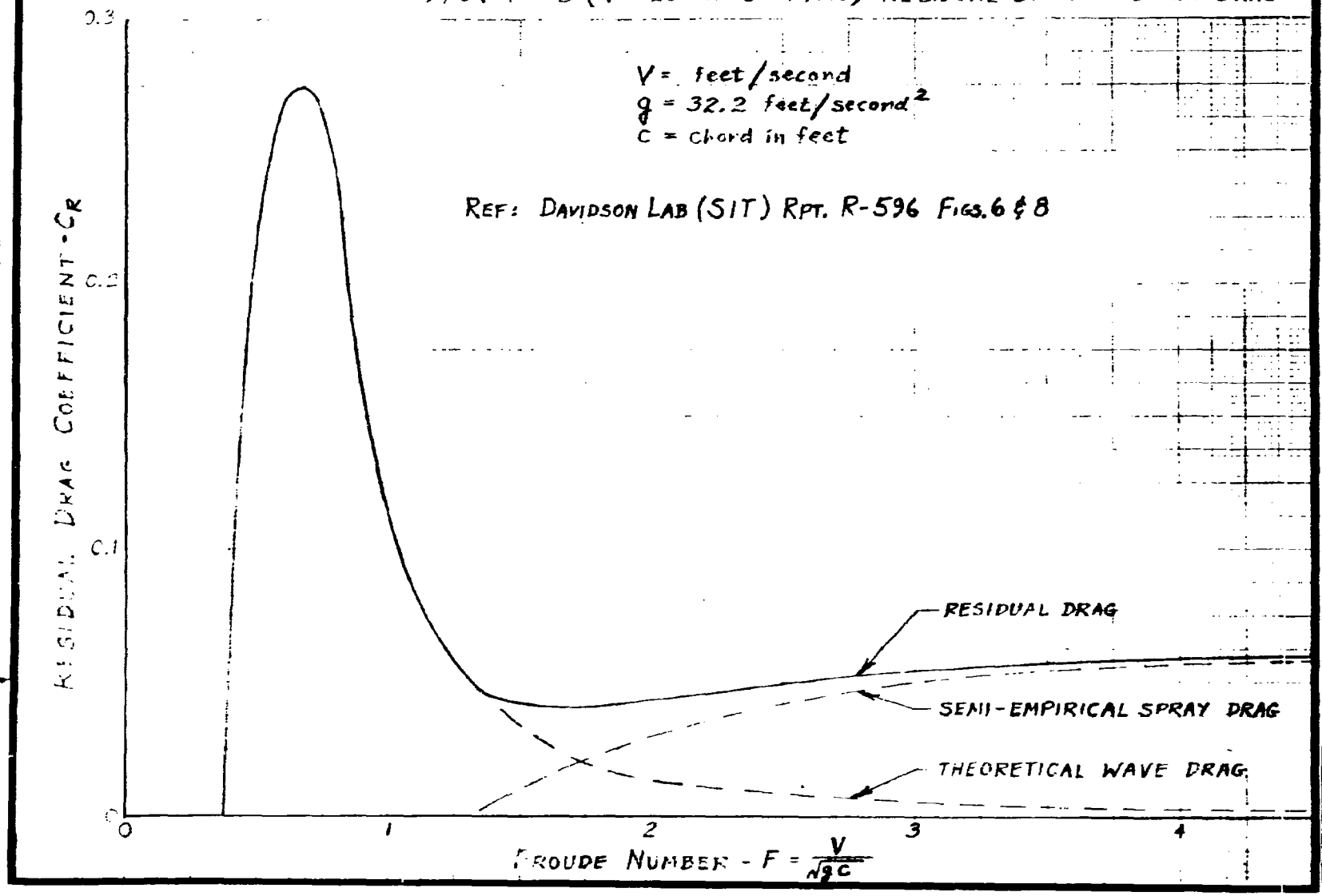

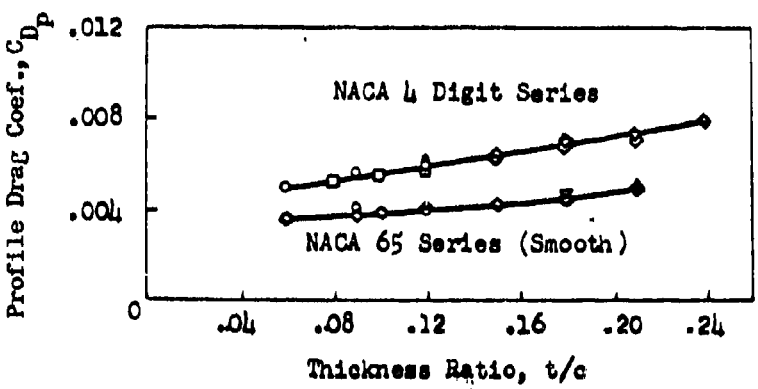

Fig. 66

PROFILE DRAG OF TWO SECTIONS AS A FUNCTION OF THICKNESS RATIO

Ref: Davidson Lab (SIT) Rept. R-596 Fig. 3

and

Theory of Wing Sections, Abbott and Doenhoff McGraw Hill 1949, pp. 152-3

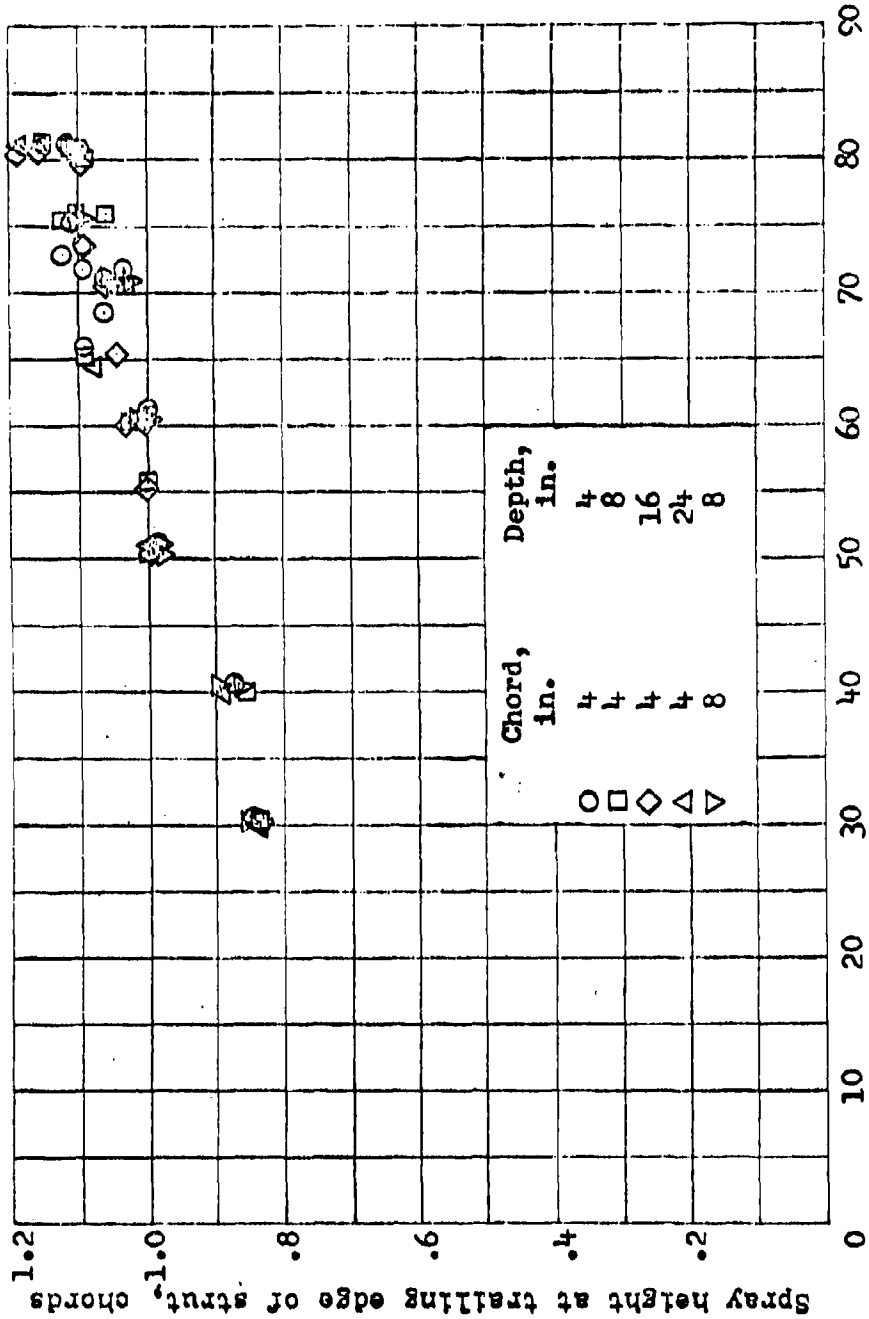

Figure 67 Spray height at trailing edge of strut. NACA 65$_1$-012 airfoil section; angle of rake, 0°.

Ref: Davidson Lab (SIT) Rept R-596 Fig. 9 and NASA TN 3092

SUPERCAVITATING
TWO AND THREE DIMENSIONAL DRAG COEFF. FOR STRUTS WITH VARIOUS LEADING EDGE ANGLES

$$\sigma = \frac{P_\infty - P_K}{\frac{1}{2}\rho V_\infty^2} = 0$$

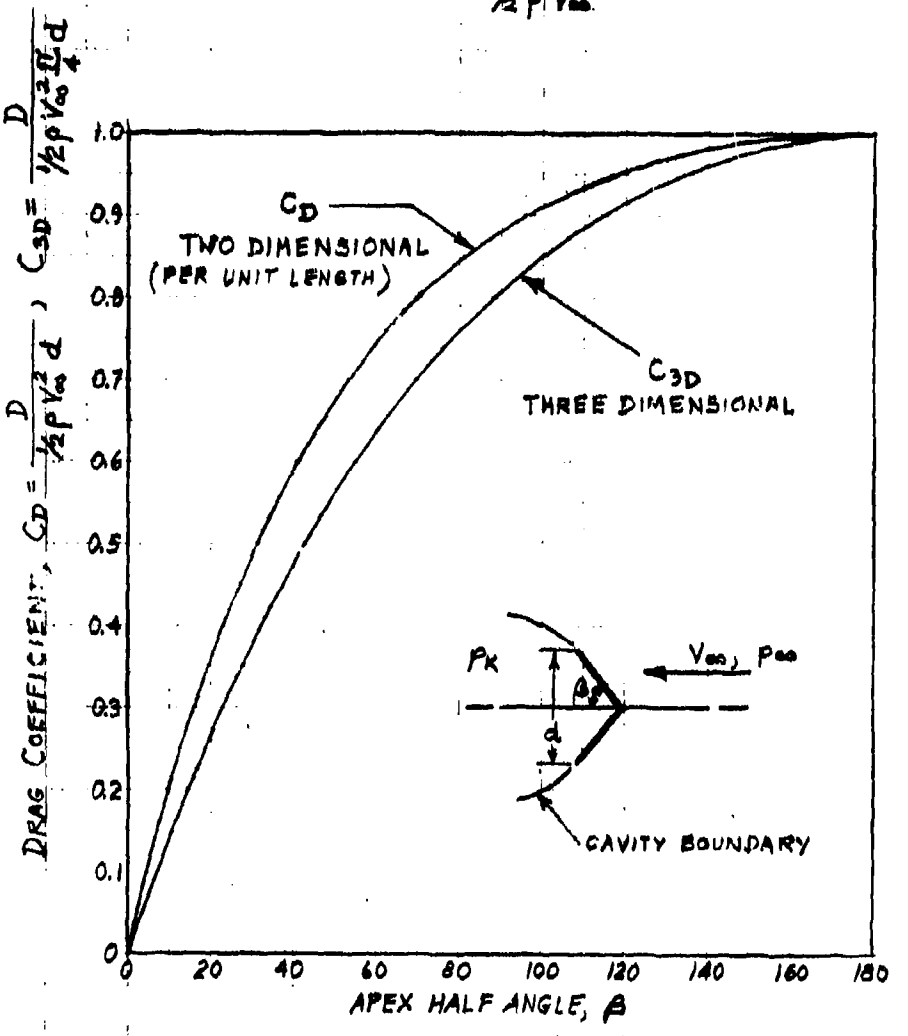

Fig. 68

Ref: Cal Tech Rept No. 47- 4 Fig. 15

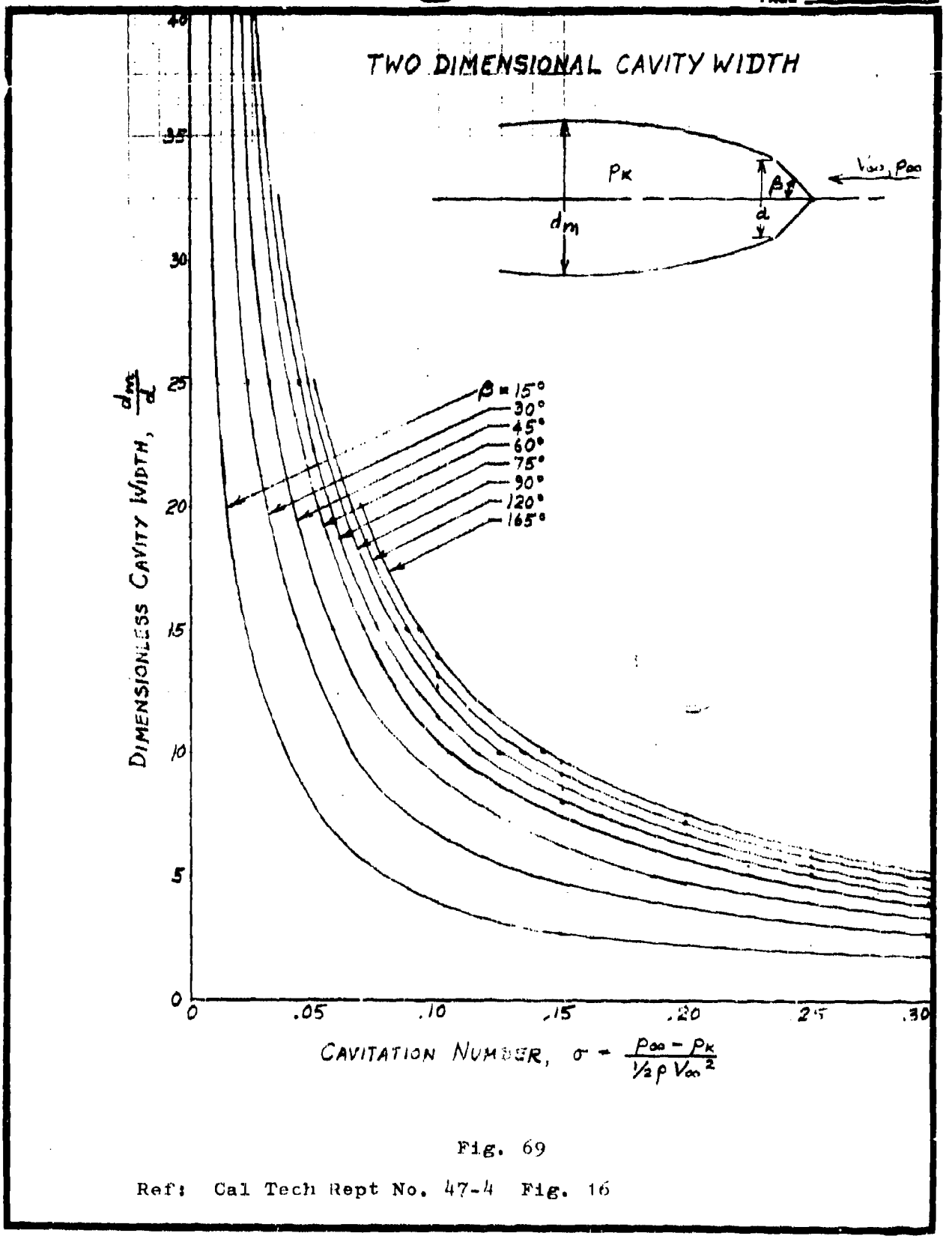

Fig. 69

Ref: Cal Tech Rept No. 47-4 Fig. 16

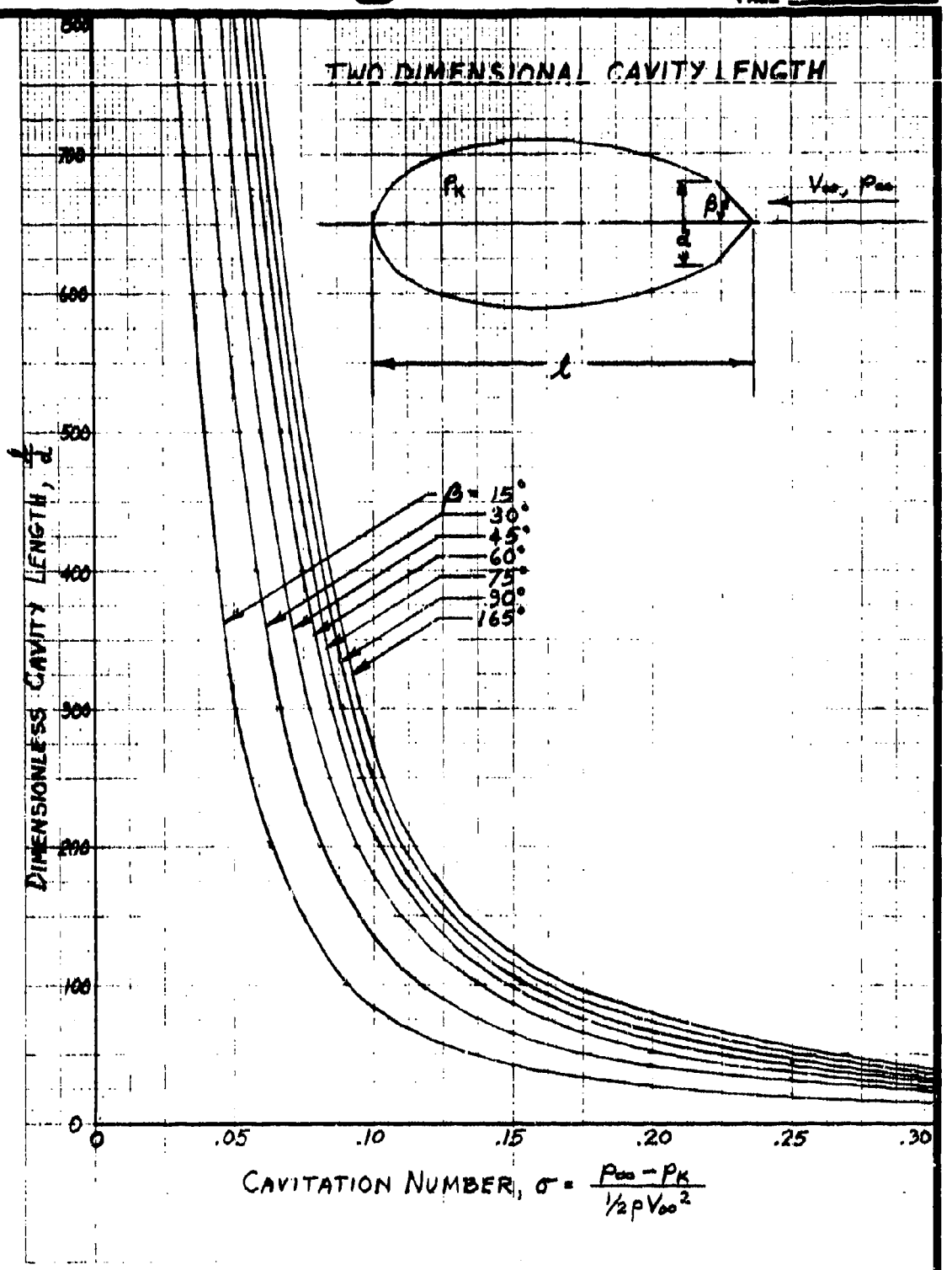

Fig. 70

Ref: Cal Tech Rept. No. 47-4 Fig. 17

V. Full Scale Hydrofoil Test Results

A. U.S. Navy JRF-5G Equipped with Grunberg Supercavitating Hydrofoil System

Under U.S. Navy sponsorship, during 1957 to 1963, the Edo Corporation designed, installed and flight tested a Grunberg supercavitating hydrofoil system on a JRF-5G (Grumman Goose) amphibian. Subsequently during 1963 and 1964 this airplane configuration was further tested and evaluated by the U.S. Navy at the Naval Air Test Center, Patuxent River, Maryland. Front and side views of the installation are given in Figure 3. This installation used the largest supercavitating hydrofoil built at that time and was the first application of a supercavitating hydrofoil to an airplane. References 42, 43 and 44 cover the work done by Edo, while reference 139 reports on the flight test evaluation performed by the Navy.

The Grunberg supercavitating hydrofoil system used on the JRF-5G was developed jointly by the Office of Naval Research, National Aeronautics and Space Administration and the Bureau of Naval Weapons. The system consists of a Tulin supercavitating surface-piercing hydrofoil (C_{l_d}=0.2) near the airplane cg and two planing bow skids, Figures 3 and 71. The bow skids were incorpated for the dual purposes of properly trimming the airplane during unporting and to prevent the airplane from diving in case of hydrofoil failure. For an operational installation, the hydrofoil would be located slightly further forward with the bow skids eliminated.

The hydrofoil was constructed of AISI 416 stainless steel heat treated to 150,000 psi tensile strength. For the purpose of providing corrosion and erosion resistance, a hard electro-plated nickel coating was applied .003 inches thick over the entire foil.

The test airplane was instrumented with a photopanel, oscillograph, and flight test boom. Water speed data were derived from airspeed recordings and wind information taken by an outside observer. The hydrofoil and skid struts were equipped with strain gauges to measure water impact loads.

The bow skids and hydrofoil could be raised and lowered hydraulically to permit operation on land or water. Land operation was limited to taxiing performed with the skids and foil raised. The main landing gear oleos were extended and stiffened to provide adequate ground clearance. Water entry was gained by taxiing down a ramp: once waterborne, the skids and foil were lowered and locked. The skids and foil remained down and locked for all water take offs and landings, as well as all flight work. Raising the bow skids in flight would make the airplane pitch up uncontrollably. The hydrofoil could be raised in flight and would permit an emergency runway landing on the stiffened landing gear in a three point attitude (to provide a ground clearance of the lowered bow skids).

A. U.S. Navy JRF-5G Equipped with Grunberg Supercavitating Hydrofoil System (Continued)

The take off maneuver was difficult to accomplish due to marginal excess thrust plus marginal stability and control existing during unporting. This, of course, was the result of the airplane not being specifically designed for hydrofoil operation coupled with the large amount of drag exhibited by this particular hydrofoil system. The bow skids created considerable spray when approaching and during hump speed, necessitating complete dependence upon the flight instruments for control of the airplane. Airborne, the airplane was nearly neutrally stable, both longitudinally and directionally, due to the large bow skids and supporting strut area. Landing technique was similar to that of a conventional seaplane and was different only because of the marginal stability of the airplane exhibited during approach.

In the hydrofoil planing condition, the pitch attitude of the airplane could be varied from the lower limit, where the bow skids contacted the water, to the upper limit, determined at low speeds by elevator control limit and at high speeds by bouncing or a heaving motion of the airplane. Figure 72 shows trim angle data, plotted against speed and the upper boundary for bounce-free operation. Bouncing occured on nearly all landings regardless of the airspeed, rate of descent and wave height. Under calm water conditions, the bouncing could be prevented by keeping sink rate and airspeed to a minimum at touch down and immediately decreasing the pitch attitude after touch down to below the bounce boundary.

When planing on the hydrofoil, the JRF-5G tended to diverge slowly from a selected heading and diverge rapidly from a selected bank angle. These tendencies, coupled with weak directional and lateral control effectiveness at the low speed end of the planing phase, required many large, rapid aileron and rudder control inputs. Both directional and lateral control power improved from barely sufficient at low speeds to satisfactory at take off speed.

The power required to plane on the hydrofoil decreased from an estimated maximum of 760 BHP at hump speed (21 knots water speed) to a minimum of 400 BHP in the 40 to 45 knot range. This data was determined during stabilized speed runs shown in Figure 73. Beyond this speed, the power required gradually increased to 560 BHP at 70 knots. Figure 74 shows photographs of the JRF-5G planing at various stabilized speeds, including side views of the accompanying spray patterns. Figure 75 shows the longitudinal acceleration of the airplane at various power settings. The hump speed is clearly defined at about 21 mph waterspeed, with minimum drag at 40 mph; corresponding to the minimum drag point shown in Figure 73.

Time histories of a take off and landing are given in Figures 76 and 77. It can be clearly seen that below 30 knots large rudder and aileron inputs are required to control the airplane.

Figure 78 presents impact normal acceleration at the

A. U.S. Navy JRF-5G Equipped with Grunberg Supercavitating Hydrofoil System (Continued)

airplane cg versus sink rate. Data are also presented in reference 139 for the foil loads versus sink speed. In both cases, the relation of load and acceleration is linear with sink speed.

Figure 79 shows the variation of elevator position, trim angle, bow skid bending stress and hydrofoil main strut compression load with waterspeed.

B. HRV-1 (LA-4A) Equipped with Thurston Aircraft Corporation Supercavitating Hydrofoil

Under U.S. Navy contracts, the Thurston Aircraft Corporation designed, installed and flight tested during 1966 to 1968 a single supercavitating, surface-piercing hydrfoil on a Skimmer LA-4A amphibian, page i. This airplane was designated Hydro Research Vehicle (HRV-1), and was the same aircraft used for previous hydrodynamic flight test work with hydro-skis. This installation was the first application of a single supercavitating hydrofoil on an airplane. References 128, 129 and 130 cover the hydrofoil test work performed during this program.

The HRV-1 hydrofoil was a 6.25 degree wedge with a 30 degree leading edge angle and a flow breakaway groove 1/4 inch behind the leading edge on the upper surface, Figure 80, and was cast from A356-T61 aluminum alloy. The projected planform area of 100 square inches satisfied both the desired foil loading speed requirement and the scale/weight relationship compared to a proposed HU-16 installation. Figure 81 shows a profile view of the HRV-1 with the hydrofoil extended to its maximum of 22 inches. The strut was a subcavitating streamlined shape with a blunt trailing edge, Figure 60. Two close-up photographs of the foil and strut installed on the HRV-1 are shown in Figure 82.

The test airplane was instrumented with an oscillograph recording strut loads, hull pressures, pitch angles and cg acceleration. Reference 129 shows the results of tests with the strut located at hull station 79, while reference 130 shows the results with the strut at station 96.25; the cg was located at hull station 106 for both strut locations.

A comparison of data for the hydrofoil versus the airplane basic hull showed the hydrofoil reduced the hull bottom pressures by about 35 percent and the normal acceleration factor by about 70 percent in calm water. Under conditions of one and one half to two foot waves, the hull pressures were reduced by about 50 percent and the acceleration again by about 70 percent, as discussed in Chapter VI. Hydrofoil take off times were reduced by approximately 30 percent compared to the basic hull performance figures.

B. HRV-1 (LA-4A) Equipped with Thurston Aircraft Corporation Supercavitating Hydrofoil (Continued)

The JRF-5G and the HRV-1 represent the only two hydrofoil seaplane configurations developed and tested in the United States to date, both sponsored by the Department of the Navy.

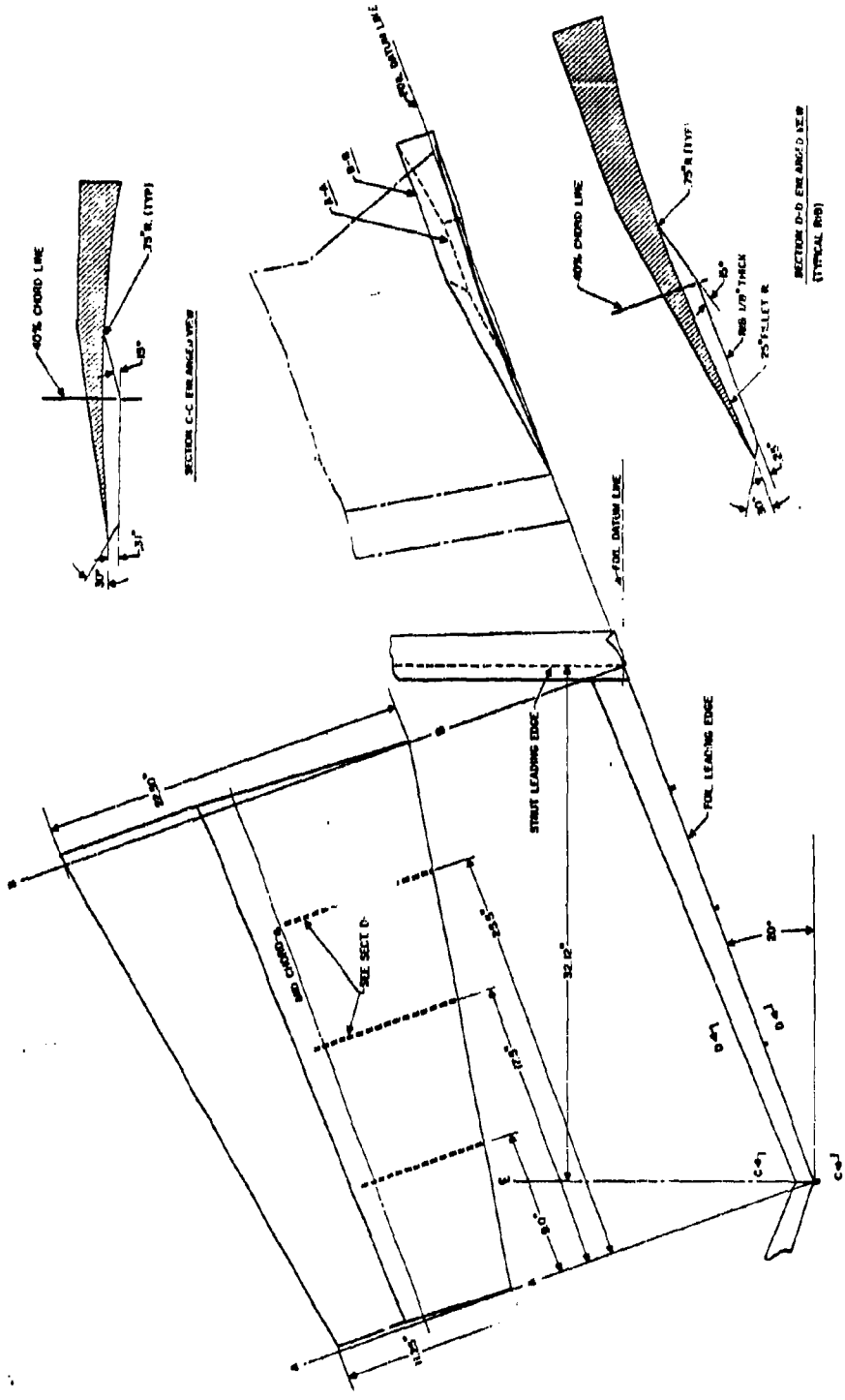

Fig. 71
JRF-5G Airplane
BuNo 37782

DETAILED DRAWING OF HYDROFOIL

Ref: U.S. Naval Air Test Center Report No. FT2121-35R-65, dated 25 July 1965

Bow Skid Configuration B
CG - 21.7% MAC
30° Flaps

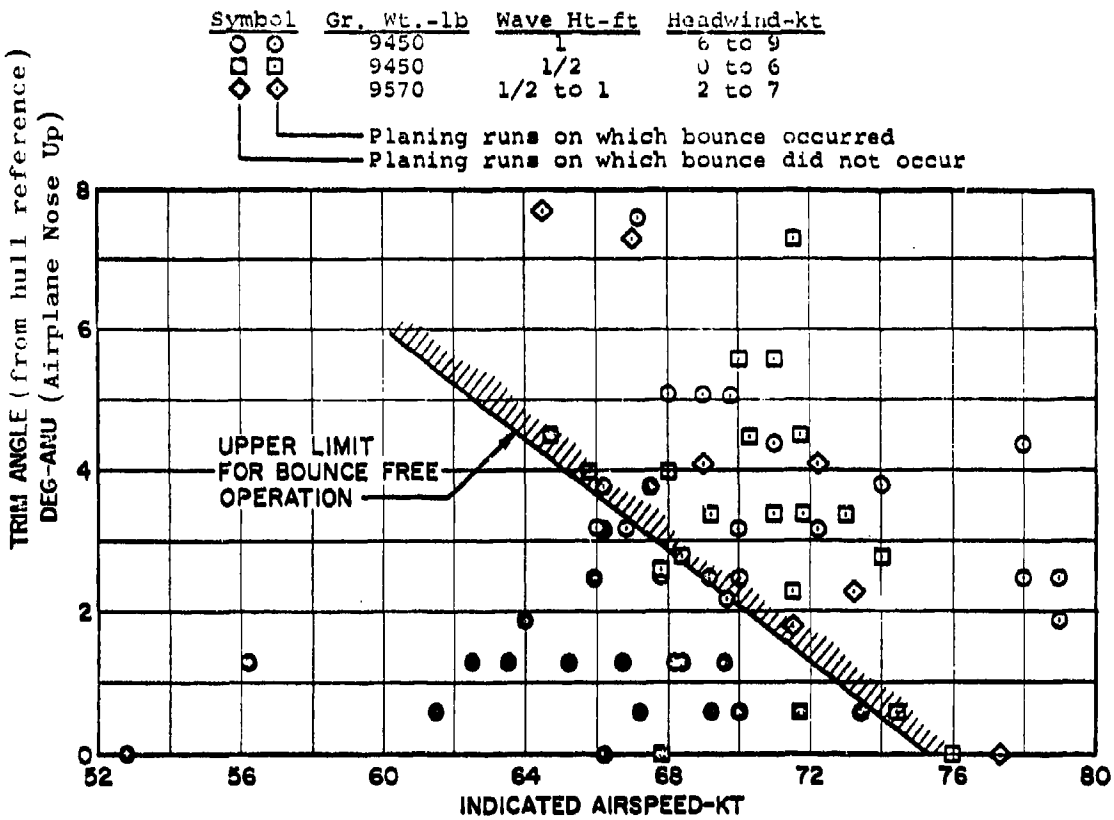

Fig. 72
JRF-5G Airplane
BuNo 37782

UPPER HYDRODYNAMIC LONGITUDINAL STABILITY LIMIT

REF: U.S. Naval Air Test Center, Report No. FT2121-35R-65, dated 25 July 1965

Bow Skid Configuration B
Gross Weight - 9,450 lb, CG - 21.7% MAC
Wave Height - 1 ft, Headwind - 5 to 10 kt
Surface Temperature - 64° F

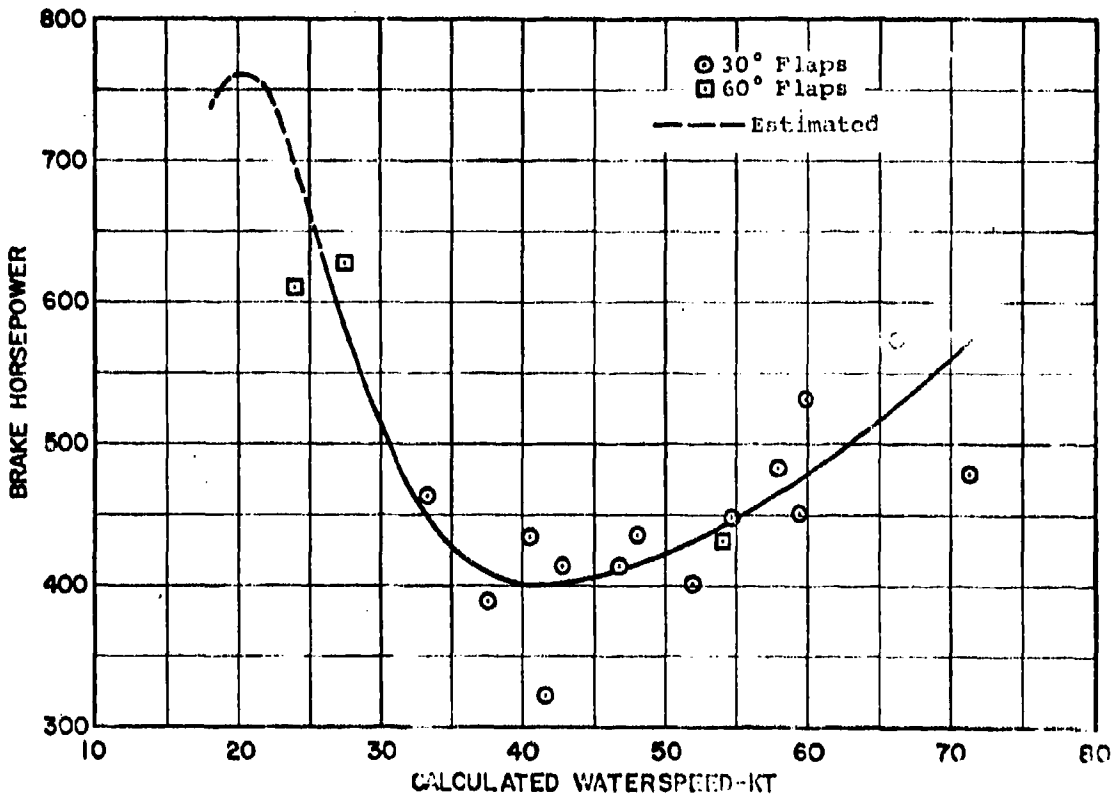

JRF-5G Airplane
BuNo 37782

POWER REQUIRED FOR PLANING VERSUS WATERSPEED

Fig. 73

REF: U.S. Naval Air Test Center, Report No. FT2121-35R-65, dated 25 July 1965

Bow Skid Configuration B
Gross Weight - 9,450 lb, CG - 21.7% MAC
Wave Height - 1 ft

Calculated Waterspeed - 26 kt
Headwind - 9.0 kt
60° Flaps

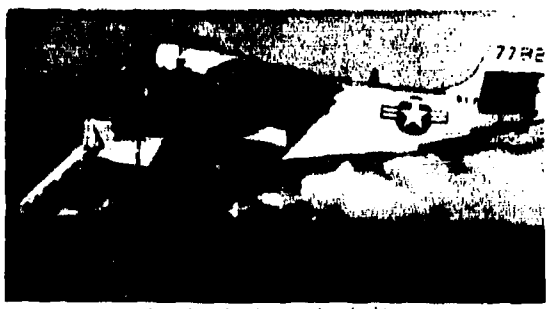

Calculated Waterspeed - 43 kt
Headwind - 9.0 kt
60° Flaps

Calculated Waterspeed - 33 kt
Headwind - 7.5 kt
30° Flaps

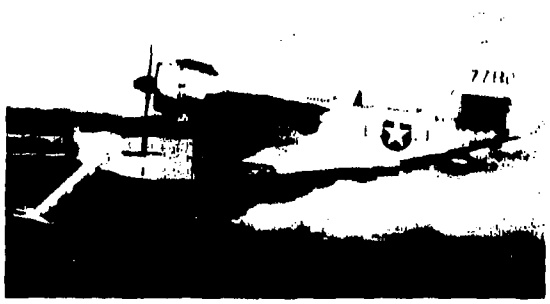

Calculated Waterspeed - 47 kt
Headwind - 9.5 kt
30° Flaps

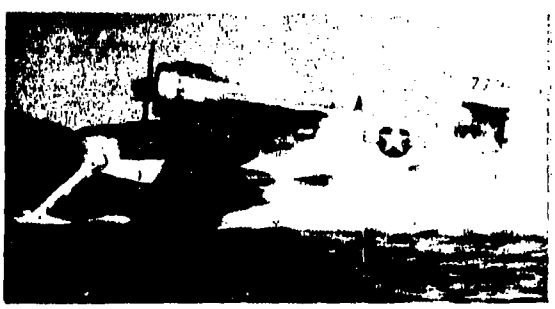

Calculated Waterspeed - 39 kt
Headwind - 8.5 kt
30° Flaps

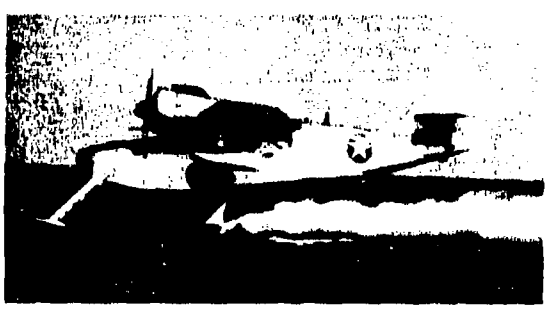

Calculated Waterspeed - 53 kt
Headwind - 7.0 kt
60° Flaps

Fig. 74
JRF-5G Airplane
BuNo 37782

SPRAY PATTERNS AT CONSTANT WATERSPEEDS

REF: U.S. Naval Air Test Center, Report No. FT2121-35R-65, dated 25 July 1965

Bow Skid Configuration B
Gross Weight - 9,390 lb, CG - 21.7% MAC
Wave Height - 1/2 ft, Surface Temperature - 58° F

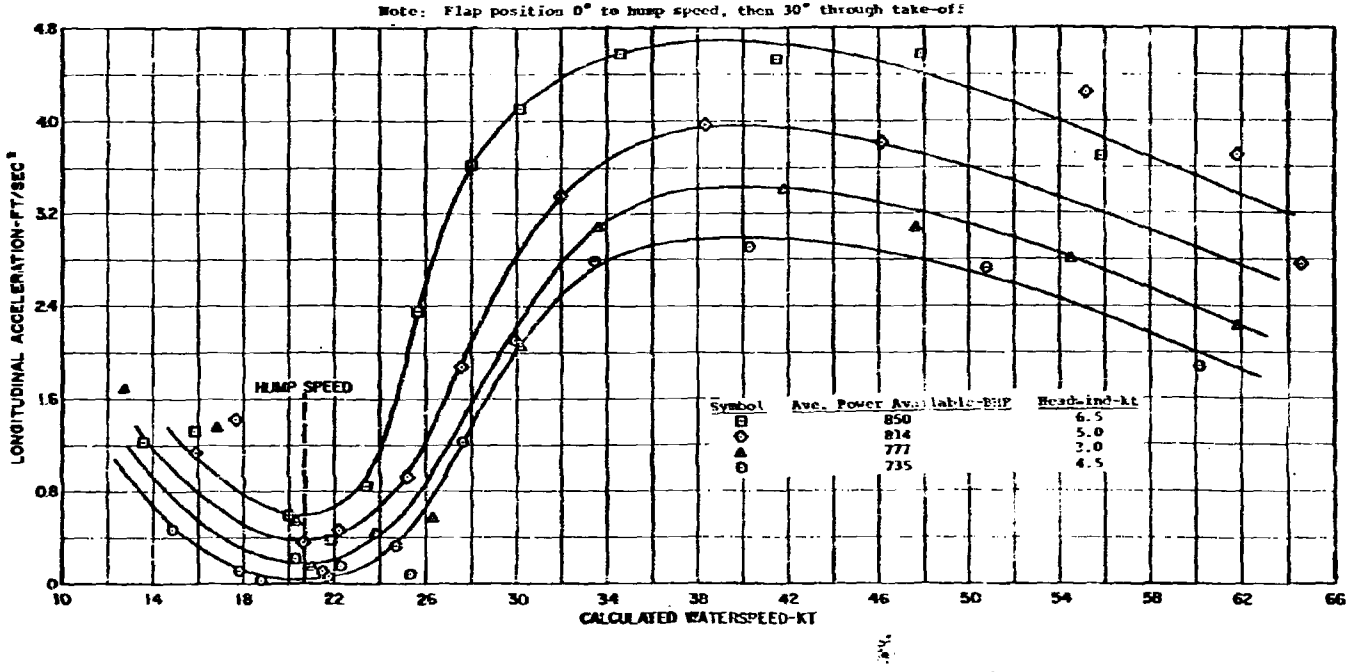

Fig. 75
JRF-5G Airplane
BuNo 37782

LONGITUDINAL ACCELERATION DURING TAKE-OFF

REF: U.S. Naval Air Test Center, Report No. FT2121-35R-65, dated 25 July 1965

Bow Skid Configuration B
Gross Weight - 9,570 lb, CG - 21.7% MAC
Wave Height - 1/2 ft, Surface Temperature - 58° F
Wind Velocity - 7 kt from 20° Left

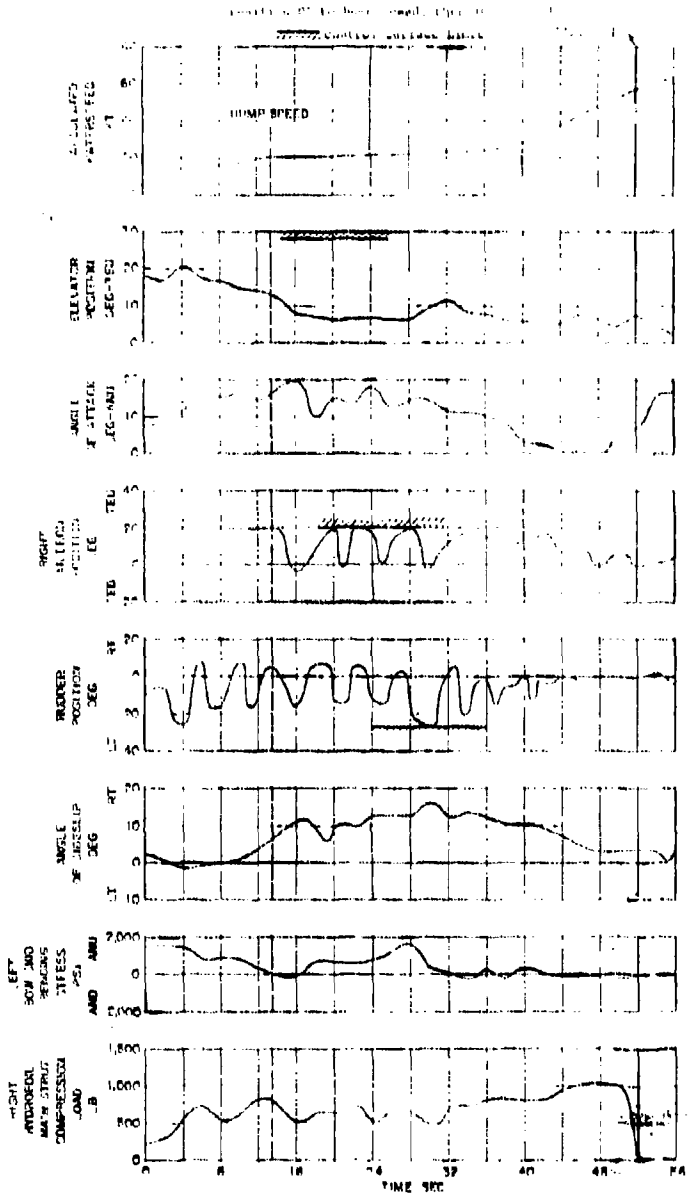

Fig. 16
JRF-5G Airplane
BuNo 37782

TIME HISTORY OF A TAKE-OFF

REF: U.S. Naval Air Test Center, Report No. FT121-15R-65, dated 23 July 1965

Bow Skid Configuration B
Gross Weight - 9,450 lb, CG - 21.7% MAC
Wave Height - 1/2 ft, Surface Temperature - 64° F
Wind Velocity - 8 kt Headwind
60° Flaps

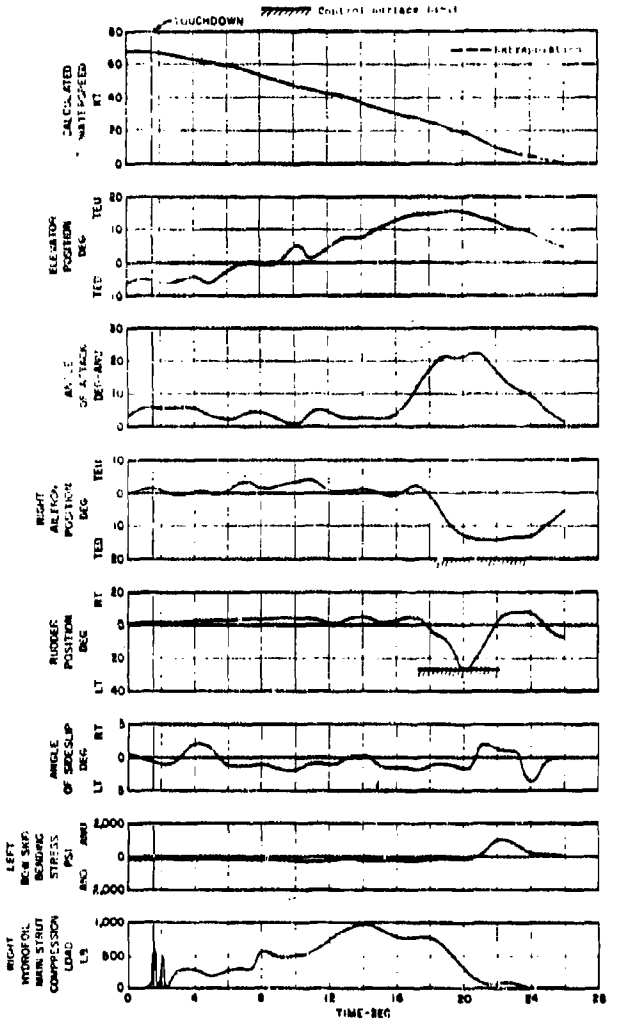

Fig. 77
JRF-5G Airplane
BuNo 37782

TIME HISTORY OF A NORMAL LANDING

REF: U.S. Naval Air Test Center, Report No. FT2121-35R-65, dated 25 July 1965

Bow Skid Configuration B
CG Position - 21.7% MAC
60° Flaps

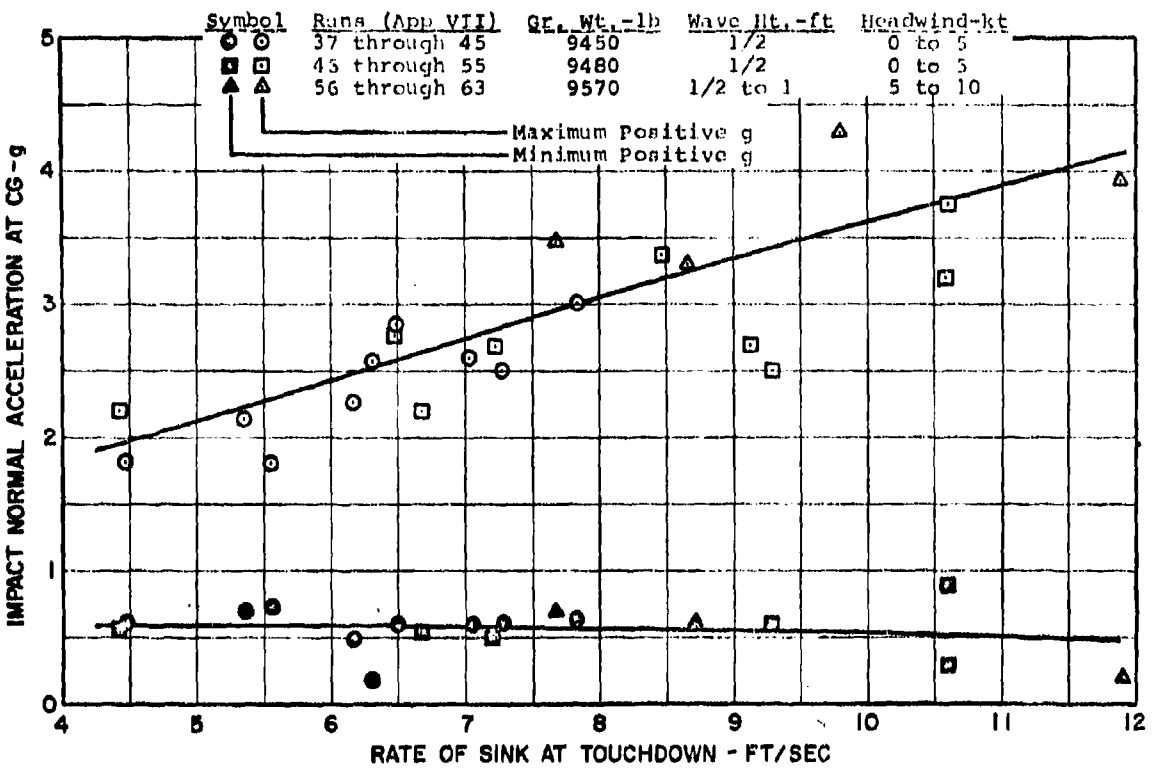

Fig. 78
JRF-5G Airplane
BuNo 37782

CG NORMAL ACCELERATION VS SINK RATE

REF: U.S. Naval Air Test Center, Report No. FT2121-35R-65, dated 25 July 1965

Bow Skid Configuration B
Gross Weight - 9,450 lb, CG - 21.7% MAC
Wave Height - 1 ft, Headwind - 5 to 10 kt

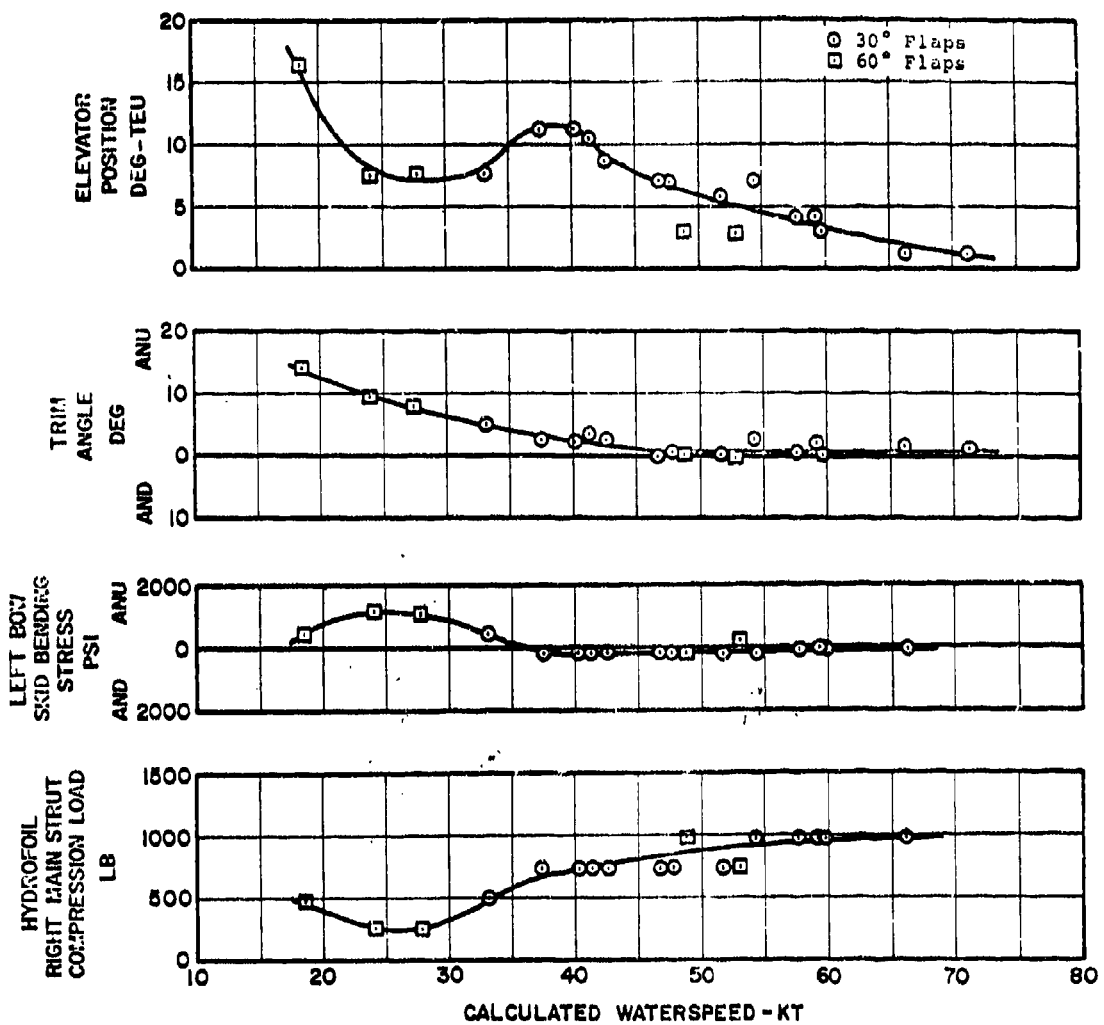

Fig. 79
JRF-5G Airplane
BuNo 37782

CONSTANT SPEED FOILBORNE CHARACTERISTICS

REF: U.S. Naval Air Test Center, Report No. FT2121-35R-65, dated 25 July 1965

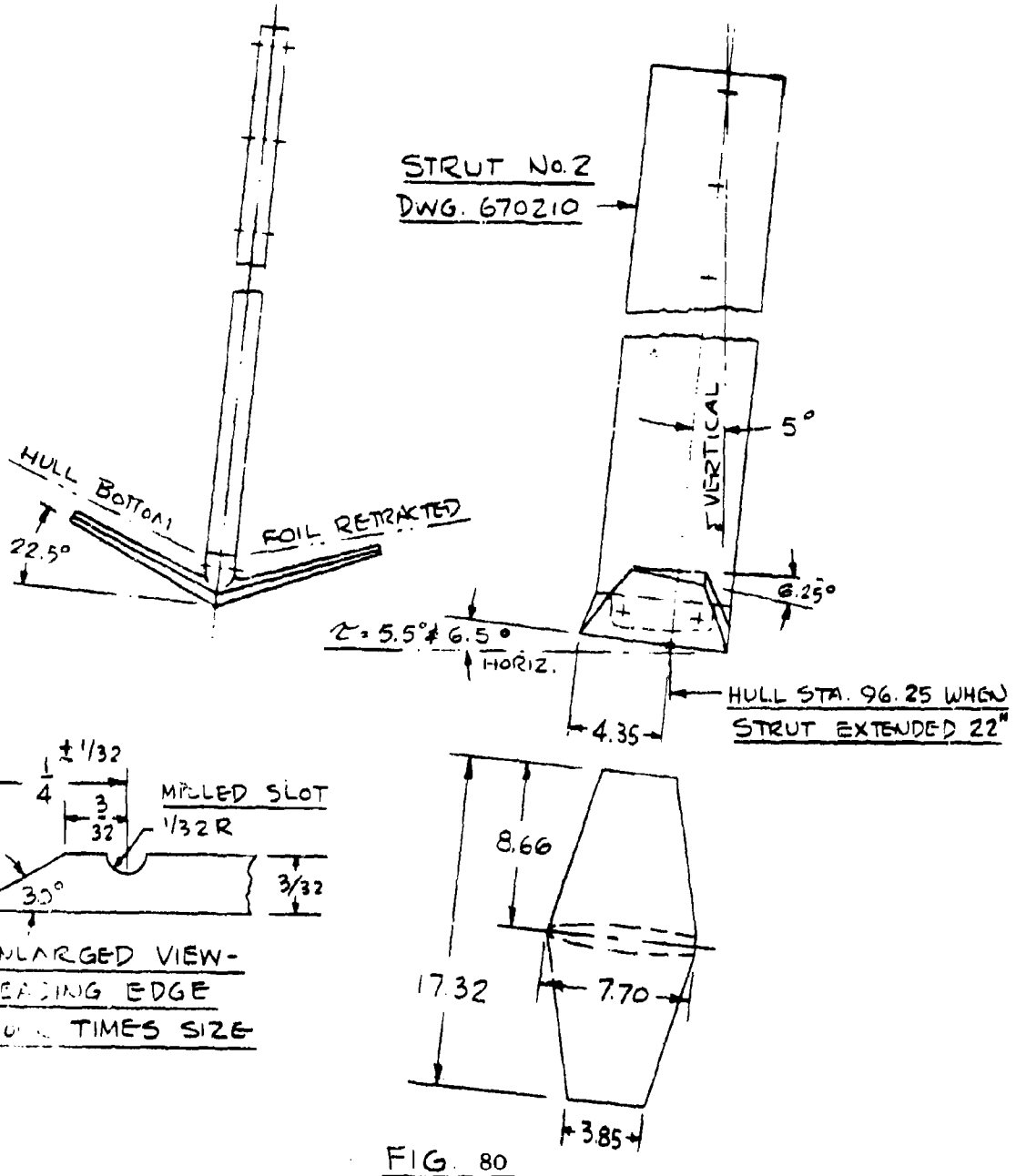

FIG. 80

HYDROFOIL NO. 1 ON STRUT NO. 2

1/8 SCALE

AFT LOCATION ANGLES TESTED

REF: Thurston Aircraft Corporation, Report No. 6902, dated February 1969 (Ref. 130).

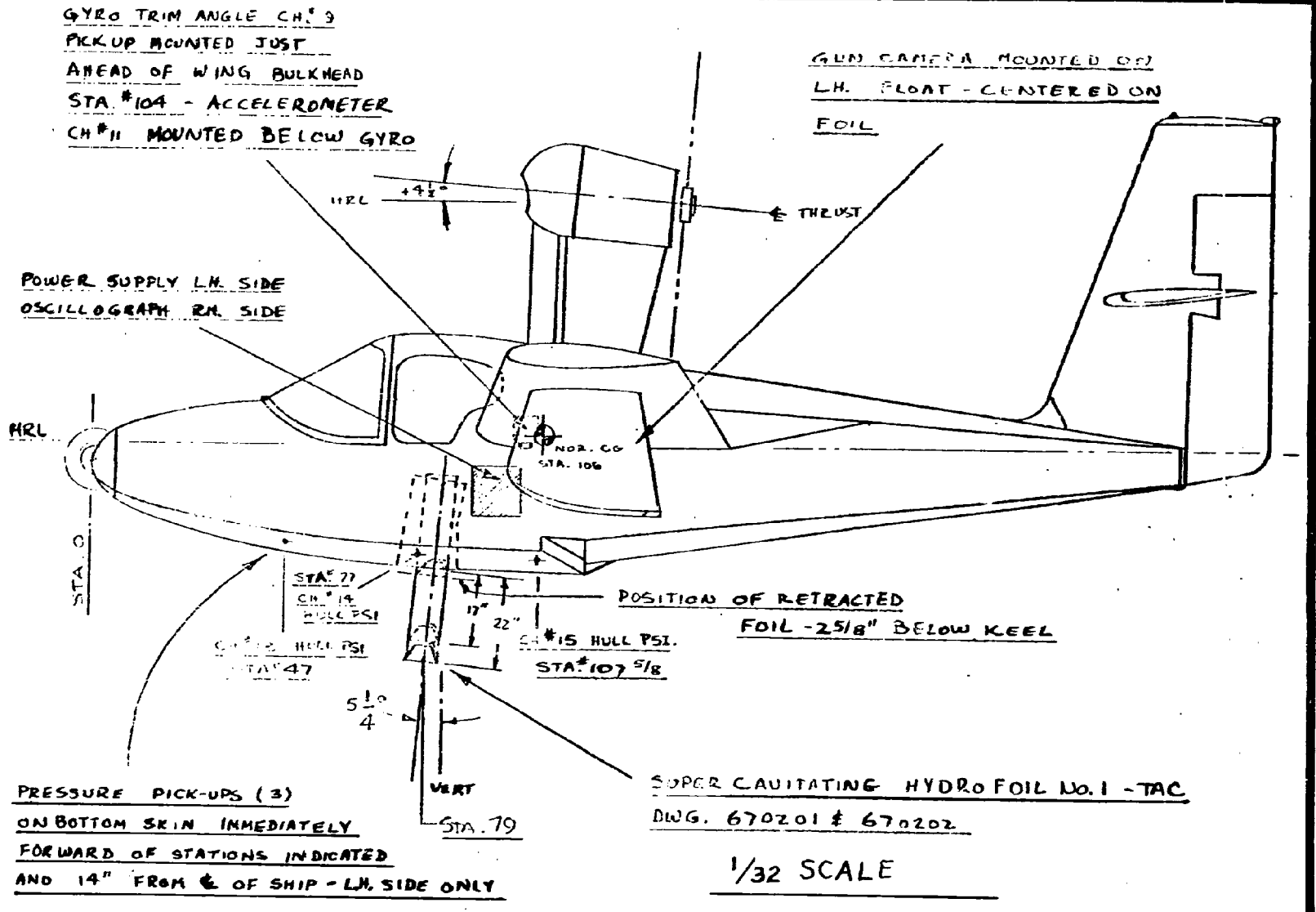

Fig. 81 HRV-1 Profile View and Instrumentation Arrangement

REF: Thurston Aircraft Corporation Report No. 6702-3, dated February 1967

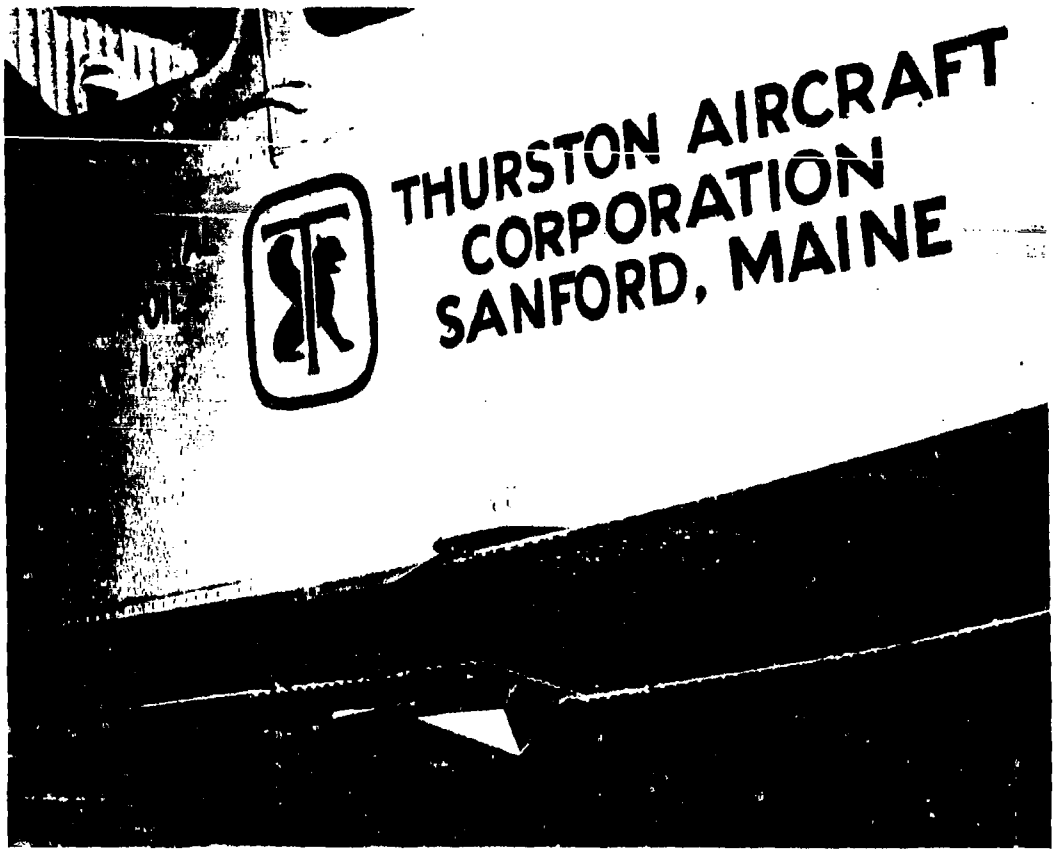

Fig.82A Hydrofoil No. 1 Retracted

Fig. 82B
Hydrofoil No. 1
Extended 22"
on Strut No. 2

(Ref. No. 129; TAC
Report 6702-3)

VI. Hydrofoil Application to Seaplane Design

A. Longitudinal Location

Development of a hydrofoil configuration for seaplane operation must be conducted parallel with the basic aircraft design. The foil longitudinal location along the hull bottom is most critical due to foil-strut L/D force vector oscillations occuring from heave, trim changes, and wave front variations experienced during take off; it is imperative that the resultant L/D vector angle does not move excessively – creating pitch trim oscillations that cannot be corrected by normal pilot control reaction.

While this operational condition is more critical for relatively small seaplanes of low mass and moment of interia compared to long range open sea boats, any sudden shift of hydrofoil resultant vector will necessitate a rapid trim correction adding to the horizontal tail load and so prolonging take off (due to increased loading of the wing and foil).

Reference 130 presents the results of an initial study concerned with the comparative location of a single surface-piercing hydrofoil on the HRV-1 test bed. Flight test data confirmed that the hydrofoil-strut combination L/D vector must be located to pass ahead of the most forward center of gravity location anticipated during seaplane operation.

The hydrofoil must be positioned with the realization that the nearer the foil-strut L/D vector approaches the seaplane cg, the greater the landing load impact factor will become relative to a more forward location. Of course, since the hydrofoil is an excellent water landing impact load alleviation device, any foil maximum landing load factor will be considerably less than that of the basic hull (Reference 129, page 16). Countering the more forward location of a foil to reduce impact loads is the additional consideration that a forward location tends to increase longitudinal pitch changes with foil lift variations during take off and will result in increased nose up pitch during the landing run out.

As an initial approximation for basic design, the single hydrofoil center of lift should be positioned .35 to .50 MAC ahead of the airplane normal cg location. The proper longitudinal location of a hydrofoil for the HRV-1 is shown on Figure 83 referred to the normal gross weight cg.

B. Extension versus Sea State Capability

While it may be properly agreed that no substitute exists for thrust and lift to reduce water contact time and run during take off, these factors cannot reduce landing impact into a rough sea to the degree possible with a surface-piercing hydrofoil. Therefore,

B. Extension versus Sea State Capability (Continued)

the amount of foil extension to provide sea state capability in rough seas becomes another major factor to be considered as the basic seaplane design develops.

Neglecting power, a hull capable of handling four foot seas should be able to negotiate eight foot waves if the hydrofoil is positioned four feet below the keel. Actually, this will not be so, since the airplane first must have the capability to climb over the hump and plane before it becomes foil borne. While excess thrust at relatively low hump speed will materially assist in reducing damaging wave impact duration, the airplane must not experience foil unporting prior to attaining sufficient speed to permit aerodynamic control about all three axes (see discussion of following Section D).

Hydrodynamically, subject to the limitation of hydrofoil support strut drag on the margin of excess thrust, a properly designed hydrofoil may be located as far below the hull as design sea state conditions require. Practically, design compromise will be necessary in the areas of handling qualities, support strut column rigidity and weight, as well as retracted storage requirements and retraction system weight.

As shown by the test results of Reference 129 and Figure 84, increasing the strut extension from 17 inches to 22 inches on the HRV-1 reduced the hydrofoil landing impact factor by 40% in rough sea conditions. Since the surface-piercing hydrofoil tends to submerge upon rough water contact, it is apparent that increased strut extension provides a greater deceleration time interval; resulting in reduced hull bottom contact velocity. (As a matter of interest, a 22 inch strut extension on the HRV-1 corresponds to a 54 inch extension for the HU-16 "Albatross" amphibian.)

While maximum strut extension is desirable for rough sea operation, intermediate extension positions should be used for take off in reduced sea state conditions. Through this procedure strut drag is reduced, permitting minimum take off run and time under conditions usually accompanied by relatively low surface wind velocities. However, it is recommended that all landings be made at maximum strut extension to reduce hull bottom plating pressure loadings.

C. Impact Load Factors and Bottom Pressures

The effect of hydrofoil extension as a landing load alleviation device to reduce maximum impact load factor and hull bottom pressures is demonstrated by test data for the HRV-1 presented in Figures 84 and 85. Impact loads with the extended foil were 1/3 the basic hull values, while maximum bottom pressure loadings were reduced 35%.

Carrying these reduced loadings into the hull structure will result in considerable savings in both airframe complexity and weight.

C. Impact Load Factors and Bottom Pressures (Continued)

For a given gross weight, a payload increase will be realized at reduced airframe cost. Experience with the hydrofoil system installed on the HRV-1 has indicated the complete system, including structural provisions and retracting mechanism, can be installed for less than 4% of the airplane gross weight. A 35% reduction in bottom pressure loadings should provide at least a corresponding weight reduction in hull bottom plating and supporting structure; a saving in weight and cost that will permit installation of the seaplane hydrofoil system as a balanced structural trade off. As a result, seaplanes designed for hydrofoil operation realize increased sea state capability without weight penalty. In fact, TAC preliminary studies have indicated that a complete hydrofoil system for a 90,000 pound seaplane designed to unport at 60 mph should weigh less than 3% of gross weight, including foil, strut, retraction system, and supporting structure. As presented in Chapter VIII, the larger the seaplane the smaller the percentage of gross weight that must be allocated to the hydrofoil system; the attendant reduction in hull weight permits incorporation of a hydrofoil system plus increased payload and sea state capability at a fixed gross weight.

To take full advantage of the hydrofoil system described in this study, hull design requirements for hydrofoil seaplanes should be revised to include load alleviation benefits associated with hydrofoil operation.

D. Hydrofoil Size

The hydrofoil size for a given seaplane configuration must be based upon:

1. desired unporting velocity
2. hydrofoil section properties
3. airplane trim angles during take off run
4. available thrust versus velocity during take off
5. hydrofoil and strut system drag versus velocity.

1. Of all these parameters, the desired unporting velocity requires most thorough initial consideration. The airplane must be aerodynamically controllable about all three axes at unporting speed or it will become unmanageable; resulting in an aborted take off, or, more likely, a damaging water loop at fairly high speed.

For small seaplanes up to 6,000 pounds gross weight, sufficient aerodynamic control should be available at unporting speeds of 45 to 50 mph; larger aircraft with higher wing loadings will require higher unporting speeds to assure sufficient aerodynamic control. Once foil-borne, the single hydrofoil seaplane is perched upon a pivot hinged

D. Hydrofoil Size (Continued)

at the water surface, requiring surface control response in sufficient degree to provide trim and stability until airborne. Therefore, unporting speed is basically an aerodynamic consideration rather than hydrodynamic, and must be established prior to determining hydrofoil area.

2. For aircraft use, as previously noted on page 19, the hydrofoil should be of supercavitating type; configuration properties are set forth in detail in Chapter III.

3. Airplane trim angles are required to determine wing and hydrofoil lift during the take off run and at unporting. The hydrofoil incidence angle relative to the seaplane reference line must be set to prevent hydrofoil lift from heaving the airplane into an unported condition prior to the desired unporting speed (and related aerodynamic control velocity). Most seaplanes trim at approximately 8 degrees during planing, and this angle could be considered for preliminary design purposes.

4. An adequate thrust margin must be available to assure rapid transition from hull displacement to the planing hydrofoil regime. This requirement is particularly critical for heavy sea state operation where wave impact duration and relative hull velocity at impact should be at a minimum. Since hydrofoil aircraft may experience two hump regions of operation, the first when the hull planes and the second when foil lift displaces the hull above the water surface, it is necessary that the thrust margin be maintained at higher velocities than necessary for basic hull transition from the displacement to the planing mode. As the foil comes into action, sufficient thrust margin must be available to overcome hull, strut, and foil hydrodynamic drag as well as the aerodynamic drag of the airplane; and with sufficient margin to continue take off acceleration through hydrofoil unporting. Complete ventilation of the hydrofoil and support strut will materially reduce system drag as velocity increases toward unporting speed.

Propeller driven aircraft characterstically experience a decrease in thrust with velocity during the take off run, and must be designed with an excess thrust margin prior to hydrofoil unporting. Turbo jet aircraft normally experience a slight thrust increase during the take off phase, permitting a matching of static thrust to the margin desired during unporting. For either type of propulsion system, other design factors such as STOL performance may determine thrust requirements; however, to assure smooth unporting and a controllable take off from the planing hydrofoil, adequate excess thrust margin must be maintained at higher speeds than is necessary for conventional hull configurations.

5. Hydrofoil and strut drag during take off must be determined with the view of establishing the minimum strut cross section necessary to provide adequate structural rigidity, and the minimum

D. Hydrofoil Size (Continued)

foil area required to provide desired lift at unporting. Examples of hydrofoil area calculation follow.

a) 2300 pound gross weight HRV-1:

Hull trim angle upon the step = 7.5°; wing C_L at this hull angle = 1.65; S_w = 170 sq. ft.; desired unporting speed of 40 knots (67.5 fps).

(i) Wing lift = $1.65 \times .00119 \times 170 \times (67.5)^2$
L_w = 1520 lbs.

(ii) Foil borne load contribution = 2300 - 1520
L_H = 780 lbs.

Foil C_L = .27 (Ref. 45, Pg.13)

ρ = 62.4/32.2 = 1.94 for fresh water

$$S_H = \frac{L_H}{C_L \rho/2\ v^2} = \frac{780}{.27 \times 1.94/2 \times (67.5)^2} = .67 \text{ sq. ft.}$$

It should be noted that an axial load of 780 to 800 pounds was frequently recorded in the HRV-1 hydrofoil support strut, but was not exceeded. The HRV-1 support strut, foil, retraction system, and hull structure reinforcement weighed 73 pounds (3.2% design gross weight).

b) 90,000 pound open ocean seaplane (preliminary design): Wing C_L at unporting = 2.2; S_w = 2000 sq. ft.; desired unporting speed of 50 knots (84 fps).

(i) Wing lift = $2.2 \times .00119 \times 2000 \times (84)^2$
L_w = 37,000 lbs.

(ii) Foil borne load contribution = 90,000 - 37,000
L_H = 53,000 lbs.

Foil C_L = .26 (Fig. 24, α = 8°, AR = 4)

$$S_H = \frac{L_H}{C_L \rho/2\ v^2} = \frac{53{,}000}{.26 \times 1.94/2 \times (84)^2} = 28.5 \text{ sq. ft.}$$

Span (AR of 4) = 13 ft.

System and structural support weight (6° wedge, steel foil) are estimated at 2540 lbs, or 2.8% of design gross weight, including hull reinforcement and retraction provisions.

NOTE: Since heavy sea state operation will normally be accompanied by surface winds which decrease the water speed for a given wing lift value, the decreased contribution of hydrofoil lift (or, conversely, the increased hydrofoil area required) will have to be taken into consideration when determining unporting speed at the design sea state conditions. The use of a flapped hydrofoil could be most beneficial under these conditions.

Fig. 83

STRUT LOCATION & EXTENSION

for the HRV-1

MAC = 52.13 in.

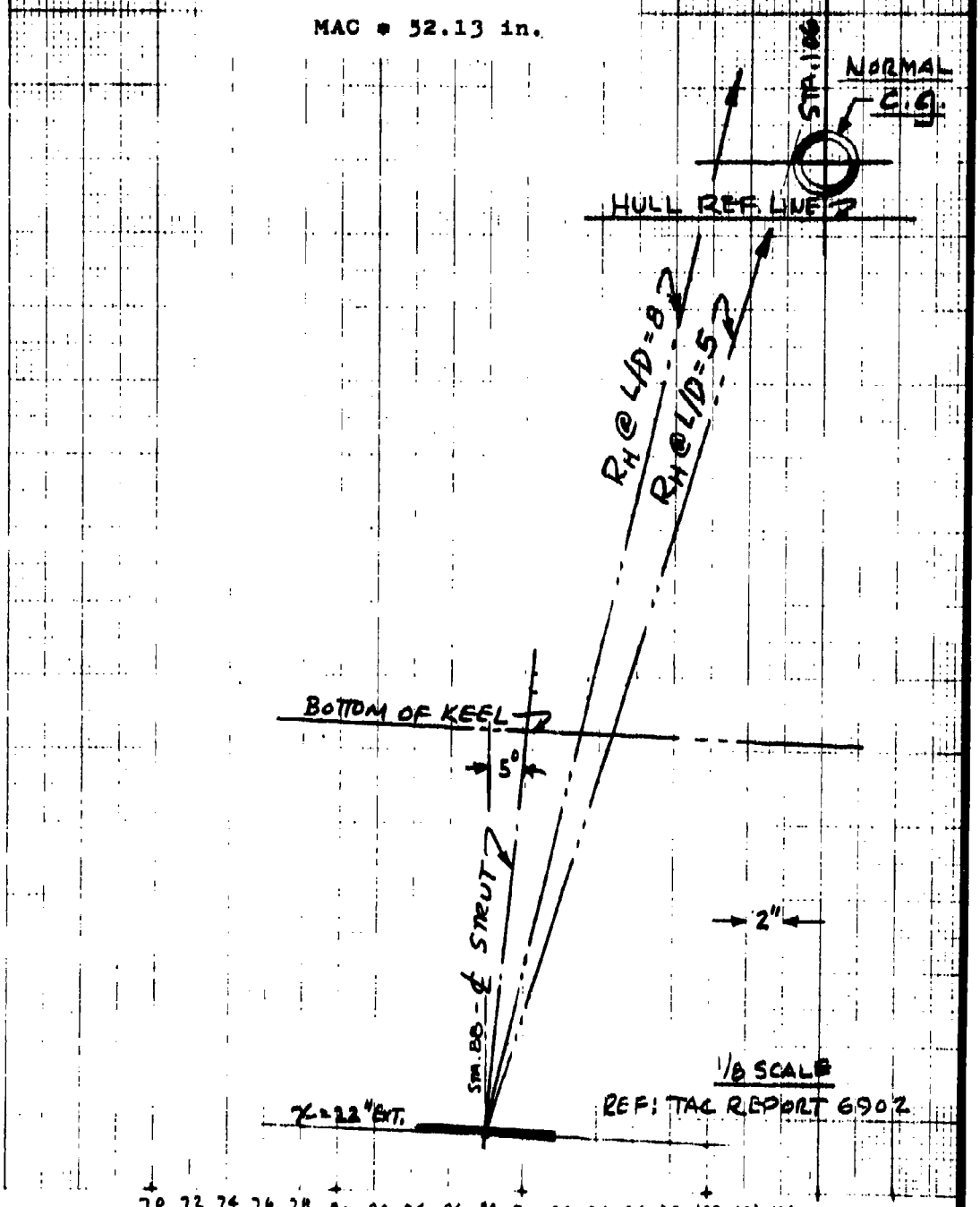

Fig. 84

RELATIVE LANDING IMPACT
LOAD FACTORS vs.
WIND & WATER CONDITIONS
for
Basic HRV-1 Hull & Hydrofoil No.1

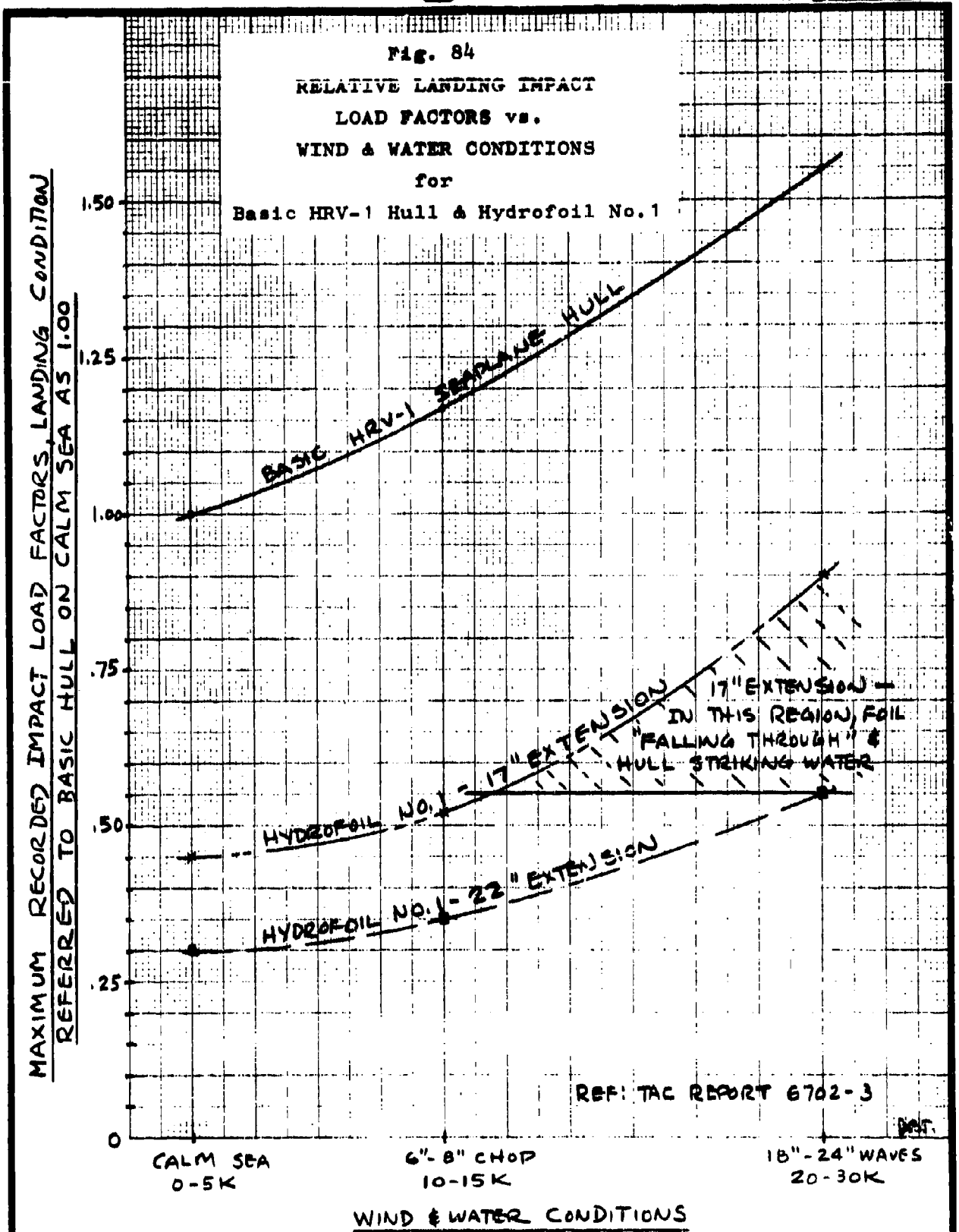

Fig. 85

HULL BOTTOM PRESSURES

vs

WIND & WATER CONDITONS

for

Basic HRV-1 Hull & Hydrofoil No. 1

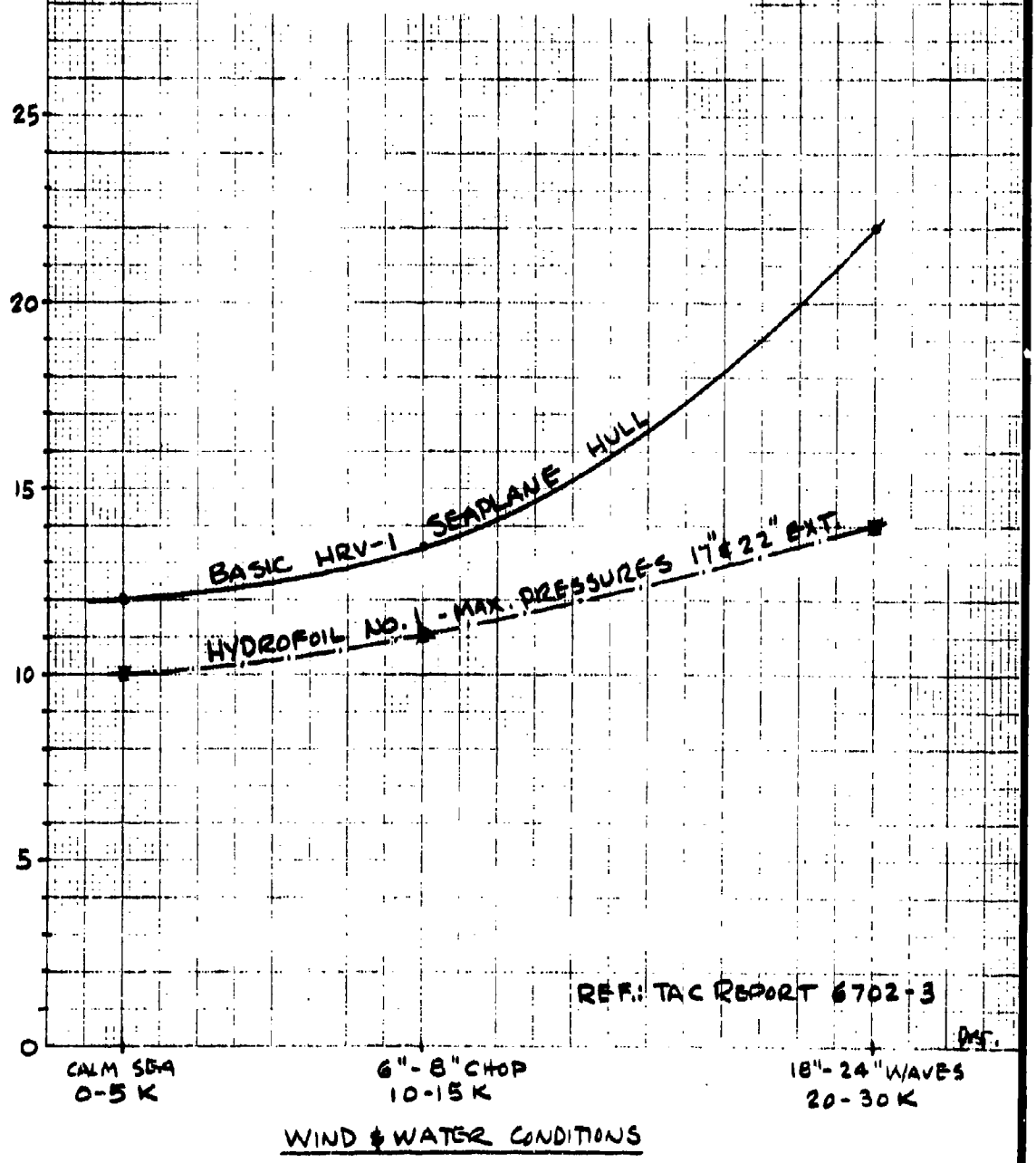

VII. Hydrofoil Seaplane Design Optimization

A. Design Factors for Integration of Hydrofoil and Seaplane

As discussed in Chapter VI, a successful hydrofoil equipped seaplane must consider hydrofoil effect upon airplane performance, handling qualities, and structural design. The hydrofoil alters the mode of operation on the water so dramatically that adding a well designed hydrofoil system to an existing seaplane without modifying the powerplant or control systems would probably result in an unsatisfactory combination.

Factors to be considered during the initial design of a hydrofoil seaplane are:

1. Hydrofoil unporting speed
2. Excess thrust at hump and unporting speeds
3. Airplane stability and control, particularly during the unporting and foilborne phases.
4. Spray pattern in relation to powerplant ingestion and airframe impingement
5. Hydrofoil performance and load capability
6. Hull design considerations reducing required hull strength, and resulting weight savings
7. Hydrofoil retracting design to maximize airborne performance.

B. Stability and Control

Experience to date with two full scale hydrofoil test seaplanes has shown that basic airplane stability and control are inadequate at the low speed end of foilborne operation. The airplane is placed atop an extended strut at speeds below stall; and must remain stable during unporting and take off acceleration maneuvers through its inherent aerodynamic stability and by the pilot's control. During planing, a conventional seaplane is acted upon by hydrodynamic and aerodynamic forces which combine to produce a stable condition in pitch and yaw, with a mildly unstable condition in roll; however, to maintain a wings level condition, seaplane ailerons are designed to provide adequate control at very low airspeeds. At higher planing speeds, the elevator and rudder become effective to provide aerodynamic pitch and yaw control.

When equipped with a hydrofoil, the seaplane is raised out of the water and the stabilizing hydrodynamic forces are replaced by a destabilizing force vector from the foil. This vector acts about the airplane cg, producing upsetting moments which can only be counteracted aerodynamically. If the design permits large foil vector moment arms about the cg coupled with inadequate aerodynamic stability and control at these slow speeds, the airplane becomes

B. Stability and Control (Continued)

uncontrollable at unporting; under such conditions transition to the planing condition would not be attainable and the take off must be aborted.

For this reason, the low speed characteristics of the airplane and the hydrofoil-strut combination must be carefully analyzed. The hydrofoil-strut resultant L/D vector must not only pass close to the cg (per Chapter VI. A), but must also stay as nearly constant as possible during unporting and at slow speeds. Any change in L/D will change the vector moment arm about the airplane cg, resulting in pitch trim changes, Figure 86.

The upsetting effects of the L/D force vector changes can be minimized by reducing the strut length. As reviewed in Chapter VI, this length normally will be a compromise between handling qualities, strut system weight, design sea state wave heights, and minimum spray pattern conditions. Since any foil will ventilate when it unports, in order to maintain nearly steady state foil conditions during unporting and the early phase of foil planing, cavitation and ventilation of the foil and strut must occur prior to unporting.

Figure 86 shows the forces acting on the foilborne airplane in the longitudinal plane. The fore and aft location of the hydrofoil is related to longitudinal control power. Moving the hydrofoil aft shortens the moment arm of the tail about the hydrofoil, thereby not only requiring more nose up trim but larger elevator deflections to maintain control. In addition, this increases the loading on the foil and wing, since the tail force is increased in the downward direction. Variations in the foil-strut L/D (R_H - resultant force of the foil) will require changes in R_T (resultant force of the tail) to maintain equilibrium and control.

From the aerodynamic viewpoint, the airplane must possess sufficient stability and control in pitch to permit holding the desired trim attitude. This can mean larger than normal control surfaces, or increased effectiveness through boundry layer control as used on some STOL airplanes.

In the roll mode, the airplane is destabilized when foilborne due to the increased foil-strut force vector moment arm acting about the cg. This decreased stability results in a more rapid "wing drop" motion requiring larger and more rapid aileron input to maintain a wings level attitude. The predominant factors affecting roll stability are strut length and foil-strut combination side forces due to yaw.

Lastly, the yaw mode directional stability is also dependent upon the longitudinal location of the foil-strut system with respect to the airplane cg as well as the side forces resulting from foil-strut yaw. Moving the foil and strut aft will reduce the side load

B. Stability and Control (Continued)

capability, improving this condition. Yaw instability is of greatest significance during the unporting phase, when the strut can make its side force contribution. After the foil unports, the strut is mostly clear of the water with its side force input essentially eliminated. The major side force contribution then comes from the foil and is of relatively minor nature, acting at higher aerodynamic speeds accompanied by more effective rudder control.

C. Performance

The waterborne performance aspects of hydrofoil seaplane design center about the excess thrust available at hump and unporting speeds. Excess thrust must provide sufficient acceleration to realize acceptable take off times and distances. To meet these requirements, available thrust must be as high as possible, consistent with other design requirements, and the airplane total drag must be kept at a minimum. Factors affecting the airplane total drag are:

1. Hump speed
2. Unporting speed
3. Hull hydrodynamic drag
4. Hydrofoil-strut combination hydrodynamic drag
5. Aircraft aerodynamic drag.

Hump speed occurs as the hull transitions from a displacement to a planing body and usually occurs at a speed where excess thrust is minimum; normally coinciding with the speed at which total drag is a maximum. In the case of a conventional seaplane without a hydrofoil system, the total drag at hump speed is predominantly hydrodynamic with a minor contribution from aerodynamic drag. This hydrodynamic drag peaks at hump speed as the displacement hull rises in the water; then diminishes as the hull begins to plane. With the addition of a hydrofoil system and its associated drag, the total hydrodynamic drag will be greater than for a conventional hull at any given speed prior to hydrofoil unporting.

The normal take off thrust-drag relationship is further altered since the hydrofoil can be designed to unport at speeds unrelated to the hump speed of the basic hull. If the hydrofoil were designed to unport at speeds below the basic hull hump speed, a comparatively large foil would be required. With such a configuration, the total drag would increase rapidly until unporting occured and then decrease. This combination is undersirable due to the unnecessarily large, heavy foil system and the poor handling qualities associated with low speed unporting operation.

The more desirable configuration would be designed to unport slightly above hump speed; permitting a reduction in foil system

C. Performance (Continued)

size combined with improved aircraft handling qualities.

If unporting is delayed to speeds considerably above hump by further reducing the foil system size, hydrodynamic drag will be reduced at any given speed; but will maintain an approximately constant level beyond hump speed, since V^2 drag of the submerged foil and strut will balance any reduction of hull drag due to hull rise. The disadvantage with this arrangement is the resulting extended period of high drag accompanied by slow acceleration; extending take off time and distance while exposing the airplane hull to increased periods of wave impact at higher speeds.

Foil size calculations and other performance parameters must also consider the landing mode, to preclude foil submergence upon landing contact due to foil overloading. This requirement is quite important since submergence of the foil would not only defeat its prime purpose of protecting the hull from wave impact loading, but could also create a strong secondary reactive force placing the airplane in undesirable attitudes leading to a high speed water loop or a violent pitch ejection high above the water surface.

D. Spray Patterns

Experiments have shown that spray height and thickness increase as foil angle of attack and submergence depth increase, occurring at the slower foilborne speeds where maximum lift coefficients are being generated. Figure 74 shows foil spray patterns for the JRF-5G with spray height maximum at a water speed of 39 knots, decreasing as speed increases. To minimize drag, it is important to minimize the amount of spray impingement on the airframe, particularly on flaps and tail surfaces. Excessive spray represents wasted thrust, resulting in increased take off time and surface run.

E. Hull Design

The hull should be designed to reflect the reduced impact loads resulting from hydrofoil operation, and to accommodate the foil system in the retracted position. Hull bottom loads should be calculated on the basis of operational speeds somewhat above unporting but well below take off. Further reductions in bottom plating should be realized from decreased bottom pressure loadings presented in Chapter VI. The resulting saving in hull weight should be greater than the total weight of the hydrofoil system (see Section D. 5 of Chapter VI, and Chapter VIII).

F. Hydrofoil System Optimization

To realize maximum performance, the hydrofoil should completely recess into the hull. A single hydrofoil having dihedral coinciding with hull deadrise, and supported by a single strut, is best suited for seaplane hull installation. The support strut could retract through the keel, with the hydrofoil housed in a hull bottom recess. The Thurston Aircraft Corporation HRV-1 design is typical of this installation (Figures 80, 81, 82 and page i).

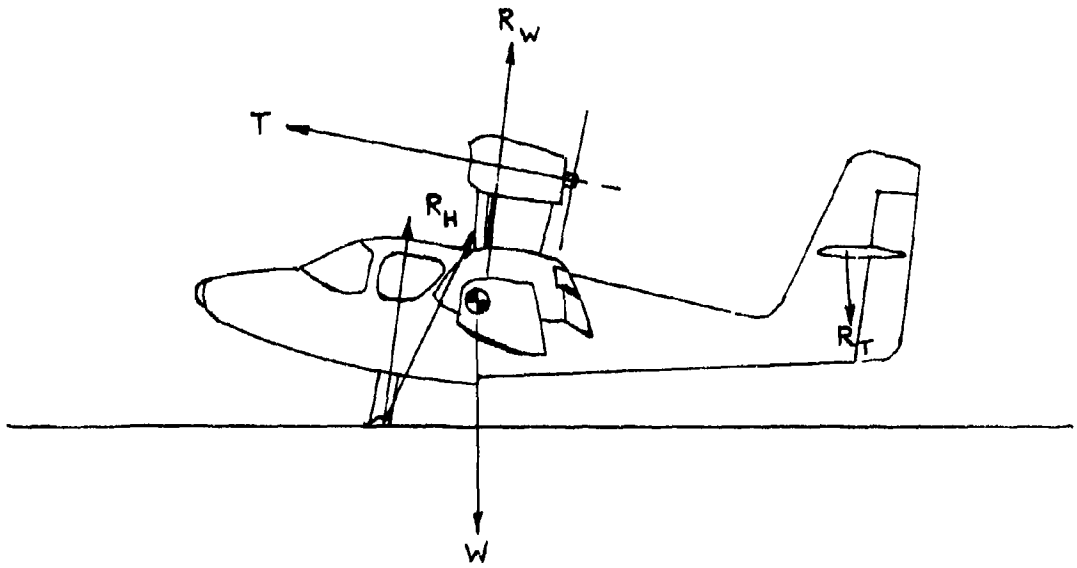

Fig. 86

Forces in

Longitudinal Plane of Foilborne Seaplane

VIII. Hydrofoil Seaplane Development

In conclusion, it is most important to understand that maximization of operational benefits offered by the hydrofoil seaplane can only be realized when the entire configuration is developed for hydrofoil operation.

In this regard, the following design areas require further study:

(a) Hull hydrodynamic configuration

(b) Hull structural loading reductions possible during displacement and impact conditions

(c) Hydrofoil system weight versus seaplane gross weight

(a) Taking full advantave of hydrofoil lift, it is quite possible that a modified semi-chine or chineless hull can be developed. In addition, a stepless, faired step, or retractable step hull configuration should be possible, using foil lift and excess thrust to assist in planing at an early point in the take off run. A proper study of these interrelated factors is beyond the scope of this report; but should permit design of a streamlined hull form capable of being pressurized with minimum weight penalty, while offering a material increase in cruising speed and range compared to prior seaplane configurations. The hydrofoil should retract flush with the hull bottom surface, presenting no increase in form drag when stowed.

(b) As noted in Section C of Chapter VI, a material reduction in impact load factors and hull bottom loading will be realized from hydrofoil operation. To take full advantage of the available reduction in hull structural weight and complexity, specification design requirements must be reduced accordingly. The savings possible from reductions in structural weight and construction complexity will offset the weight and cost of the hydrofoil system, while providing increased sea state capability and a probable increase in payload for a given gross weight. Any serious effort to design a new open ocean seaplane should be preceded by an investigation of hull loading reductions possible with the hydrofoil operating in heavy sea state conditions.

(c) As shown in Figure 87, the weight of the hydrofoil system referred to seaplane gross weight should reduce slightly with seaplane size. While this presentation is based upon preliminary parametric studies, further detail design will be required to integrate a working hydrofoil system into the seaplane configuration and operational specification requirements. For preliminary design study, the percentage of gross weight set forth in Figure 87 indicates that with attendant reductions in hull weight the hydrofoil will permit development of a superior seaplane without weight penalty.

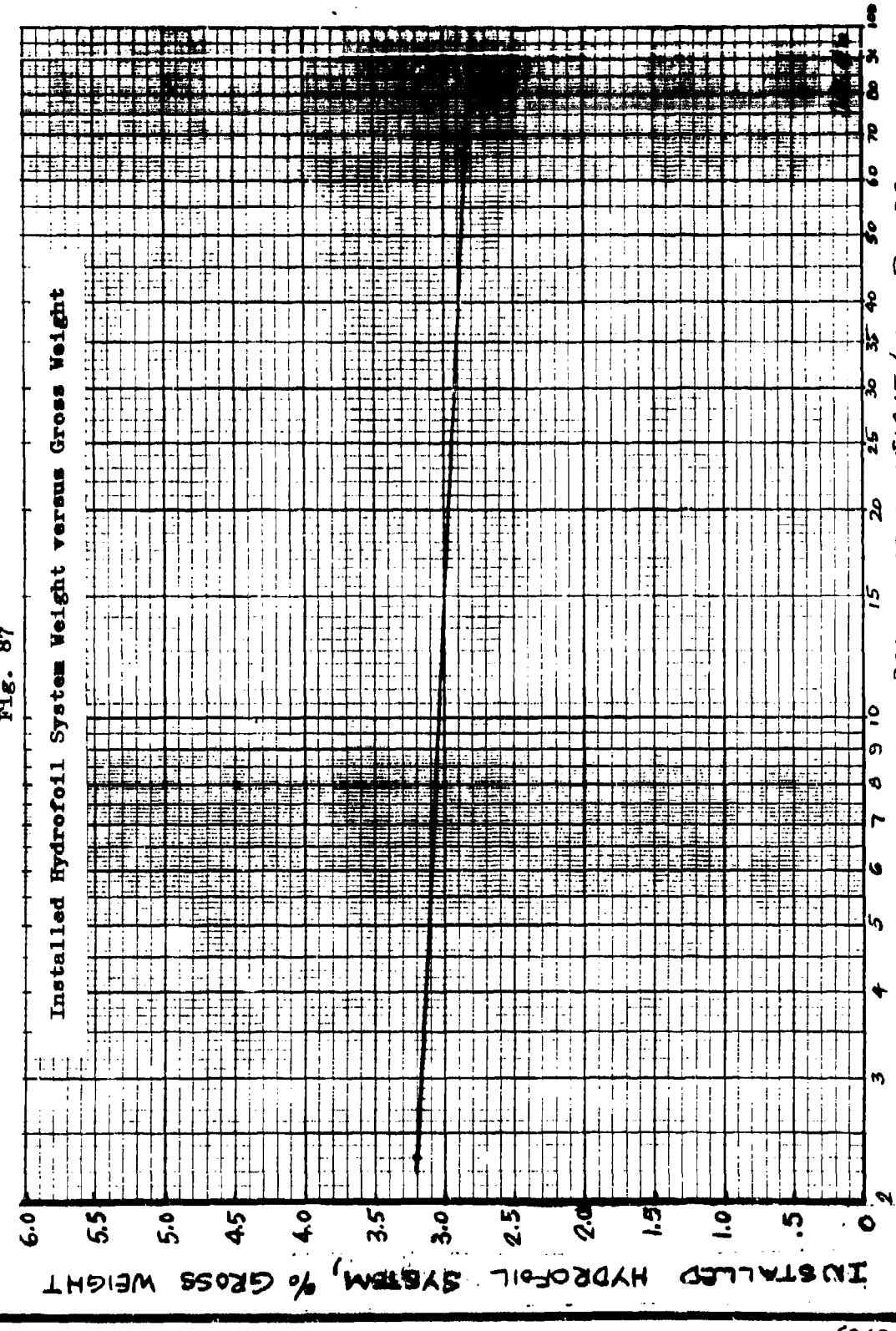
Installed Hydrofoil System Weight versus Gross Weight
INSTALLED HYDROFOIL SYSTEM, % GROSS WEIGHT
6.0
5.5
5.0
4.5
4.0
3.5
3.0
2.5
2.0
1.5
1.0
.5
0
2
3
4
5
6
7
8
9
10
15
20
25
30
35
40
50
60
70
80
90
100
HYDROFOIL SEAPLANE DESIGN GROSS WEIGHT/1000, POUNDS

Fig. 87

IX. Bibliography and Reference List

A. Historical References

1. Aeromarine Origins; H.F. King; Putnam and Company Ltd. (Aero Publishers Inc. in the USA), 1966.

2. British Flying Boats and Amphibians 1909-1952; G.R. Duval; Putnam and Company Ltd. (Aero Publishers in the USA), 1966.

3. Jane's All the World's Aircraft, 1932.

4. The Hydrofoil Boat, Tietjens; Werft-Reederei-Hafen and The Yearbook Deutsche Luftfahrtforschung p. 1361, 1937.

5. Hydrodynamic Lift Through Hydrofoils, Design of a Stable Foil System, Grunberg; L'Aerotechnique No. 174 and L'Aerotechnique No. 217, p. 61, June 1939.

6. Brief Historical Review of the Hydrofoil Boat; H.O. Hollenberg; Systems Analysis Division, Report No. RRSY-60-53, Bureau of Naval Weapons, Washington, D.C., August 1960.

B. Hydrofoil Bibliography Lists

7. Hydrofoil Bibliography; Glen J. Wennagel; Dynamic Developments, Inc., Babylon, N.Y., September 1957.

8. Hydrofoils, An Annotated Bibliography SB-60-36; K.D. Carroll; Lockheed Missiles and Space Division, Sunnyvale, California, September 1960.

C. Hydrofoil Study Reports

California Institute of Technology

9. Report No. 47-2 April 1955 by Parkin, Perry and Wu; "Pressure Distribution on a Hydrofoil Running Near the Water Surface"

10. Report No. 47-3 December 1956 by Parkin and Peebles; "Calculation of Hydrofoil Sections for Prescribed Pressure Distributions"

11. Report No. 47-4 September 1955 by Wu and Perry; "Comparison of The Characteristics of a Hydrofoil Under Cavitating and Noncavitating Operation"

California Institute of Technology

12. Report No. 47-6 February 1956 by Parkin;
"Experiments on Circular Arc and Flat Plate Hydrofoils in Noncavitating and Full Cavity Flows"

13. Report No. 47-7 February 1956 by Kermeen;
"Water Tunnel Tests of NACA 66-012 Hydrofoil in Noncavitating and Cavitating Flows"

14. Report No. 47-9 December 1957 by Parkin;
"A Note of the Cavity Flow Past a Hydrofoil in a Liquid with Gravity"

15. Report No. 47-10 February 1957 by Parkin and Kermeen;
"Water Tunnel Techniques For Force Measurement on Cavitating Hydrofoils"

16. Report No. 47-11 March 1960 by Cumberbatch and Wu;
"Cavity Flow Past Two Slender Pointed Hydrofoils"

17. Report No. 47-12 May 1960 by Cumberbatch;
"Cavitating Flow Past a Large Aspect Ratio Hydrofoil"

18. Report No. 47-13 June 1960 by Cumberbatch;
"Accelerating, Supercavitating Flow Past a Thin Two-Dimensional Wedge"

19. Report 47-14 September 1960 by Kermeen;
"Experimental Investigations of Three Dimensional Effects on Cavitating Hydrofoils"

CONVAIR

Aeromarine Test Center, San Diego, Cal.

20. Report ZH-083A - May 1952;
"An Exploratory Investigation of the Practical Aspect of Hydrofoils as Applied to Waterbased Aircraft"

21. Report ZH-102 - July 1955;
"Model Experiments with Hydrofoils and Wedges for Rough Water Seaplane Design"

22. Report ZH-123 - August 1957;
"A Hydrofoil System for the JRF-5 Airplane"

23. Report ZH-127 - March 1958;
"Hydrodynamic Characteristics of Two MACH 3 Designs"

24. Report ZH - 132 - February 1959;
"Supersonic Attack Seaplane - Final Report of Design Studies"

CONVAIR
Aeromarine Test Center, San Diego, Cal.

25. Report ZH-136 - April 1959;
"A Hydrofoil System for a MACH 3 Seaplane"

26. Report GD/C - 63-021A - February 1963;
"Supercavitating Hydrofoil Studies"

27. Report No. U419-67-011 - September 1967, Conolly and Ball;
"Towing Basin Tests with a One-Eleventh Scale Model of a High Density Seaplane Configuration"

Cornell Aeronautical Laboratory

28. Cal. Report No. BB-1629-S-1 - August 1962, Crimi and Statler; "Forces and Moments on an Oscillating Hydrofoil"

Dynamic Developments, Inc.

29. Report No. 107, Application of Supercavitating Hydrofoils to High Performance Seaplanes
Part I Summary Report; John Lueck 1958

30. Report No. 108, Application of Supercavitating Hydrofoils To High Performance Seaplanes
Part II Steady State Hydrodynamic Loads Calculations;
John Lueck, March 1958

31. Report No. 109, Application of Supercavitating Hydrofoils To High Performance Seaplanes
Part III Structural Considerations; Thomas Shervington, March 1958

32. Report No. 110, Gruen Tech. Rpt. 66, Prepared by Gruen Applied Science Laboratories, Inc. Application of Supercavitating Hydrofoils to High Performance Seaplanes
Part IV Aerodynamic Considerations

33. Report No. 111, Gruen Tech. Rpt. 67, Prepared by Gruen Applied Science Laboratories, Inc. Application Of Supercavitating Hydrofoils To High Performance Seaplanes
Part V Foil Flutter and Airplane Waterborne Stability Considerations

EDO Corporation

34. Report No. 4769 - 17 July 1958 by J. Kapsalis;
"Structural Design Criteria: Grunberg Hydrofoil System on JRF-5 Airplane"

EDO Corporation

35. Report No. 4815 - 2 October 1958;
"The Development of a Damping Hydrofoil for Rough Water Landings of Seaplanes"

36. Report No. 4869 - 9 December 1958;
"An Experimental Investigation of the Effect of Size on the Hydrodynamic Characteristics of a Surface-Piercing Hydrofoil"

37. Report No. 4912 - 22 January 1959 by J. Kapsalis:
"Water Loads for the Grunberg Hydrofoil System on JRF-5 Airplane"

38. Report No. 4999;
"Structural Analysis of Installation of Grunberg Hydrofoil System on the Grumman JRF-5 Airplane"
Part I Forward Skid Installation
Part II Stress Analysis of Hydrofoil and Supporting Struts
Part III Bow Skid and Hydrofoil Carry Through Structure

39. Report No. 5741 - 13 April 1962;
"The Equilibrium Configuration of a Towed Hydrofoil - Strut System in Two-Dimensional Steady Flow"

40. Report No. 5743;
"Final Report on the Development and Preliminary Design of a Helicopter-Towed Hydrofoil Sea Pallet"

41. Report No. 6487 - 5 May 1964;
"Proposal For The Model Test Development of a Penetrating Superventilating Hydrofoil Installation for The Grumman HU-16 Airplane"

42. Report No. 6651 - November 1964;
Final Report "Design and Installation of Grunberg Hydrofoil System on the JRF-5 Airplane"

43. Report No. 6652 - October 1964
Final Engineering Report "Instrumentation and Preliminary Flight Tests of the JRF-5 Equipped with a Grunberg Hydrofoil System"

44. Report No. 6653 - January 1965
Final Engineering Report "Flight Tests of the JRF-5 Equipped with a Grunberg Hydrofoil System"

45. Report No. 7016 - 7 February 1966 by L. Kaplan and R.J. Miko; "The Design and Model Testing of a Small Single Hydrofoil Installation for the HU-16 Airplane"

EDO Corporation

46. Report No. 7140 - 25 March 1966;
"Development of Ogive Hydrofoils for Mk 3 Mod 0 Seaborne Equipment, Final Report"

47. Report No. 7489-1 - 23 December 1966 by P.A. Pepper and L. Kaplan; "Survey on Seaplane Hydro-Ski Technology Phase I: Qualitative Study"

48. Report No. 7489-2 - 28 March 1968 by P.A. Pepper and L. Kaplan; "Survey on Seaplane Hydro-Ski Technology Phase II: Quantitative Study"

Grumman Aircraft Engineering Corporation

49. Report No. PDR-140-1 - 12 April 1957;
"Summary Report - JRF Hydrofoil and Dynamic Model Test Program" Phase I

50. GAEC & DDI - 3 October 1958;
"Study of Hydrofoil Seacraft"
Volumes I and II

Volume I contains chapters on sub and supercavitating hydrofoils, struts and bodies of revolution, estimates of strut and hydrofoil weights.

Volume II, devoted entirely to hydrofoil boats, contains useful information on hydrofoil configurations, hull structure to which the struts are attached, and some applicable preliminary design analysis.

51. Report No. DA10-480.3 - 7 February 1962 by Baird, Squires & Caporali;
"Investigation of Hydrofoil Flutter"

52. Report No. STR-MAR-100, 1 May 1962 by Dulmovits;
"Hydroelastic Effects on The Lift of High Speed Hydrofoils"

53. Report No. DA Nonr - 3989.3 - November 1963 by Squires;
"Hydrofoil Flutter, Small Sweep Angle Investigation"

Hydronautics, Incorporated

54. Report 001-1 - June 1960
"Optimum Wing-Strut Systems for High Speed Operations Near a Free Surface"

55. Report 0016 - January 1961 by V.E. Johnson, Jr. and M.P. Tulin; "The Hydrodynamic Characteristics of High-Speed Hydrofoils"

Hydronautic , Incorporated

56. Report 120-1 - March 1961 by M.P. Tulin;
"80 Knot Wing-Strut System Design and Performance"

57. Report 001-7 - April 1962 by J. Auslaender
"Low Drag Supercavitating Hydrofoil Sections"

58. Report 001-16 - September 1962 by V.E. Johnson, Jr. and S.E. Starley;
"The Design of Base-Vented Struts for High-Speed Hydrofoil Systems"

59. Report 001-15 - November 1963 by V.E. Johnson, Jr. and S.E. Starley;
"Low-Drag Base Vented Hydrofoils Designed for Operation Near the Free Surface"

60. Report 343-1 - March 1964 by J.O. Scherer and J. Auslaender;
"Experimental Investigation of the 5-Inch Chord Model of the Buships Parent Supercavitating Hydrofoil"

61. Report 463-1, Chapter 4 - September 1964 by R.A. Barr;
"Trim Attitude and Pre-Takeoff Resistance of Hydrofoil Craft"

62. Report 463-6 - January 1965 by T. Hsieh;
"Passive Load Alleviation on Supercavitating Hydrofoils"

63. Report 457-1 - November 1965 by R.J. Altmann;
"Measurement of Cavity Shapes Above Ventilated Hydrofoils"

64. Report 498-1 - November 1966 by R.J. Altmann;
"Model Tests of a 20-Ton Hydrofoil Sled"

65. Report 744-1 - March 1968 by R.J. Altmann;
"Hydrofoil Craft Designer's Guide"

66. Report 001-14 - April 1968 by R.J. Altmann;
"The Design of Supercavitating Hydrofoil Wings"

67. Report 121-5 - April 1965 by Marshall P. Tulin;
"The Shape of Cavities in Supercavitating Flows"

68. Report 343-3 - September 1965 by Scherer and Auslaender;
"Experimental Investigation of a Supercavitating Hydrofoil with Trailing Edge Flaps"

69. Report 463-4 - June 1964 by B. Yim;
"On a Fully Cavitating Two-Dimensional Flat Plate Hydrofoil with Non-Zero Cavitation Number Near a Free Surface"

Hydronautics, Incorporated

70. Report 463-5 - July 1964 by C.C. Hsu;
"On Full Cavitating Hydrofoils Entering Gusts Under a Free Surface"

71. Report 465-1 - December 1965 by T.T. Huang and H.H. Shih;
"Investigation of Base Vented Hydrofoils"

Iowa, State University of

72. Proj. No. S-R009-01-01 July 1961;
"Tests of a Cavitating Hydrofoil"

The Martin Company

73. Report ER9433 - June 1957 by E.G. Band and J.W. Cuthbert;
"Preliminary Design Data for Water-Based Aircraft with Hydrofoils or Skis"

74. Report ER10135 - March 1958;
"Configuration and Model Lines of the Martin M329 E-8 Supersonic Seaplane"

University of Minnesota
St. Anthony Falls Hydraulic Laboratory

75. Tech Paper No. 30, Series B, April 1960 by J.M. Wetzel;
"Experimental and Analytical Studies of the Longitudinal Motions of a Tandem Dihedral Hydrofoil Craft in Regular Waves"

76. Proj. Report No. 64 - September 1960 by Wetzel and Schiebe;
"Lift and Drag on Surface Piercing Dihedral Hydrofoils in Regular Waves"

77. Tech Paper No. 36, Series B - December 1961 by Lorenz G. Straub, Director;
"Ventilated Cavities on Submerged Three Dimensional Hydrofoils"

78. Tech Paper No. 37, Series B - December 1961 by Wetzel and Maxwell;
"Long Motions and Stability of Two Hydrofoil Systems Free to Heave and Pitch in Regular Waves"

79. Proj. Report No. 61 - May 1962 by Lorenz G. Straub, Director; "Tandem Interference Effects of Flat Noncavitating Hydrofoils"

University of Minnesota
St. Anthony Falls Hydraulic Laboratory

80. Proj. Report No. 72 - October 1964 by Schiebe and Wetzel; "Further Studies of Ventilated Cavities on Submerged Bodies"

81. Proj. Report No. 68 - March 1965 by Wetzel and Foerster; "Force Characteristics on Restrained, Naturally Ventilated Hydrofoils in Regular Waves"

82. Tech Paper No. 51, Series B - May 1965 by R. Oba; "Performance of Supercavitating Hydrofoils with Flaps, with Special Reference to Leakage and Optimization of Flap Design"

National Advisory Committee for Aeronautics

83. WRL-725 - March 1944 by K.L. Wadlin; "Preliminary Tank Experiments with a Hydrofoil on a Planing-Tail Seaplane Hull"

84. RM No. L9A17 - March 1949 by King and Rockett; "Preliminary Tank Investigation of the Use of Single Monoplane Hydrofoils for High Speed Airplanes"

85. TN-2453 - September 1951 by R.F. Smiley; "An Experimental Study of Water-Pressure Distributions During Landings and Planing of a Heavily Loaded Rectangular Flat-Plate Model"

86. RM L52D15 - September 1952 by Land, Chambliss and Petynia; "A Preliminary Investigation of the Static and Dynamic Longitudinal Stability of a Grunberg Hydrofoil System"

87. RM L52J10 - December 1952 by King and Land; "Effects of Sweepback and Taper on the Force and Cavitation Characteristics of Aspect Ratio 4 Hydrofoils"

88. TN 2981 - July 1953 by Weinstein and Kapryan; "The High Speed Planing Characteristics of a Rectangular Flat Plate Over a Wide Range at Trim and Wetted Length"

89. TN 3092 - December 1953 by Coffee and McKann; "Hydrodynamic Drag of 12 and 21 Percent Thick Surface Piercing Struts"

90. TN 3951 - March 1957 by K.A. Christopher; "Investigation of the Planing Lift of a Flat Plate at Speeds up to 170 Feet per Second"

National Advisory Committee for Aeronautics

91. RM L57A15 - March 1957 by Roy Steiner;
"Statistical Approach to the Estimation of Loads and Pressures on Seaplane Hulls for Routine Operations"

92. RM L57G05 - October 23, 1957 by Petynia, Hasson and Spooner;
"Aerodynamic and Hydrodynamic Characteristics of a Proposed Supersonic Multijet Water-Based Hydro-Ski Aircraft with a Variable Incidence Wing"

93. TR-1355 - 1958 by C.L. Shuford, Jr.;
"A Theroretical and Experimental Study of Planing Surfaces Including Effects of Gross Section and Plan Form"

National Aeronautics and Space Administration

94. Memo 5-9-59L - June 1959 by McGehee and Johnson;
"Hydrodynamic Characteristics of Two Low Drag Supercavitating Hydrofoils"

95. TN D-16 - August 1959 by Maki and Giulianetti;
"Low Speed Wind Tunnel Investigation of Blowing Boundry Layer Control on Leading and Trailing Edge Flaps of a Full Scale Low Aspect Ratio, 42 degree Swept Wing Airplane Configuration"

96. TN D-119 - November 1959 by Johnson and Rasnick;
"Investigation of a High Speed Hydrofoil with Parabolic Thickness Distribution"

97. TR R-14 - 1959 by Wadlin and Christopher;
"A Method for Calculation of Hydrodynamic Lift for Submerged and Planing Rectangular Lifting Surfaces"

98. TN D-166 - November 1959 by Vaughan;
"A Hydrodynamic Investigation of the Effect of Adding Upper Surface Camber to a Submerged Flat Plate"

99. TN D-187 - January 1960 by Christopher and Johnson;
"Experimental Investigation of Aspect Ratio 1 Supercavitating Hydrofoils at Speeds Up to 185 Feet per Second"

100. TN D-220 - February 1960 by Stubbs and Hoffman;
"A Brief Investigation of a Hydro-Ski Stabilized Hydrofoil System on a Model of a Twin Engine Amphibian"

National Aeronautics and Space Administration

101. TM X-191 - February 1960 by McKann, Blanchard and Pearson; "Hydrodynamic and Aerodynamic Characteristics of a Model of a Supersonic Multijet Water Based Aircraft Equipped with Supercavitating Hydrofoils"

102. TN D-728 - March 1961 by K. Christopher; "Experimental Investigation of a High Speed Hydrofoil with Parabolic Thickness Distribution and an Aspect Ratio of 3"

103. TR-93 - 1961 by V. Johnson, Jr.; "Theoretical and Experimental Investigation of Supercavitating Hydrofoils Operating Near the Free Water Surface"

Southwest Research Institute, San Antonio, Texas (Administered by DTMB) (Now NSRDC)

104. Tech Report No. 2 - 1 Nov. 1962 by Ransleben and Abramson; "Experimental Determination of Oscillatory Lift and Moment Distributions of Fully Submerged Flexible Hydrofoils"

105. Tech Report No. 4 - 15 December 1963 by Abramson and Ransleben; "A Experimental Investigation of Flutter of a Fully Submerged Subcavitating Hydrofoil"

106. Phase I Tech Report Task 1719, SWRI Project No. 0Z-1546 by G. Ransleben, Jr.; "Experimental Determination of Oscillatory Lift and Moment Distributions on a Fully Submerged Supercavitating Hydrofoil"

107. Tech Report No. 1 - 15 August 1958 by Abramson and Chu; "A Discussion of the Flutter of Submerged Hydrofoils"

Stanford University

108. Tech Report No. 17 - September 1963 by Nimr and Perry; "Cavity Flow Around Cambered Hydrofoils"

Davidson Laboratory, Stevens Institute of Technology

109. Report No. 517 - December 1959 by P. Kaplan; "Longitudinal Stability and Motions of a Tandem Hydrofoil System In a Regular Seaway"

Davidson Laboratory, Stevens Institute of Technology

110. Report No. 596 - January 1956 by J.P. Breslin and J.W. Delleur; "The Hydrodynamic Characteristics of Several Surface-Piercing Struts"

111. Report No. 668 - October 1957 by J.P. Breslin and R. Skalak; "An Exploratory Study of Ventilated Flows About Yawed Surface Piercing Struts"

112. Report No. 698 - October 1958 by P.W. Brown; "The Force Characteristics of Surface Piercing Fully Ventilated Dihedral Hydrofoils"

113. Report No. 704 - June 1959 by Paul Kaplan and W. Jacobs; "Dynamic Performance of Scaled Surface-Piercing Hydrofoil Craft in Waves"

114. Report No. 731 - July 1959 by P.W. Brown; "A Generalized Theory of the Impact Characteristics of Surface-Piercing, Fully Ventilated Dihedral Hydrofoils"

115. Report No. 732 - October 1959 by G. Fridsma; "Longitudinal Stability of Surface-Piercing Hydrofoil Systems Water-Based Aircraft"

116. Report No. 795 - November 1960 by G. Frisma; "Force and Moment Characteristics of a Surface-Piercing, Fully-Ventilated, Dihedral Hydrofoil"

117. Report No. R-856 - September 1961 by C.J. Henry; "Hydrofoil Flutter Phenomenon and Airfoil Flutter Theory Volume I - Density Ratio"

118. Report No. R-911 - July 1962 by C.J. Henry and M. Raihan Ali; "Hydrofoil Flutter Phenomenon and Airfoil Flutter Theory Volume II - Center of Gravity Location"

119. Report No. 952 - October 1963 by G. Fridsma; "Ventilation Inception on a Surface-Piercing Dihedral Hydrofoil with Plane Face Wedge Section"

120. Tech Memorandum No. 133 - April 1965 by J.P. Breslin; "Simplified Procedures for Estimation of the Cavitation Inception Speed on Two-Dimensional Foil Sections"

121. Letter Report No. 1096 - November 1965 by R.L. Van Dyck; "Development Tests of HU-16 Hydrofoil Aircraft"

122. Report No. 1115 - December 1965 by C.J. Henry and M. Railhan Ali; "Hydrofoil Flutter Phenomenon and Airfoil Flutter Theory Volume III - Sweep and Taper

Davidson Laboratory, Stevens Institute of Technology

123. Report No. 1118 - June 1966 by S. Tsakonas and C.J. Henry; "Finite Aspect Ratio Hydrofoil Configurations in a Free Surface Wave System"

124. Letter Report No. 1180 - November 1966 by John Mercier; "Force Measurements on a Rotating Variable Sweep Hydrofoil"

125. Letter Report No. 1332 - January 1969 by John Mercier; "Tests of a Variable Sweep Hydrofoil with Cavitation and Ventilation"

126. Letter Report SIT-DL-69-1347 - October 1969 by R.L. Van Dyck; "Model Tests of Hydrofoil Equipped Floats"

Technical Research Group (TRG)

127. TRG-141-FR - July 31, 1961 by Bluston and Kaplan; "Lateral Stability and Motions of Hydrofoil Craft in Smooth Water"

Thurston Aircraft Corporation

128. Report No. 6702 -1 September 1966 by David B. Thurston; "Structural Analysis of HRV Hydrofoil No. 1"

129. Report No. 6702-3 - February 1967 by David B. Thurston; "Final Summary Report: HRV-1 Equipped with Hydrofoil No. 1 on Strut No. 2"

130. Report No. 6902 - February 1969 by David B. Thurston; "Final Report: HRV-1 Flight Test with Aft Location of Hydrofoil No. 1 on Strut No. 2"

Ministry of Aviation, United Kingdom

131. R & M No. 3285 - December 1958 by Arlotte, Brown, Crewe; "Seaplane Impact - A Review of Theoretical and Experimental Results"

U.S. Navy
David Taylor Model Basin
(Naval Ship Research and Development Center)

132. Report 1607 - April 1962 by Donald L. Blount; "Resistance Characteristics of a 70 Foot Hydrofoil Missile Range Patrol Boat"

U.S. Navy
David Taylor Model Basin
(Naval Ship Research and Development Center)

133. Report 1676 - January 1963 by Ficken and Debay;
"Experimental Determination of the Forces on Supercavitating Hydrofoils with Internal Ventilation"

134. Report 1723 - August 1963 by Nathan K. Bales;
"A Method for Predicting the Probable Number and Severity of Collisions Between Foilborne Craft and Floating Debris"

135. Report 1801 - December 1963 by Jerome Feldman;
"Experimental Investigation of Near Surface Hydrodynamic Force Coefficients for a Systematic Series of Tee Hydrofoils, DTMB Series HF-1"

136. Report 1778- October 1965 by Wilburn and Haller;
"Experimental Measurements of the Steady Lift, Drag and Moment on Surface-Piercing Struts"

137. Report 2160 - March 1966 by Eugene P. Clement;
"The Development of Efficient Hull Forms for Hydrofoil Boats"

U.S. Navy
U.S. Naval Air Test Center, Patuxent River, Maryland

138. "Hydrodynamics Manual," Flight Test Division - May 1958, by R.N. deCalles

139. Tech Report FT2121-35R-65 - 21 July 1965 by LCDR Nicholas J. Vagianos;
"Evaluation of the Hydrodynamic Characteristics of the JRF-5G Hydrofoil Seaplane"

U.S. Navy
U.S. Naval Ordnance Test Station

140. NOTS TP 2346 NAVORD Report 6606 - 19 October 1959 by T.G. Lang; "Base Vented Hydrofoils"

U.S. Navy
Office of Naval Research

141. Contract No. N62558-2896 Task No. NR.062-287 by J.K. Lunde and H.A.A. Walderhaug;
"Surface Piercing Hydrofoils with Self Adjusting Incidence and Shock Absorbers"

U.S. Navy
Naval Ship R & D Center, Washington, D.C.

142. Report No. 2424 - June 1967 by George Springston, Jr.;
"Generalized Hydrodynamic Loading Functions for Bare and Faired Cables in Two-Dimensional Steady State Cable Configurations"

Papers

143. Journal of Ship Research, Vol. No. 2 pp 5-13, by
H. Norman Abramson and Wen-Hwa Chu;
"A Discussion of the Flutter of Submerged Hydrofoils"

144. Journal of Ship Research, Vol. No. 3, pp 20-27 by
Wen-Hwa Chu and H. Norman Abramson;
"Effect of the Free Surface on the Flutter of Submerged Hydrofoils"

145. Journal of the American Society of Naval Engineers - May 1959
by CMDR S.R. Heller, Jr. USN and H. Norman Abramson;
"Hydroelasticity: A New Naval Science"

146. Am. Inst. of Aeronautics and Astronautics, Paper No. 68-472
1 May 1968 by E. Yates, NASA Langley Res. Center;
"Flutter Prediction at Low Mass Density Ratios with Application to the Finite-Span Noncavitating Hydrofoil"

147. Society of Naval Architects and Marine Engineers
Hydrofoil Symposium, 1965 Spring Meeting

148. Am. Society of Mech. Engineers, 10 May 1962 by D.L. Stevens;
"Flying on Hydrofoils"

149. Journal of Hydronautics Vol. 4, No. 1, January 1970 by
P. Crimi;
"Experimental Study of the Effects of Sweep on Hydrofoil Loading and Cavitation"